SOME STUDIES ON TRANSPORT PHENOMENA IN PRESENCE OF A BLUFF BODY

Thesis submitted by

SUDHIR CHANDRA MURMU

Doctor of Philosophy (Engineering)

Department of Mechanical Engineering,

Faculty Council of Engineering & Technology

Jadavpur University

Kolkata, India

2018

JADAVPUR UNIVERSITY

KOLKATA-700032

<u>**INDEX NO**</u>. 20/14/E

1. **Title of the thesis:**   **Some Studies on Transport Phenomena in Presence of a Bluff Body**

2. **Name, Designation &**   Dr. Himadri Chattopadhyay
    Institution of the Supervisor/s: Professor
                                            Department of Mechanical Engineering
                                            Jadavpur University

    Dr. Amitava Sarkar
    Professor(Retired)
    Department of Mechanical Engineering
    Jadavpur University

3. **List of publication:**

    1 **Sudhir Chandra Murmu**., Himadri Chattopadhyay, Transport Phenomena around bluff body at varying inlet turbulent intensity, *Heat transfer research*, *accepted*.

    2 **Sudhir Chandra Murmu,** Himadri Chattopadhyay, Effect of different bluff bodies on heat transfer enhancement in a channel flow- *Progress in Computational fluid dynamics - Under Review*.

    3 **Sudhir Chandra Murmu,** Himadri Chattopadhyay, Augmentation of heat transfer in a channel using a triangular prism with varying inlet turbulent intensity, Journal of enhanced heat transfer- *Under Review.*

4. **List of Patents:**   Nil

5. **List of Presentations in**   1. S. C. Murmu, H. Chattopadhyay, A. Sarkar,
    National / International :   "Numerical simulation of flow and heat transfer around circular cylinder" 1st International

ISHMT-ASTFE Heat and Mass Transfer Conference, 17-20 December, 2015, ISRO, Kerala.

2. S. C. Murmu, H. Chattopadhyay, A. Sarkar, **"**Numerical simulation of flow and heat transfer around triangular prism**",** 6th International & 43rd National Conference on Fluid Mechanics and Fluid Power, 15-17th December,2016,MNNIT Allahabad, Uttar Pradesh.

3. S.Saha, S.C. Murmu, A. Chatterjee, H. Chattopadhyay, "Transport phenomenon around a diamond shape bluff body",6thInternational and 43rd National Conference on Fluid Mechanics and Fluid Power, Dec 15-17,2016,ISBN 978-93- 5267-408-4MNNIT Allahabad, India.

4. S.Saha, A.Chatterjee, H. Chattopadhyay," Augmentation of heat transfer a channel in presence of a diamond shape bluff body "National Conference on Advances in Thermal Engineering, Dec 23-24,2017 Jadavpur university, Kolkata, India.

5. S. C. Murmu, H. Chattopadhyay, **"**Transport phenomena over bluff bodies at varying inlet turbulent intensity**",** Computational Science Symposium, 16-18 March 2017, IISC, Bangalore.

CERTIFICATE FROM THE SUPERVISORS

This is to certify that the thesis entitled **"Some Studies on Transport Phenomena in Presence of a Bluff Body"** submitted by **Shri Sudhir Chandra Murmu** who got his name registered on 20th August 2014 for the award of Ph.D. (Engg.) degree of Jadavpur University is absolutely based upon his own work under the supervision of *Dr. Himadri Chattopadhyay*, Professor, Department of Mechanical Engineering, Jadavpur University & *Dr. Amitava Sarkar (Retired)* Professor, Department of Mechanical Engineering, Jadavpur University and that neither his thesis nor any part of the thesis has been submitted for any degree/ diploma or any other academic award anywhere before.

Signature of Supervisor with seal　　　　　　　　**Signature of Supervisor with seal**

Seal of the Supervisor　　　　　　　　**Seal of the Supervisor**

को अद्धा वेद क इह प्र वोचत्कुत आजाता कुत इयं विसृष्टिः ।

अर्वाग्देवा अस्य विसर्जनेनाथा को वेद यत आबभूव ॥

(RigVeda, Mandal 10)

(But then who can say where the creation started and where from? Even the Gods came after that.)

*Dedicated to
My family*

ACKNOWLEDGEMENT

My deep gratitude goes first to Dr. Himadri Chattopadhyay, and Dr. Amitava Sarkar whose guidance helped me through my graduate education and who shared his ever evolving knowledge throughout the excitement of 4 years of discovery. His staunch enthusiasm has kept me constantly engaged with my research, and his personal generosity helped make my time at Jadavpur enjoyable. The way he guides his students is undoubtedly the best. No words are enough to express my indebtedness for his dedicated support, without which this work would have been imperfect.

I would like to thank my committee members for their valuable advices and encouragement which helped in shaping up this work better.

I am very thankful to Head of Department, faculty members of Mechanical Engineering and fellow lab mates and my close friends for their support without which accomplishment of the present work cannot happen.

Above all, I am indebted to my parents and my brothers and sisters and the full family, whose value to me only grows with age. And finally, I acknowledge my wife Sara Hansda, who whole heartedly supported me in completing this herculean task.

Sudhir Chandra Murmu

ABSTRACT

Transport phenomena around bluff bodies have been a subject of considerable research interest. Heat transfer characteristics inside a channel in presence of bluff body and effect of turbulence level on transport process around a bluff bodies encompassing laminar and turbulent regime covering a Reynolds number range of 10-2,00,000 along with turbulence intensities varying from 5% to 40% are studied in this work. Here bluff bodies of five different shapes are considered, namely-a) Circular cylinder, b) Square cylinder, c) Equilateral triangular prism, d) Diamond and e) Trapezium shape bluff bodies.

The effect of turbulence intensity on the transport phenomena over two dimensional bluff bodies is investigated. The governing equations of continuity, momentum, and energy equations are solved along with transition SST Model for closure of turbulence. The simulation results are validated with experimental correlations which show good agreements. This work demonstrates that transition SST Model can effortlessly bridge all flow regimes for predicting the heat transfer. The study quantifies the effect of inlet turbulence intensity on enhancing heat transfer from the bluff bodies. The drag and pressure coefficients are found to be unaffected by inlet turbulent intensity.

A operative study of different bluff bodies are incorporated in this work. The bluff bodies are taken triangular prism, diamond and trapezoidal shape bodies with the identical hydraulic diameter D, which is further the non-spatial length scale. The flowing medium i.e., air is consider to have constant Prandtl number (0.71). This work explains that transition SST Model can effortlessly link all flow regimes for predicting the heat transfer. The study quantifies the effect of inlet turbulence intensity on improve heat transfer from different bluff bodies.

As part of the present work, an attempt has been made to study augmentation of heat transfer on a channel wall in presence of bluff body of different shapes. Heat transfer enhancement in a channel in presence of bluff bodies of different shape has been numerically investigated in the turbulent flow regime with Reynolds number ranging from 100-2,00,000.The hydraulic diameter of the bluff body (Three different shapes namely Triangular Prism (TP), Diamond and Trapezoidal are consider in this work) is taken as characteristics length. The inlet turbulent intensities is varied from 5% to 40%.The aspect ratio between channel to the bluff body is fixed at 4. The velocities and pressures were predicted using semi

implicit pressure linked equations (SIMPLE) scheme.The results show that in presence of triangular prism, heat transfer in a channel is augmented by around 10%. The presence of TP enhances heat transfer all through the downstream region. Analysis shows that the amount of enhancement increases with inlet turbulent intensity. The study quantifies the effect of inlet turbulence intensity on enhancing heat transfer from all other bluff bodies. Augmentation is associated with higher values of skin friction coefficient on channel wall.The Augmentation is also expressed as a percentage increased of heat transfer from a similar system without the diamond bluff body. For trapezoidal bluff body different configurations as: (a) large edge of trapezium facing the flow (b) small edge facing flow and (c) trapezium is symmetrically placed is considered. Results show that the small edge facing upstream show better heat transfer performance. The thermo hydraulic efficiency for three bluff bodies are also computed.

Research Publications from this Thesis

▪ *Journals*

1. Sudhir Chandra Murmu., *Himadri Chattopadhyay, Transport Phenomena around bluff body at varying inlet turbulent intensity, Heat transfer research, accepted.*

2. Sudhir Chandra Murmu, *Himadri Chattopadhyay., Numerical simulation of flow and heat transfer over bluff body at varying inlet turbulent intensity, Heat Transfer Research - Under Review.*

3. Sudhir Chandra Murmu, *Himadri Chattopadhyay, Effect of different bluff bodies on heat transfer enhancement in a channel flow- Progress in Computational fluid dynamics - Under Review.*

4. Sudhir Chandra Murmu, *Himadri Chattopadhyay, Augmentation of heat transfer in a channel using a triangular prism with varying inlet turbulent intensity, Journal of enhanced heat transfer- Under Review.*

▪ **Conferences**

1. S. C. Murmu, *H. Chattopadhyay, A. Sarkar, "Numerical simulation of flow and heat transfer around circular cylinder" 1st International ISHMT-ASTFE Heat and Mass Transfer Conference, 17-20 December, 2015, ISRO, Kerala.*

2. S. C. Murmu, *H. Chattopadhyay, A. Sarkar,* **"***Numerical simulation of flow and heat transfer around triangular prism***",** *6th International & 43rd National Conference on Fluid Mechanics and Fluid Power, 15-17th December,2016,MNNIT Allahabad, Uttar Pradesh.*

3. S.Saha, S.C. Murmu, *A. Chatterjee, H. Chattopadhyay, "Transport phenomenon around a diamond shape bluff body",6thInternational and 43rd National Conference on*

Fluid Mechanics and Fluid Power, Dec 15-17,2016,ISBN 978-93- 5267-408-4MNNIT Allahabad, India.

4. S.Saha, A.Chatterjee, S.Murmu, *H. Chattopadhyay, " Augmentation of heat transfer a channel in presence of a diamond shape bluff body "National Conference on Advances in Thermal Engineering, Dec 23-24, Jadavpur university, Kolkata, India.*

5. S. C. Murmu, *H. Chattopadhyay,* **"***Transport phenomena over bluff bodies at varying inlet turbulent intensity***",** *Computational Science Symposium, 16-18 March 2017, IISC, Bangalore.*

6. S. C. Murmu, *H. Chattopadhyay, Augmentation of heat transfer in a channel using a triangular prism with varying inlet turbulent intensity***",** *December 27-30, 2017, BITS Pilani, Hyderabad,.*

7. S. C. Murmu, *H. Chattopadhyay, "Numerical simulation of flow and heat transfer around trapezoidal shape bluff body", 1st International Conference on Mechanical Engineering, 4th - 6th January, 2018, Jadavpur University, Kolkata.*

8. S.C. Murmu, *H. Chattopadhyay, "Numerical simulation of flow and heat transfer around trapezoidal shape bluff body, 5th International Conference on Computational Methods for Thermal Problems***,** *9th – 11th July, 2018, IISC Bangalore, India*

TABLE OF CONTENTS

List of figures

List of Tables   *Page no.*

Nomenclatures

Abbreviations

RANS   Reynolds Averaged Navier-Stokes

SST   Shear Stress Transport

Symbols

a   transitional model constant

A   transitional model constant

B   Slot jet width, m

C_d drag coefficient

C_f Skin friction coefficient

C_p Pressure coefficient

D   Diameter of the bluff body, m

E   model destruction terms

F_1, F_2 blending functions in SST model

f   Friction factor

H   Height of the computational domain, m

h   heat transfer coefficient w/m^2-k

k   thermal conductivity

L   Length of computational domain, m

Nu   Nusselt number based on diameter

$\overline{Nu}$ Average Nusselt number

p   pressure, Pa

P   model production term

Pr   Prandtl number

Re   Reynolds number based on bluff body diameter

S   absolute value of the shear strain rate, s^{-1}

TI   turbulence intensity

T_s bluff wall temperature, K

T_∞ free stream temperature, K

U_∞ free stream velocity, m/s

x_i tensor coordinate direction

x, y, z Cartesian coordinates

Greek symbols

α thermal diffusivity, m^2/s

β_1, β_2 SST model constants

μ dynamic viscosity. kg/m-s

κ turbulent kinetic energy, m^2/s^2

ν kinematic viscosity, m^2/s

σ Prandtl-like diffusivities

γ intermittency

η thermo-hydraulic performance parameter

ω specific rate of turbulence dissipation, s^{-1}

Π intermittency adjunct function

ρ density, kg/m^3

Θ dimensionless temperature

Θ azimuthal angle, degree

τ wall shear stress, N/m^2

Subscripts

avg   average

eff   effective property

i, j   tensor notations

turb   turbulent

x, y, z   Cartesian coordinates

Chapter

1

Introduction

1. 1. Background

Flow around a bluff body in ducts and channels have been investigated intensively by many researchers both experimentally and numerically. Over the decades meticulous research efforts have been carried out to a broader understanding of the fluid flow and heat transfer past bluff bodies of various cross section geometries. Most of the effort is dedicated in analyzing the complex flow physics and thermo-fluid transport phenomenon for circular, square and rectangular shaped bodies. Fluid flows are classified as external flow and internal flow, depending on whether the fluid is flowing over the surface or in the conduit. External flow generally shows a very different characteristic with respect to internal flow. A bluff body (i.e. external flow) is one in which the length in the flow direction is close or equal to the length perpendicular to the flow direction.Otherwise a body is referred to as bluff and a significant pressure drag is associated with it. In general, the value of Reynolds number is large for heating, cooling systems for nuclear power plant. However, in lines, offshore structures, buildings, chimneys, stints, grids, screens, and cables, in both air- and water-flow where recently lot of emphasis is being given, Re can be relatively low. In specific terms, the flow around circular cylinders shows various important physical phenomena, such as separation of flow, vortex shedding and also the shifting of flow from laminar to turbulence. It is the shape of the bodies which determined the form of flow and the energy transformation and flow characteristics.

1.1.1 Drag force

A body moving through a fluid experiences a drag force, which is usually divided into two components :(a) frictional drag, and (b) pressure drag. Frictional drag comes from friction between the fluid- and the surface over which it is flowing.This friction is associated with the development of the boundary layers, and it scales with Reynolds number.Pressure drag comes from the eddying motions that are set up in the fluid by passage of the body.This drag is associated with the formation of wake, which can be readily seen behind a passing boat, and it is usually less sensitive to Reynolds number than the frictional drag. Formally, both types of drag are due to viscosity (if the body was moving through an inviscid fluid there would be no drag at all), but the distinction is useful because the two types of drag are due to different flow phenomena. Frictional drag is important for attached flows (that is, there

is no separation), and it related to the surface area exposed to the flow. Pressure drag is important for separated flows, and it related to cross sectional area of the body.

1.1.2 Bluff bodies and streamlined bodies

When the drag is dominated by viscous drag, then it is called streamlined, and when it is dominated by pressure drag, then the body is called bluff body. Whether the flow is viscous-drag ruled or pressure drag ruled depends completely on the format of the body. A streamlined body views alike a fish, or an airfoil at small angles of attack, whereas a bluff body looks like a brick, a cylinder, or an airfoil at extensive angles of attack. For streamlined bodies, frictional drag is the controlling origin of wind resistance. In case of bluff body, the ruling source of drag is pressure drag. For a given frontal region and velocity, a streamlined body will continually have an inferior resistance compare to a bluff body. Pressure drag and frictional drag which are based on the pressure variation between the upstream and downstream facial of the substance. Fig 1.1 illustrates a bluff body and streamlined body.
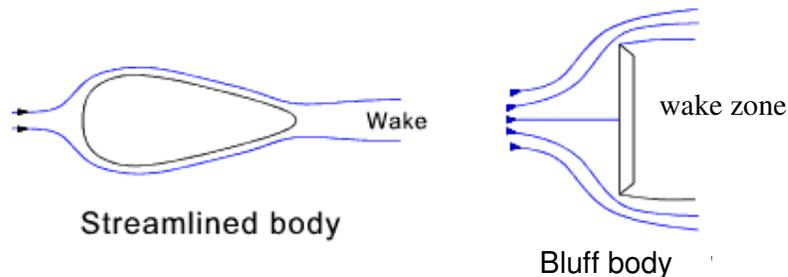
Figure 1.1: Streamline and bluff body

Especially bluff body can be characterized as a body that, as a result of its shape, has divided flow over a significant section of its surface. An valuable features of the bluff body flow is that there is a real powerful communication between the viscous and in viscous domains. Break-up may happen either from sharp corner or from a maintain surface. Forecast of break-up point from a constant surface is specifically tough the formate of the adjacent wake zone. Further the separation location may change in feedback to pressure gradients appoint by unsteady flow features in wake. Normally bluff bodies induce flow disengagement

at the location where the velocity at the border of the edge layer is higher than the free stream velocity. This leads to a huge ratio of shedding of circulation which in shift leads to a big drag also due to the production and shedding of comprehensible whirlpool, wide unsteady forces may grow, especially in a direction across to the flow direction. Spheres, cylinders, triangular prism etc. are treated bluff bodies because at wide Reynolds number the drag is govern by the pressure fall in the wake. Circular cross division members are a universal shape used in offshore design and therefore it is fortunate that the circular cylinder is further the most thoughtful bluff body structure. Currently, the unstable viscous flow past bluff bodies and the effect vortex shedding have been the centre of attention of plentiful numerical investigation and experimental analyses. The variation of drag coefficient with Reynolds number is shown in figure 1.2 and the corresponding flow structures are shown figure 1.3. We noticed that as the Reynolds number rise the difference of drag coefficient (based on cross sectional area) drop, and over a wide area in Reynolds number it is approximately consistent.
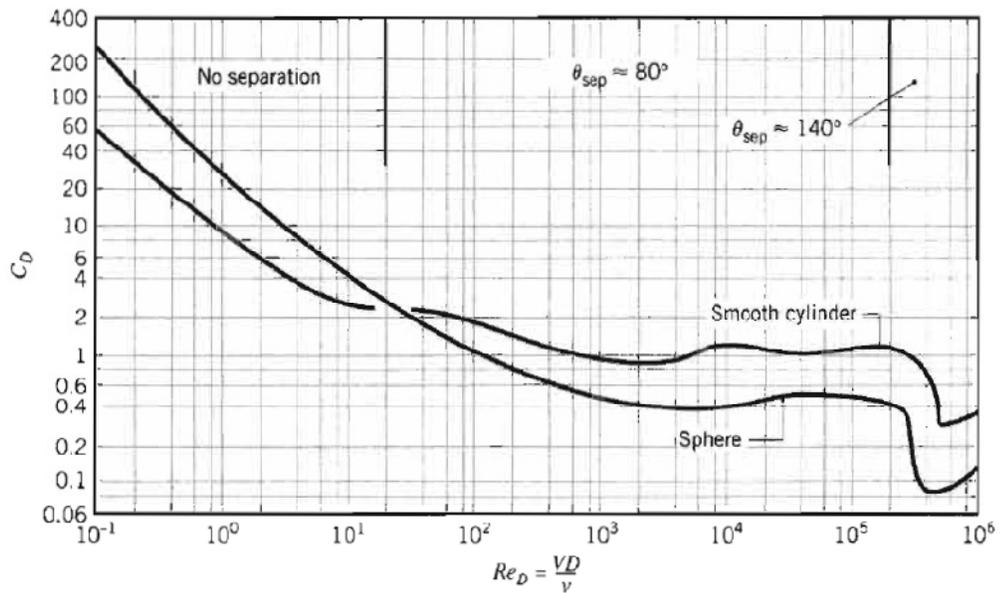
Figure 1.2: Drag coefficient as a function of Reynolds number for smooth circular cylinders and smooth spheres (Incorpera, 2006)
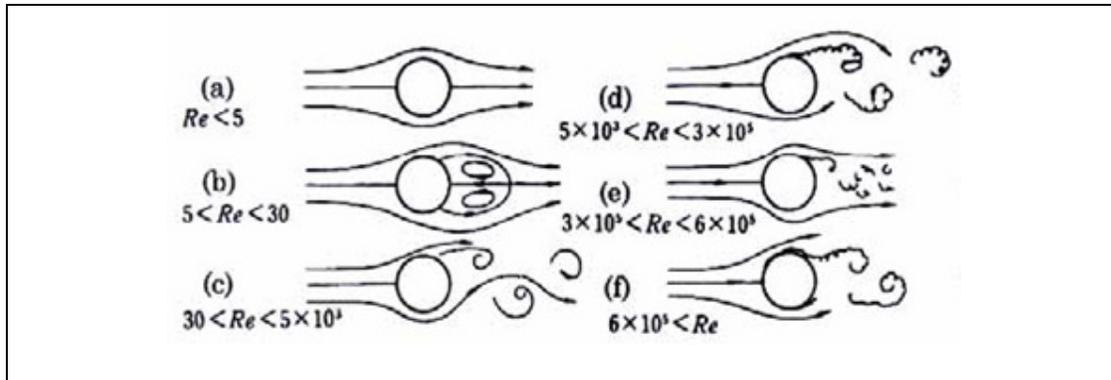
Figure 1.3: Flow arrangement at various Reynolds numbers over circular cylinder (Incorpera, 2006)

1.1.3 Aero dynamic body and bluff body

Aero dynamic bodies are those characterized by thin boundary layers completely attached over their whole surface, which leave behind them generally thin and steady wakes containing vorticity.The aerodynamic forces acting on these bodies may be evaluated through the potential flow-boundary layer procedure. Conversely, bluff bodies are characterized by a more or less precocious separation of the boundary layer from their surface, and by wakes having significant lateral dimensions and normally unsteady velocity fields.

1.1.4 Application of bluff bodies

On the engineering application, there are a number of devices in mechanical, civil and other engineering, where circular and cylindrical structures are used. Cylinder-like structures are found in both alone and in a group, in the designs for heat exchangers for locomotive, cooling system for nuclear power plants, offshore structures, buildingchimneys, power lines, grids, screens and cables, in both air and water as the flowing medium. Tube banks of different cross sections are also often encountered.

1.1.5. External flows

External flows are characterized as the flows deeply involved in an unbounded fluid. A body immersed in a fluid experiences a resultant force due to the communication between

the body and fluid ambience. In few cases, the body shift in static fluid medium (like movement of an airplane) while in few occasion, the fluid passes around a fixed article (such as motion of wind over a replica in a air channel). In several case, one can fix the coordinate system in the body and treat the condition as the flow past a static body at a uniform velocity U_∞, well-known as upstream/free-stream velocity. Though, there are significant cases where the flow is not uniform. Even, the flow in the proximity of the object can be irregular in the case of a steady, consistent upstream flow. For cases, when air blast over a towering building, various velocities are sense at highest and lowest portion of the building. But, the unstableness and non-consistency are of lesser significant somewhat the flow nature on the surface of the body is grater valuable. The pattern of the body (like cutting-tip, blunt or streamline) influence design of an external flow. For study view point, the bodies are normally classified as, two-dimensional objects (infinitely lengthy and fixed cross-section), axi-symmetric bodies and three-dimensional objects. In such a flow border coatings grow openly without restraint set by adjoining surfaces. Appropriately there will consistently exist a area of the flow outside the boundary layer in which temperature, velocity, and/or consolidation slop are trivial. For examples fluid movement around a flat plate (this may be inclined or parallel to the free flow velocity) and flow around arc facial e.g. a cylinder, airfoil or turbine blade, sphere.

There are a number of attracting phenomena that happen in an external viscous flow past an item. For a given structure of the object, the features of the stream depend much actively on deliberate parameters like size, orientation, speed and fluid properties.

1.1.6. Flow Separation: The appearance of the fluid viscosity sluggish down the fluid fragment much adjacent to the solid facial and create a lean lazy-moving fluid coating called a boundary layer. The stream velocity is zero at the surface to gratify the no-slip boundary condition. Indoors the border layer, flow momentum is quite low since it knowledge a substantial viscous stream resistance. Thus, the boundary layer stream is sensible to the outer pressure slop (while the shape of a pressure force acting upon fluid fragments If the pressure reduce in the direction of the stream, the pressure slope is spoken to be favourable. In this circumstance the pressure force can help the fluid motion and there is no stream delay. However, if the pressure is rising in the direction of the flow, an conflicting pressure slop

situation as so it is called exist More to the existence of a substantial viscous force, the fluid fragments now have to shift against the rising pressure force. That's why, the fluid fragments could be interrupted or turned around, causing the bordering fragments to shift abroad from the surface. This phenomenon is called the boundary layer separation.

1.1.7. Bluff body wake: Consider a fluid particle flows within the boundary layer over the circular cylinder. From the pressure allocation calculated in a previous experiment, at the stagnation point, the pressure is a highest and uniformly diminishing along the frontal part of the cylinder. The flow hold connects in this favourable pressure zone as expected. Still, the pressure beginning to raise in the back half of the cylinder and the fragment presently knowledge an opposing pressure slopes. Therefore, the flow split from the surface and developing a highly turbulent zone following the cylinder which called the wake. The pressure interior the wake zone debris low as the flow split and a profiting pressure force (pressure drag) is formed. Many researchers investigate the wake characteristics behind the bluff body. Some of works are describe below.

"Dutta et al.(2004)" studied the impact of coordination on the wake of a square cylinder at laminar region. The experimental research of flow past a square cross section of cylinder at Reynolds number range of Re=97-187 is stated. Cylinder coordination of 0^0-60^0 with regard to the mean flow has been treated. Two part hotwire anemometry has been take-up for calculations of velocity. The cylinder's wake has been anticipated with a pulsed laser coat to know the flow formation. Calculations have been performed at the near wake, mid wake and far wake of the cylinder. The impact of coordination and Reynolds number on drag coefficient, Strouhal number, time average and rms velocity allocation, collapse of velocity oscillations and power spectra are of concern. The drag coefficient and Strouhal number are comparing to the angle of cylinder. A variation in the cylinder adjustment experienced to an initial arrival of quasi-periodicity and therefore, three dimensionality, unpaid to the irregular kind of the wake. The structure of the mean velocity portrait, oscillations and the rate of collapse display a active reliance on the cylinder adjustment in the adjacent wake, however dependency decrease in the far wake. In a group of angle considered, the wake of a cylinder whose orientation is 22.5^0 with regard to the incoming flow is unusually energetic and display powerful three-dimensionality.

"Samani and Bergstrom (2015)" had performed the influence of a solid wall on the wake design of an infinite cylinder of square cross-section when it is placed in proximity to the wall. Three different values of the gap ratio were considered, namely g=D 0,0.5 and 1, also to the reference case of a cylinder in a free stream with no wall. The Reynolds number which based on the cylinder width and free stream velocity was Re =500. A coarse-grid Large Eddy Simulation was employ to anticipate the resolved-scale velocity and pressure fields.

An experimental analysis into logical design in the wake behind a circular disk was performed by Lee et al.(1992).The spectral study and a conditional phase averaging method are used. In order to help clearup the form of the wake design, the velocity fluctuations were split into two manners: positive (+ve) mode and negative (−ve) mode, and the conditional averaging method was used to each mode individually. The wake exhibits a predominant vortex-shedding frequency and the corresponding Strouhal number is about $0 \cdot 138$. The phase angle between velocity fluctuations in the wake at the shedding frequency, measured by two hot-wires, changes very little for circumferential angular separations Ψ, below $\pm 70°$ and changes very quickly through $180°$ near $\Psi = 90°$. On average, vortices are shed alternately from diametrically opposite sides of the disk. Negative mode velocity fluctuations are dominant at small angular separations between the reference probe and the measurement probe. The probability of occurrence of the −ve mode decreases steadily and that of the +ve mode starts to increase with increasing angular separation between the probes and becomes dominant at $\Psi = 180°$. At $\Psi = 90°$, the two modes, which have velocity fluctuations that are $180°$ out of phase with each other, occur equally, and hence the velocity fluctuations cancel each other when they are averaged together in a conventional phase-averaging way.

Forbes et al. (2017) studied a progression of the computational methods in reproducing experimental data for a generic sports utility vehicle (SUV) geometry and an assessment on the influence of fixed and rotating wheels for this geometry. Initially, comparisons are made in the wake structure and base pressures between several CFD codes and experimental data. It was shown that steady-state RANS methods are unsuitable for this geometry due to large scale unsteadiness in the wake caused by separation at the sharp trailing edge and rear wheel wake interactions. unsteady RANS (URANS) offered no improvements in wake prediction despite a significant increase in computational cost. The detached-eddy simulation (DES) and Lattice–Boltzmann methods showed the best agreement with the experimental results in both

the wake structure and base pressure, with LBM running in approximately a fifth of the time for DES. The study then continues by analysing the influence of rotating wheels and a moving ground plane over a fixed wheel and ground plane arrangement. The introduction of wheel rotation and a moving ground was shown to increase the base pressure and reduce the drag acting on the vehicle when compared to the fixed case. However, when compared to the experimental standoff case, variations in drag and lift coefficients were minimal but misleading, as significant variations to the surface pressures were present.

1.1.8. Vortex Shedding: The boundary layer split from the surface forms a free shear layer and is highly changeable. This shear layer will ultimately revolve into a various vortex and separate from the surface (a phenomenon called vortex shedding).Additional kind of flow inconsistency appear while the shear layer whirlpool shed from both the highest and lowest surfaces connect along one another. They shed alternatively from the cylinder and produce a continues vortex design (known as Karaman vortex street) in the wake. The whirlpool shedding take place at a various frequency and is a function of the Reynolds number. The dimensionless frequency of the whirlpool shedding, the shedding Strouhal number, St = f D/V, is almost identical to 0.21 when the Reynolds number is greater than 1,000.

1.1.9. Vortex-Induced Vibrations: When whirlpool shed from the cylinder, unbalanced pressure allocations establish between the top and bottom surfaces of the cylinder, producing an fluctuating aerodynamic loading (lift) on the cylinder. This unsteady force can induce important vibrations on a design, particularly if the "resonance "situation is connect. The best popular example is the breakdown of bridge in 1940 under the action of wind-induced vibrations. It is trust that natural whirlpool shedding frequency trailing the bridge matches one of the sonorous method of the bridge and eventually lead to a disaster vibration that damage the bridge.

Hydraulic diameter

For flow through non circular pipes the Reynolds numbers is based on the hydraulic diameter. It is expressed as given below.

$$D_h = \frac{4A}{P}$$

A cross sectional area and P   wetted perimeter of the cross section

Hydraulic diameter is mainly employ for computation for turbulent flow. Hydraulic diameter is further utilizing in calculation of heat transfer in internal flow problems. In figure 1.5 some geometry and their formulas are given below.

Type of Geometry	Hydraulic diameter
	Square $$D_h = \frac{4B^2}{4B} = B$$
	Trapezium $$D_h = \frac{(A+B) \times H}{2(A+B+C+D)}$$
	Circular $$D_h = \frac{4(\pi D^2)}{4\pi D} = D$$
	Equilateral triangle prism, $$D_h = \frac{A}{\sqrt{3}}$$
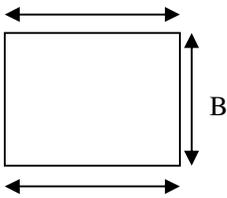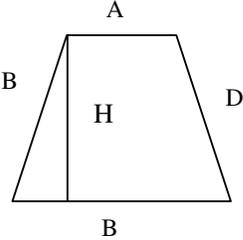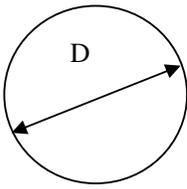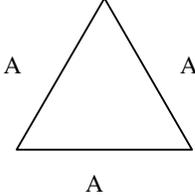
Figure 1.4: Formula of hydraulic diameter for different geometry

1.2 Thesis Organization

The present thesis comprises of seven chapters.

- In the chapter **1**, a brief introduction has been given on about difference between bluff body and stream line body, its applications, flow field and its classifications. Also given details about hydraulic diameter of circular, square and rectangular ducts and their formulas.

- *Chapters 2 include* an extensive Literature review of the entire thesis which has assisted the research methodically, technically and mathematically. Chapter 2 is divided into four parts so as to authorize to envision various aspects of the current investigation. This consists of literature survey of numerical simulation around bluff body, vortex flow around bluff body and augmentation on channel wall. Based on the literature survey objectives were itemized in the final part of chapter two.

- *Chapter 3* deals with the mathematical modeling of computational method which is utilize for current research task. Parameters apply to evaluate performance like surface averaged Nusselt number) and envision flow design (contour) are also explain.

- *Chapter 4* deals with analysis of transport phenomena around different shapes bluff body. This analysis further cover the effect turbulence intensity on heat transfer covering a large range of Reynolds number containing laminar, transition and turbulent regimes. Also, TI effect on drag value and pressure coefficient is studied here.

- The next *Chapter 5* that deals with augmentation on channel wall in presence of a bluff body. The bluff bodies are again considered of different shapes.

- *Chapter 6* briefly describes the conclusions drawn from the analysis done in this study. Future prospects of studies are also pointed out in this chapter.

Chapter

2

Literature Review

CHAPTER 2

LITERATURE REVIEW

The subject of heat transportation with numerical simulation and vortex flow around bluff body has been introduced in Chapter 2. In this section a detailed state-of-art is presented.

2. STATE OF ART

2.1 Literature review on transport phenomena around bluff body

2.1.1 Studies on numerical simulation around bluff body

Distribution of local pressure and skin friction around a smooth circular cylinder in cross-flow has been studied by "**Achenbach (1968)"** with large range of Reynolds number up to $Re = 5 \times 10^6$. The higher Reynolds number were achieve in test channel which could be pressurized up to 40 bar .New experiments were carry out for measure the local pressure and skin friction distribution around the cylinder. The total drag, pressure drag, and friction drag were computed. By means of skin friction allocation the location of the separation point, transition point or separation bubble can be bounded. This results grant to define three category of flow: sub-critical flow, where the boundary layer separates laminarly, critical flow, where a separation bubble, followed by a turbulent reattachment, happen and super critical flow, in which an instantaneous transition from laminar to turbulent boundary layer is found at a critical gap from the stagnation point.

"**Brian (1983)"** performed an **experimental study** of transport procedure in the near wake of a circular cross section of a Reynolds number, Re=1, 40,000. The wake of flow is measured using X-array hotwire probes which are mounted on a pair of rotating arm. These hot were approach raise the relative velocity component on the axis of probe. For generating an intermittency signal an analogy circuit is used and fast surface pressure sensor was used to produced a phase signal integrate by the vortex shedding technique. The protections of turbulence signify that turbulent energy is formed at the largest scale of the flow and soon after relocated by a cascade technique to lower scale. The evidence of this experiment is that

sizeable fractions of the turbulent energy is formed mainly at intermediate or even short scales near saddle in the flow decoration and is later transported to and gather at centre whose larger scale may be carefully visible in uniform spectra or interrelation.

The computations of incompressible high Reynolds number flow over a circular cylinder with surface roughness are studied by **"Kawamura et al. (1985)".** These are analyzed by direct integration of the Navier Stokes equations with finite difference method. A statement coordinate setup is used so that a enough number of grids point are distributed in the wake and boundary layer region. The computations are done at Reynolds number, Re=1,200 and the corresponding results are compared with experimental results which show reasonable good agreement. The computations series were find out on the flow over the circular cylinder with surface roughness. In this computation, the height of roughness is 0.5% of the diameter. No turbulence model is used for the Reynolds number ranges from 1,000-1,00,000. Sudden decline of drag coefficient is noticed close at Re=20,000. This signifies that the critical Reynolds number is captured in the current computation.

"Nakamur and Ozono (19987)" made a study on the work of the effect of free flow disturbance on the mean pressure allocation ahead the break-up droplet develop on a flat plate with rectangular best-side calculus. It is examined experimentally in a wind tunnel with disturbance generating grids. Attention is located on discovery the impact of turbulence scale. The ratio between turbulence scale and plate thickness was around 0.5 to 24 for two values of TI of around 7 and 11

It is observed that the major impact of free-flow disturbance is to decrease the break-up droplet. It is gradually decrease with increasing turbulence intensity. The average pressure allocation along the decrease break-up droplet is unresponsive to altering turbulence scale up to a scale ratio of about 2**.** Furthermore increase in the scale ratio it asymptotes towards the smooth-flow allocation. There is no hint of communication between disturbance and circular current shedding (the impinging-shear-layer fluctuation) in the average pressure allocation.

"Okajima et al.(1990)" perform a numerical approach of flows around cylinders with rectangular cross-section of different width -to height ratios of 0.4 to 8 have been calculate in the Reynolds number range from 100 to 1.2×10^3. It is observed that a few impressive phenomena by which a flow over the cylinder with a B/H ratio of 2 is completely detached from the superior edge at the Reynolds number at about Re=800, even though for the B/H ratio of 2.8, a fully detached flow changes to an substitute reattachment flow with failing of time at the Re=1.2×10^3, and two ingredient with various Strouhal frequencies arrive in a

flow field around the cylinder with the B/H ratio of 6 at the Re=800. Specifically , the flow arrangement critically modified when the B/H ratio is 2.8 and 6 about Re=500 to1.2×10^3. It is explain through the numerical simulation that the part with a large Strouhal frequency is induced through the vortices detached from the following edges and that the small Strouhal element is due to the fluctuations of flow up the edge surfaces guide by the change of detach bubble.

"Norberg (1993)" has concern an experimental investigation of the flow over rectangular cylinders at angles of attack 0^0-90^0. Pressure forces and moments for cylinders with side ratios *B/A* = 1, 1.62, 2.5 and 3 (shortest side A = 20 ram) were approximated from analysis of static pressure allotment at midspan. Strouhal numbers and wake frequencies were determined from hot wire measurements in the close to wake regions (A = 4 and 20 mm). The free stream turbulence intensity was less than 0.06%, blockages less than 5% and aspect ratios *L/A* greater than 50 are used in this work. Here, Reynolds number ranging from Re=400-30,000 is used (Pressure calculation about Re=30,000).

Drag coefficient and Strouhal number are plotted against H/D in figure 2.1. A normal agreement with past analysis was found (**Nakaguchi, 1968, Bearman, 1972 Nakamura1975, Knisely, 1990, Courchesne, 1979, Igarashi1, 1987).** The most important characteristics is that in the range H/D=0-1, drag value undergoes convincing turnover while Strouhal number changes slightly though the reverse is true in the range H/D=2-3. The drag value reaches maximum at nearby H/D=0.6
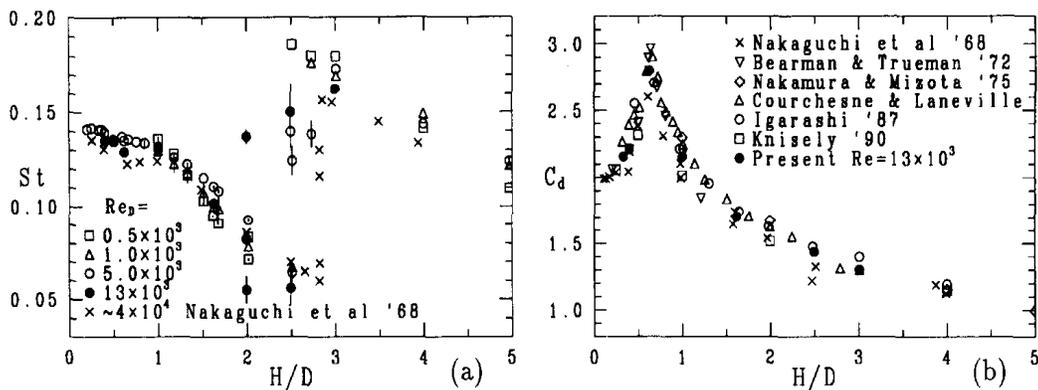
Figure 2.1. Strouhal number (a) and drag coefficient (b) vs *H/D* at low free stream turbulence, Norberg (1993)

"Kondjoyan and Daudin (1995)" have shown the effect of free stream turbulence intensity on heat and mass transfer at a surface of circular cylinder and an elliptical cylinder. Turbulence intensity ranging from 1.5 to 40% and of Reynolds number ranging from 3,000 to 40,000 on transfer coefficients has been measured for a circular cylinder in cross-flow. The effect of turbulence intensity is important as the influence of velocity and it seemed to be independent of the pressure gradient and of the degree of turbulence isotropy. It also seen that the heat transfers are much less affected by the cylinder axis ratio than by the air flow properties. Their work also confirms that the local transfer coefficient is much higher at the stagnation point of a circular cylinder than elsewhere at the surface.

An experimental analysis is performed to study the effect of free stream turbulence on surface pressures on a flat plate with rectangular cross section by **"Li et al. (1995)"** applying turbulence producing grids. The measured mean and crest pressure coefficients, standard deviation, pressure coefficients are reported and explained.

"Mittal and Balachandar (1995)" has presented a comprehensive review on the impact of three dimensionality on the lift and drag of nominally two dimensional cylinders. It has been admitted that two dimensional numerical computations of flow around two dimensional bluff bodies at Reynolds number for which the stream is basically three dimensional, starts to defect guess of the drag and lift co-efficient.

In appropriate, for flow past a natural flat plate **(International Symposium on Nckzsteady Fluid Dynamics, edited by J. A. Miller and D. P. Telionis, 1990, pp. 455-464) and circular cylinders [J. Wmd Eng. Indus. Aerodyn. 35,275 (1990)],** it has been notable that the C_D value measured from two dimensional computation is undoubtedly greater than what is obtained from experiments. Moreover, it has been found that three dimensional simulation of flows influence to exact guess of drag **[J. Wind Eng. Indus. Aerodyn. 35, 275 (1990**)]. The fundamental reasons for this difference is that the surface pressure allocation achieve from two dimensional computations does not match up with that get from experiments. In this study, the two and three dimensional results of flow past circular and elliptical cylinder have been uniformly distinguished in an struggle to identify the accurate reason for the defective prediction of the lift and drag by two dimensional simulations. This study further contributes a detailed way of how the oscillations affect the mean pressure distribution and the aerodynamic forces on the body.

A CFD study on unsteady flow field past a square cross section of two dimensional cylinders is inspected by **"Murakami et al. (1995)".** The precision of the conclude results by numerical simulation is checked from different viewpoints. In the early part of the work, the

comparison of the outcome of large eddy simulation (LES) for 2D and 3D simulations are represent. The LES results obtained from 3D simulation admit well with the experimental results, but the outcomes obtained from 2D computation are different from those located on 3D simulation including from those disposed from experiments. In the second section of the paper interest thorough verification of 3D LES simulations for the study of periodic and hypothetical oscillations, for which specific experimental results are available. The LES computation results are compared with those obtained from Reynolds-averaged Navier-Stokes equations model (RANS) including those from experiments. Lastly 3D LES simulation results of unsteady pressure field and wind force performing on the fluctuating square cylinder are conferred.

Convective heat transfer and pressure loss aspect in rectangular tunnel with staggered bunch of drop-structure pin fins in mixed flow of air was experimentally investigated by "**Chen et al. (1997)".** The effects of plans of pin fins on heat transfer and opposition are explained and the row-by-row differences of the average Nusselt numbers are given. By way of the heat/mass transfer similarity and the method of naphthalene sublimation, the film coefficients on pin fins and on edge wall of the tunnel have been gain accordingly. The complete average heat transfer coefficients of pin fin tunnels are determined and the opposition coefficients are further examined.

"Li et al. (1997)" have been carried out an experimental study to analyze the heat transfer and pressure drop nature in rectangular duct along staggered bunch of shortened elliptical pin fins in a air's cross flow. By apply the heat and mass transfer similarity and the naphthalene sublimation approach, the mean heat transfer coefficients on pin fins and on the base plate of the channel have been reported, commonly. The total mean heat transfer coefficients and resistance coefficients of pin fins are find out. The empirical results display that the heat deportation of a channel with elliptic pin fins is slightly bigger than that with circular pin fins while the struggle of old much lessened than that of the recent in the Reynolds number ranging from 1,00 to 10,000.

The analysis of the flow around rectangular cylinders was numerically predicted by **"Nathan Steggel (1998)".** The viscous flow around rectangles defined by after body length, *B,* and cross-stream dimension, *A,* is analyzed by a hybrid discrete vortex approach. For uniform flow conditions the effects of varying the side ratio, *B/A,* the angle of incidence, *a,* and the Reynolds number, *Re,* are all considered. Pulsating flow results are recorded for rectangular

cylinders with *B/A* values of 0.62, 1.0, 2.0 and 3.0, a *B/A=1.0* cylinder inclined at 45° and a circular cylinder.

At a settled Reynolds number, Re=200, the alternation of drag coefficient with side ratio display C_D increasing with decreasing B/A ratio. This variation with the accepted result at higher Reynolds number, $10^4 \leq Re \leq 10^5$, for which a maximum drag happen close to B/A=0.6. A peak is seen in both the Strouhal number and lift coefficient near to B/A=0.30. This is made clear by the after body elimination of the shear layer interaction. In the case of the square cylinder, results are granted for the alternation of drag coefficient and Strouhal number with Reynolds number, $50 \leq Re \leq 5 \times 10^3$. Good agreement with experiment is shown although for Re~500 the calculated Strouhal number is dual valued. This study also contribute a detailed view of how the oscillitation.

The 'lock-in' natures under pulsating flow are shown to be extremely dependent on body geometry. All the cylinders are shown to display an asymmetric resonant mode within which the shedding frequency is controlled at half the forcing frequency and the mean forces increase. Several different shedding designs are predicted across this asymmetric synchronisation range. A 'quasi-symmetric' mode is also seen for few cylinders characterized by near wake symmetry and a substantial reduction in mean forces. A pseudo-phase lag is defined which relates a moment of the lift cycle to a moment of the forcing oscillation. This is shown to change across the synchronisation range of each cylinder considered and the change is found to be greater at lower forcing amplitude.

"Scholten and Murray (1998)" has studied unsteady heat transfer and velocity profile of a cylinder in cross flow for Low free-stream turbulence. A method has been developed for making simultaneous measurements of time-resolved velocity, using laser Doppler anemometry, and local heat flux, using a hot film sensor, at the surface of a cylinder in cross flow. The results that they found are the magnitude of fluctuations in heat transfer at the front of the cylinder is very small.

The simulation at low-Reynolds-number flow around a square cylinder at incidence which was numerically investigated by **"Sohankar et al. (1998)"**. The problem is 2D and angle of incident α = 0°-45° are used. The low Reynolds numbers are applying (45-200) so that the flow is purely laminar. A Von Kármán vortex sheet is observed behind the cylinders with a periodicity which good agreements with experiments**.** Strouhal number and drag, lift and moment coefficients are reported here.

"Fred et al. (1998)" studied the pressure field over a rectangular prism using a advanced turbulence creation technique with constant turbulence intensity. Applying jets blowing parallel to the vital flow and impediment, the method produce turbulent flow of variable scales. The effect of turbulence on the aero-elastic stability of long-span bridges was reported here. The necessary scales of the incident flow had meaningful impact on the flow form happen in changes in rms, mean and contradictory peak pressure allocation. Fluctuating scale have shown that scales have meaningful effects on the flow form. Up to critical value, growth of integral scale, with the related decreases in small scale content essential to keep up constant turbulent intensity, changed mean, rms and bad crest pressure distribution. The crest of this allocation moved closer to leading edge and the shapes of the distributions grow narrower on either side of the crest.

Unsteady turbulent adjacent wake of a rectangular cross section of cylinder in tunnel flow has been performed experimentally by using a laser Doppler velocimetry (LDV) which was analyze by **"Nakagawa et al. (1999)".** The time averaged and phase -averaged stats were calculated for the cylinder which having different width to height ratios, b/h. It is observed that the turbulent intensities on centre line of the channel have their maxima adjacent the back stagnation point of a recirculation domain. The profile of consistent vorticity and streamline create precisely the shed vortices from the cylinder noticed by the flow visualization. The natures of the flow field are explain and meaningful donation of the understandable form to the flow field is explain. Additionally the turbulent kinetic energy budget has been investigated.

Taylor, Ian J. (1999) Study of bluff body flow fields and aero elastic stability using a discrete vortex method. A two dimensional discrete vortex method has been developed to simulate the unsteady, incompressible flow field and aerodynamic loading on bluff bodies. The method has been validated successfully on a range of simple bluff geometries, both static and oscillating, and has also been validated on a wider range of problems including static and oscillating suspension bridge deck sections. The results have been compared with experimental data and demonstrate good qualitative and quantitative agreement, and also compare favourably with other computational methods. Most notably, the method has been used to study the aeroelastic stability of a recent bridge deck, with accurate predictions of the critical flutter velocity. A thorough literature review is presented, considering the nature of bluff body flows and the aeroelastic phenomena associated with the unsteady flow field. Analytical methods are considered for studying these phenomena and other computational

methods are reviewed. The basis of the method is the discretisation of the vorticity field into a sense of vortex particles, which are transported in the flow field that they collectively induce. In the method presented herein, the time evolution of the system of particles is calculated by solving the vorticity transport equation in two stages : employing the Biot-Savart law to calculate particle velocities and random walks to simulate flow diffusion. The Lagrangian approach to the calculation avoids the necessity for a calculation grid, and therefore removes some of the problems associated with more traditional grid based methods. These include numerical diffusion and difficulties in resolving small scale vortical structures. In contrast, vortex methods concentrate particles in areas of vorticity, and can provide high quality representations of these small scale structures. Dispensing with a calculation mesh also eases the task of modelling a more arbitrary range of geometries. In particular, vortex methods are well suited to the analysis of moving body problems. The vortex method presented herein was originally developed to study dynamic stall on pitching aerofoils. The necessary modifications to enable the method to be used as a tool to study bluff body flow fields are presented. These include improvements to the modelling around sharp comers and an empirical procedure to account for three dimensional effects in the wake. Also, a more efficient algorithm for the velocity calculation has been implemented, reducing the computational operation count from $O(N_2)$ to $O(N+MogN)$. The procedure uses a zonal decomposition algorithm, where the velocity influences of a group of vortex particles can be calculated using a series expansion. Results of the validation exercise are firstly presented for a range of simple bluff geometries to give confidence in the results before moving on to more complex geometries. These results include the effect of incidence on the aerodynamic loading for a stationary square cylinder, and also a study of the effect on aspect ratio for rectangular cylinders. This includes the limiting case of a flat plate. Vortex lock-in is studied on a square cylinder undergoing a forced transverse oscillation, for a range of frequencies and amplitudes. The results in each of these cases are in good agreement with experimental data. The flutter instability on a recent bridge design and also on the original Tacoma Narrows bridge section are considered. Predictions of the flutter derivatives and of the critical flutter velocity on each section indicate the capability of the method to analyse the stability of bridge sections. A study of flow control devices, which are used to increase structural stability has been made, demonstrating how the vortex method could potentially be used as part of a design process to investigate a range of possible designs. It is anticipated that future work on the vortex method will include a link to a structural solver to give a full aeroelastic model that can be used to analyse the flow around a wide range of geometries.

Another work, the turbulent wake behind a square cylinder has numerically investigated by "**Saha et al. (2001)**". The problem is considered as two dimensional and Reynolds number are taken 20,000 for this study. Two approaches are highlights between in terms of time averaged flow, Strouhal number and aerodynamic forces. Simulations are done through direct solution and calculation by using turbulence model. The time averaged drag value and rms fluctuation which is obtained by direct calculation is higher than the results coming out by turbulence model. The time averaged drag value was decreasing with increase the shear parameter up to assured value. After that it increases further increasing the shear parameter. Diversely lift coefficient increases with increases the shear parameter. It is observed that Strouhal number decreases with increase in shear parameter though rms value of lift and drag coefficient increases with shear parameter.

The unsteady incompressible flow simulation of drag crisis past a circular cylinder are find out by "**Singh et al.(2001)**". The 2-D Navier Stokes equations are solved with a finete element method with Steamline Upwind/Petrov-Galerkin(SUPG) and Pressure-Stabilizing/Petrov-Galarkin(PSPG) for large Reynolds number(Re=10^5-10^6) to compute drag crisis. The mean drag value are compared with experimental values. It is seen that flow at Re=10^6 seperates much later from thesurface of the cylinder compare to the Re=10^5. Also the wake is narrower in case of Re=10^6 compare to the Re=10^5. The time avereged flow field display a continuing bubble just downstream of the flow seperation pointfor the Re=10^5 where it is not observed at Re=10^6.

E(k) is compuated by suming $\bar{E}(k)$ over a slim shell over k. Fig 2.2 display the effect of number of bands of k over energy spectra. Invariable changeof E(k) is seen when the number of bands within the range of 200-300.But when the number of bands is crossed tha range of 2,000, the spectrum convert oscillatory.Both gradient are seen when number of band is around 300.
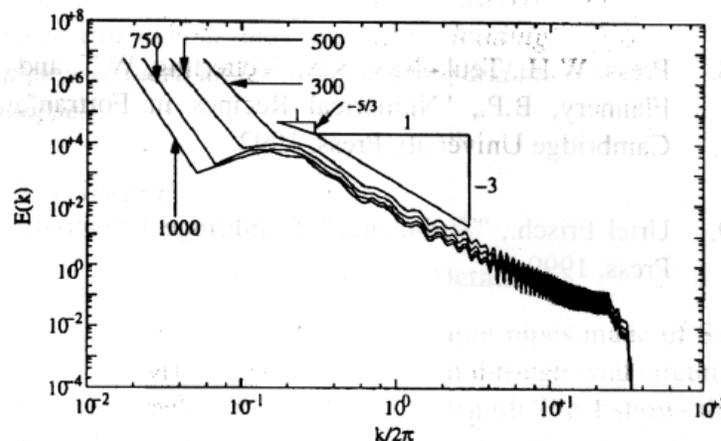
Figure 2.2: Effect of number of band of k over energy spectra at Re=10^6(**Singh et al. (2001).**

Figure 2.3 shown the comparison of energy spectra for two different Reynolds number (Re=10^5 and10^6). It is observed that flow display the characteristics of 2D turbulence. The energy casced is shown at k^{-3}. An revers energy cascade is observed which varies according to k$^{-5/3}$. Seeing that no turbulence model is being used and the resolution is not neat enough to solve the Kolmo-gorov scale.So this propose that the numerical dissipation received by the stabilization terms is not sufficient to drag out the energy at broad wavenumbers and thats why an proper turbulence model is required.
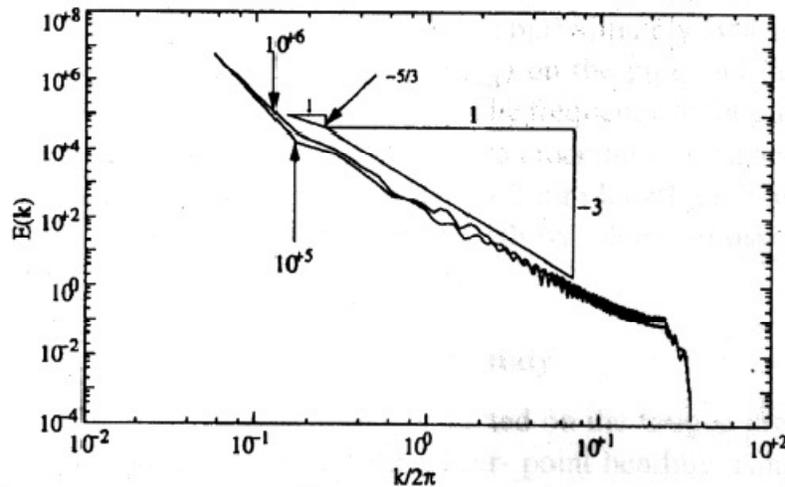
Figure 2.3: Comparison of energy spectra at different Reynolds number (**Singh et al.(2001).)**

Large eddy simulation are applied for the flow over a bluff body to display that it is attainable to get correct results in a rough grid simulation, was carried out by "**Krajnovic et al. (2002)**". The defective decision is satisfy for through the employment of a one equation subgrid range model. In this place two one equation sub grid models are apply for modelling the subgrid - scale stress tensor. The turbulent stress and time averaged velocities are calculated and distinguished with the experimental results which show good agreement with each other. Universal quantities like drag coefficient, lift coefficient and vortex shedding frequency are reported. The relocation of turbulent energy and reversal transmission of energy was forecast. Comprehensible structure and other flow appearance were further investigated. The results display excellent agreement with the experiments results.

"**Sohankar et al. (2002)**" observed that the large eddy simulation of flow and heat transfer around square cylinder along one side covering the upcoming flow at Reynolds number ,

$\mathrm{Re} = 2.2 \times 10^4$. Three distinct sub-grid scale model are namely the Smagorinsky, the standard dynamic, and a dynamic one-equation model, used in this study. An incompressible finite volume code which is established on a fractional step technique and a non-staggered cell arrangement was used. Strouhal number .mean and rms value of lift and drag are calculated. The results which are found out by dynamic one equation provide the superior agreement with experiments compare to the other two sub grid model.

The turbulent characteristics of the flow around a bluff body of circular cylinder in the near wake and in the near wall upstream domain with the Reynolds number of 1, 40,000 was analysed by "**Djeridi et al. (2003**)". The geology of average and turbulent velocity fields engaging a moderate blockage and aspect ratio is provide in order to use the modern outcome for direct comparisons with realizable 3D-Navier Stokes computation. Two experiment are used using PIV and LDV techniques respectively where both supply a purify grid of survey points and the flow structure is examine by these two techniques. The motion of the break-up domain, the growth and decay "**Nakaguchi et al. (1968)**" investigate an experimental study on aerodynamics drag of rectangular cylinders with Reynolds number upto Re=6× 10^4. It is show that the drag value change significantly accompanying the d/h ratio of rectangles and that the C_D value is maximum is about 2.6 for d/h of 2/3 compared with C_D value is 2.0 for the cases of flat plate and square cylinder. The Strouhal number of the vortex shedding are remain nearly constant for d/h upto 1.0 , again moderately decreases for larger values of d/h and then increases unexpectedly at d/h ratio of about 2.0, where the flow reconnect on the sideways surface of the cylinder.

"**Gupta et al. (2003)**" have been numerically investigating the two-dimensional steady flow of a power-law fluid past a square cylinder in a plane channel. The momentum and energy equation were solve with finite difference method. Rheological and kinematic ambiance are considered power law index n=0.5-1.4, Re=5-40 and Peclet number, Pe=5-400. The constant heat flux and isothermal condition has been investigated and fixed blockage ratio of $\beta = \dfrac{1}{8}$ are used for this study. Drag co-efficient and Nusselt number value (both individual and overall) is marginally upper unity in shear thining fluids and marginally below unity in case of dilatants fluids. Reynolds number effect on flow arrangement is approximately same which notice for Newtonian fluids is.

The laminar flow over a square cross section of circular cylinder seated inside a plane channel (β=1/8) was carried out by "**Breuer et al. (2002)**." Here, two distinct numerical approaches used, i.e. lattice-Boltzmann automata (LBA) and a finite volume method (FVM).

So to restrict the way to 2D computations, the biggest Reynolds number was elect of Re=300 based on the highest inflow velocity and chord length of the cylinder. The lattice a Boltzmann automaton was developing on the D2Q9 model and the single recreation time technique called the lattice-BGK method. The finite volume code which based on an incompressible Navier -Stokes solver for inconsistent non-rectangular and frame fitted grid. The two numerical techniques are second order skill in slot and time. Proper computing was perform on grids accompanying various resolutions. The outcome which are coming out from both methods, were check out and analyse in details. There magnificent agreement was create between LBA and FVM computations. The global quantity like drag coefficient, Strouhal number, and recirculation length were reported.

"Catalano et al.(2003)" illustrated, numerical simulation of the flow around a circular cylinder at high Reynolds number. Large Eddy simulation was used with wall modelling for high Reynolds number in the super critical regime. A understandable wall stress model is engaged to supply exact boundary conditions to the large eddy simulations. The results are correlate with those obtained from steady and unsteady RANS solutions with experimental result's data. The LES simulations results are appreciably more authentic than the RANS results. They catching the deferred boundary layer separation and shortened drag coefficients regular with experimental calculation after the drag crisis. The mean pressure allocation is anticipate fairly good at $Re_D=5\times 10^5$ and10^6. However, the Reynolds number confidence is not capture and therefore results becomes lesser authentic at increased Reynolds number.

Swirling flow past a cross section of square cylinder placed in a channel is computationally studied by **"Kim et al. (2003)"** with large eddy simulation (LES). The major objective of this investigation are to broadly check the experimental results of **Nakagawa et al. [Exp. Fluids 27(3) (1999) 284]** with Large Eddy Simulation and to analyze the appearance of flow past a square bluff body bounded in a channel in comparison with the regular one in an vast region. The simulation results obtained are in good agreement by experiment both collectively tentatively. Karman vortex shedding is observed. Mean drag and fluctuation lift force is increases significantly by the vortices. The rolled up vortex is connected together with the interrelated Karman vortex, they develop a counter rotating vortex couple. From table 1 which is given below, it can be understood that at the same Re, the drag force, lift fluctuation and Strouhal number is larger in case of square cylinder confined in a channel compare to square cylinder in an infinite domain.

Table 1

Comparison of characteristics of wakes for simulations with the two conditions, Re ¼ 3000

	Confined in a channel (20% blockage ratio)	Infinite domain
St	$0.124(f\frac{h}{U_b})$	$0.125(f\frac{h}{U_m})$
C_{Dmean}	2.76	1.97
C_{Drms}	0.49	0.43
C_{Lrms}	2.06	1.15
L_r/h	0.67	0.96

Here, L_r is the recirculation length behind the square cylinder, and C_{Drms} and C_{Lrms} represent RMS fluctuations of C_D and C_L, respectively. U_b is the mean stream wise velocity at the cylinder location. C_D and C_L are based on U_m.

The comparisons of St and C_D mentioned above which are summarized in Tables 2.

Table 2

Comparison of Strouhal numbers

	Author	St
Confined channel	Nakagawa et al. [8] ($f\frac{h}{U_b}$)	0.13
	Present($f\frac{h}{U_b}$)	0.124
Infinite domain	Okajima [6] ($f\frac{h}{U_m}$)	0.126
	Present($f\frac{h}{U_m}$)	0.125

Figure 2.4 shows distribution of the mean wall shear stress on the channel wall along the plate. It is seen that the maximum value obtained at x/h=-0.8 where the flow accelerated because reduction of cross sectional area and maximum occur at the location where flow separation take place in order to produce vortex counter rotating across the Karman vortex shed from the square bluff body. The gradient of mean stream wise velocity on the channel wall become lower compare to the other location.
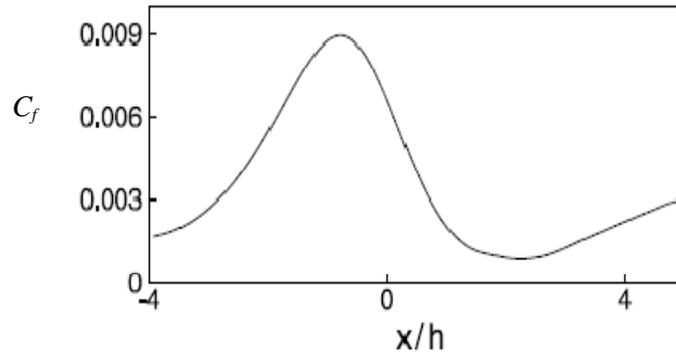
Figure 2.4: Mean shear stress along the square cylinder [Kim et al.(2003)]

Figure 2.5 shown the distribution of turbulent kinetic energy along the centre line of the square cylinder .It is clearly observed that magnitude of fluctuation is increased towards the cylinder and flow is undoubtedly affected by the cylinder.
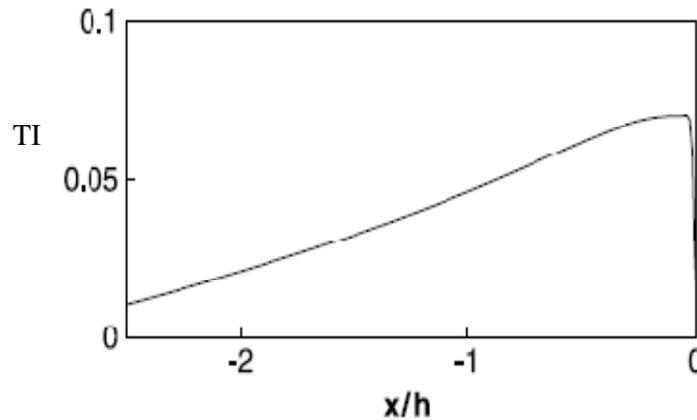
Figure 2.5: Distribution of turbulent kinetic energy upstream of the square cylinder along the centre line [Kim et al.(2003)]

Figure 2.6 shows the comparison of turbulence intensity with that over a square bluff body at infinite zone at fixed Reynolds number .It is noticed that contour pattern of the maximum zone are various. In infinite domain, the local maximum zone of stream wise velocity fluctuation rear both trailing edges which is shown in Fig.11(a), don't exist. Comparison of turbulence intensity with that around a square. So it is proposed that the channel has a perfect effect on high stream wise turbulent fluctuation in the normal direction in the close wake zone.
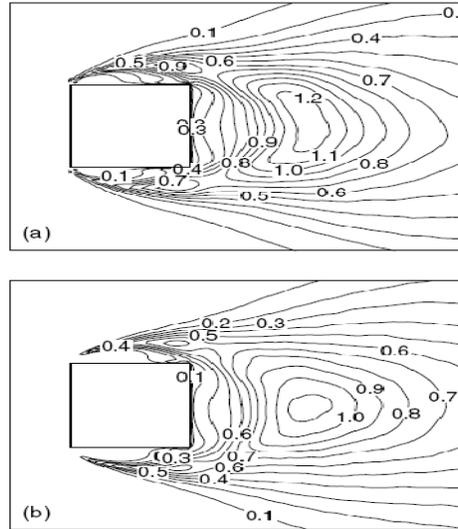
Figure 2.6: Comparison of turbulence intensity ($U'_i U'_i / U^2_m$) increment: 0.1): (a) square

cylinder in the channel and (b) square cylinder in an infinite domain **[Kim et al.(2003)]**.

The momentum and forced convection heat transfer nature for an incompressible and constant free stream flow of power law liquids over a square cylinder have been performed by "**Paliwal et al. (2003)**".The momentum and energy equations have been discretized with finite different method. Power law index is used n=0.5-1.4 so that housing both shear thinning and shear thickening behaviour and Reynolds number Re=5-40, Peclet number Pe=5-400 are used in this study. Only one blockage ratio is considered ($\frac{L}{H} = \frac{1}{15}$) for all computation. The shear thinning cut down the size of the wake region but it also setback the wake formation and shear thickening behaviour.

"**Isaev et al. (2004)**" carried out a numerical computing of the parameters of unsteady -state flow and heat transfer under circumstance of laminar crosswise stream of viscous incompressible fluid past a circular cylinder with Reynolds number upto, Re=14.The forming of Karman vortex is treated, including the cyclic heating of the close and distant wake following the heated cylinder. Major concentration is given to investigate of the nature of the basic attribute of flow and heat transfer and allocation of friction, pressure and coefficient oh heat transfer on the surface of cylinder, including to interaction of the parameters of stream and temperature at elected specific location in the proximity of the cylinder.

The three-dimensionality of vortex shedding from a trapezoidal bluff body using direct numerical simulation method at Re_d=250 which is analyse by "**Najjarand Balachandar**

(1998)". Numerical procedures presently applied in this work which is classified into two categories. The first one is direct numerical simulations method which is used to solve the Navier-Stokes equation directly, and the second one is averaging of the Navier-Stokes equation. Flow around triangular prism has received significant attention from researchers.

"Sanitjai and Goldstein (2004)"study the Local and average heat transfer by forced convection from a circular cylinder. A Reynolds numbers ranging from 2,000 to 90,000 and Prandtl number from 0.7 to 176 has been considered. Their results are interesting for subcritical flow. The local heat transfer measurement indicates three flow regions including laminar boundary layer region, reattachment of shear layer region and periodic vortex flow region. In each region, the average heat transfer is calculated and correlated with the Reynolds number and the Prandtl number. Also the Nusselt number in each region depends on the Reynolds number and the Prandtl number. An empirical correlation is developed for predicting the overall heat transfer from the cylinder in these three regions.

Application of a modified k-ε model for prediction the aerodynamic characteristics of rectangular cross-section cylinders of infinite and different breadth to depth ratios ranging from B/D=0.6-8.0 were study by **"Shimada et al. (2001)"** In spite of the numerical method is considered two dimensional, a physically fairly smooth, cyclic vortex shedding was achieve, uniform in the high Reynolds number range .this nature cannot be simulated by common 2-D study which do not include a turbulence model. Different conventional aerodynamic appearance were favourably obtained, specially including the discontinuity in Strouhal number at the detracting portion of B/D=2.8 AND 6.0.In addition to, drag coefficient and mean surface pressure distribution were in reasonable good agreement with the experimental results and the 3D study for the range of B/D ratio. The prediction of force and pressure variations which is presently available RANS model are capable of performing to examine the periodic components and not hypothetical components. The total fluctuations in lift force and surface pressure were significantly miscalculate in few cases, distinguished with those deliberate in experiments and computed from 3D examination.

"Sharma and Eswaran (2004)" had shown the flow structure and heat transfer characteristics of an isolated square cylinder in cross flow. It is investigated numerically for both steady and unsteady periodic laminar flow. The problem is considered two-dimensional where Reynolds numbers of 1 to 160 and a fixed Prandtl number of 0.7. The isotherm pattern, heat transfer from cylinder and the effect of vortex shedding on the cylinder is discussed. The correlations of heat transfer between Nusselt number and Reynolds number are presented for boundary condition of uniform heat flux and constant cylinder temperature.

Three-dimensional computational analysis of the flow around the cross section of rectangular cylinders with different side ratios of D/H, from 0.2 to 2.0, was performed by "**Rokugou et al. (2003)"** for Reynolds number of 1000 with using a multi directional finite difference method. It is observed that simulation results are good agreement with experimental results. It is seen that fluid dynamics nature of rectangular cross section replacement between high pressure and low pressure mode of the base pressure for D/H=0.2-0.6.Privately show that this development is induced by the modification of the flow arrangement around rectangular cylinder.

"Singh and Mittal et al. (2004)" studied numerically the flow past a circular cylinder with resolving the unsteady incompressible two dimensional Navier-Stokes equations by way of steady finite element organization. Reynolds number are considered as Re=100 to 10^7.It is very strongly known that beyond $Re \sim 200$ the flow expand significant three dimensional characteristics. Thus, two dimensional simulations are wonted to decline well short of predicting the flow correctly at high Reynolds number. In the present computations, the frequency of the shear layer vortices good agree with the $Re^{0.67}$ fluctuation noticed by different investigator from experimental analysis. The major aim of this paper is to find out a probable relationship between the drag crisis (abrupt deficit of drag at $Re \sim 2 \times 10^5$) and imbalance of the detached shear layer.

When Re is increased the transition point of shear layer, beyond which it is changeable, shift challenging. The transition point is situated much close to the point of flow separation at critical Reynolds number. The lag of flow separation is correlate with shortening of wake, increase in Reynolds shear stress close the shoulder of the cylinder and important decline in the drag and base suction coefficient. As in two-dimensional isotropic turbulence, E(k) change as $k^{-5/3}$ for wave numbers greater than energy dose scale and as k^{-3} for inferior wave numbers. The current simulations propose that the shear layer vortices play a bigger act in the transition boundary layer from laminar to turbulent.

The numerical simulation of flow around triangular prism situated vertically on a level with moderate aspect ratio by using Large-eddy simulation method which studied by "**Camarri et al. (2006)"**. The outcomes are compared with available and fresh experimental statistics in order to achieve proof on the physical source of the velocity oscillation interior and over the wake. Both the numerical and the experimental velocity signs are studied through time–frequency approach placed on the wavelet and Hilbert transforms in order to define the time

alternation of the amplitude and frequency of the various distinguishable oscillating parts. It is exhibit that the numerical simulation, even though relating to a Reynolds number that is lone rule of magnitude lesser than in the experiments, supply values of the rms wake oscillation that are in excellent reconciliation with those achieve from the hot-wire calculation. Moreover, it admit the form of the top adjacent wake to be defined, and provides valuable clues on the dynamics of the vorticity designs emerge from the free edge of the body and on their feasible contact with the wake oscillating flow range.

"**Dalal et al. (2006)"** observed numerical simulation of unconfined flow past a triangular cylinder. Reynolds number taken are in the range of 10 to 250.A finite volume method, 2nd order correct in space and time, applying non-staggered settlement of the variables with momentum initiation for the coupling of pressure velocity is developed. Comprehensive method study forecast $\text{Re}_{cr} = 39.9$ which affirm the outcomes of previous research. The phenomena of vortex shedding are found to be identical to the cylinder of square cross section with no second ramification in the range of Reynolds number studied. A analysis on the time-averaged coefficient of drag, rms of lift coefficient and Strouhal number are discussed.

The flow over bluff body from moderate to high Reynolds number which was performed by **"Sohankar et al.(2006)".** Large eddy simulation is used to study the uniform flow over a square section cylinder where Reynolds number varying from $1,00$ to 5×10^{6}. Smagorinsky and a dynamic one-equation model are used. The Strouhal number, the mean lift and RMS values of drag coefficient are reported here. This show good agreement with the experimental results.

The two dimensional flow over an infinite long circular cylinder is analyze numerically by **"Posdziech et al. (2006)"** using spectral element method. Precise analysis of the reaction of resolution and enlargement of the computational territory on drag and lift forces, Strouhal number, and base pressure coefficient are carry out in the laminar region. Asymptotic outcome are achieve by rising the length of the computational territory to assorted thousand of cylinder diameters. it is observed that in compare to the Strouhal number, base pressure coefficient, and the force coefficients are fully dependent on the decision and even greater on the size of the computational territory. The Reynolds number communications are compared to computational and experimental info from the literature. The database is favourable both for confirmation of computational codes and calculation proofs where the partition of physical appearance and effect of experimental plans are regularly an free question.

Turbulent flow past a circular cylinder at the critical regime was studied by "**Benim et al. (2007)".** The flow is considered incompressible flow. Numerical simulation over circular cylinder was done by using RANS model (Transition SST model) up to Reynolds number 10,000-5, 00,000.For the velocity -pressure coupling, SIMPLEC scheme and low turbulence intensity (0.01%) is used in this study. The major parameter non dimensional wall distance y^+ value is calculated as $y^+=(y/\nu)(\tau_{w/\rho})^{0.5}$ where, y, ν, τ_w, p represents the cell to wall distance, kinematic viscosity, wall shear stress and density receptively. The drag co efficient value which are obtained in present simulation, compared with measured value from the literature.

"Benim et al. (2011)" simulated flow around cylinder using RANS, URANS as well as LES and found that LES predict the drag coefficient closer to experimental values. the Reynolds numbers consider are (Re) 2500, 5000 and 25,000 and the Prandtl number is identical to 0.7 for whole computations. For Re=2500 and Re= 5000 three-dimensional URANS (3D URANS) and Large Eddy Simulations (LES) are also performed. In the RANS and URANS computations, the Shear Stress Transport (SST) model is used as the turbulence model. The Wall-Adapting Local Eddy-Viscosity (WALE) subgrid-scale model is used in LES. It is predicted that the heat transfer at the channel wall can be enhance by the triangular prism, where the forecast features depends on the modeling method employ. URANS and LES predict mainly enough higher Nusselt values compared to RANS, and, thus, point out a enough powerful heat transfer enhancement by the triangular prism. It is explain that the impact of the unsteady movement of the understable whirlpool design behind the prism, which are primarily liable for the heat transfer enhancement cannot be sufficiently describe by a RANS model, and an unsteady approach (URANS/LES) is necessary for a superior forecast. The comparison between 2D URANS and 3D URANS exhibit, on the other hand, that three-dimensional impact in large scales can further play few act, depending on the Reynolds number, which could fairly be prove for Re =2500. The forecast crest time-averaged Nusselt numbers in the downstream zone of the prism by LES produce to be much higher than those of URANS, due to small but intense vortical design in the wall proximity, that are solve by LES. Still, more downstream, LES and URANS converge and display a fairly identical asymptotic attitude.

 While **"Ding et al. (2004)"** applied mesh free method to analyze flow field over a cylinder, lattice Boltzmann method was applied by "Shueet al. (2005)" for rotating cylinders successfully.

Two and three-dimensional numerical heat transfer modelling from different circular cylindrical particles have been performed by **Motlagh and Hashemabadi (2008)"** with the commercial CFD software, FEMLA. In this work four distinct position (a) infinite cylinder in cross-flow, (b) cross-flow on finite cylinder with different aspect ratio in a rectangular duct,(c) axial-flow on finite cylinder and d) axial-flow on finite cylinder with upstream turbulence are used. All body forces have been neglected and the standard κ–ε turbulence model has been used for calculation of eddy viscosity of flow. The computation results were validated with experimental data and also experimental correlations from different research papers and show reasonable good agreement with each other.

The 2-D flow around a porous expanded trapezoidal cylinder using a finite volume method, based on the body-fitted, non-orthogonal grids and multi-block technique which was analyzed by **"Chen et al. (2009)"**. The Brinkman-Forcheimmer lengthy model was employ to control the flow in the porous medium zone. At its junction, a shear stress bounce that contains the inertial impact was enforcing, together with a constancy of common stress. Discovering – The current model was verify by comparing with the for the flow over a tight circular cylinder. Outcomes for flow over absorbent extend trapezoidal cylinder are granted with flow structure for various Darcy number, 10^{-2} to 10^{-7}, porosity ranging from 0.4 to 0.8, and Reynolds number Re=20 to 200. The flows grow from steady to unsteady intermittent whirlpool shedding state. The early coefficient β has a greater notable impact, whereas the second coefficient $\beta 1$ has much low impact, consistent for Re = 200. The impact of the porosity, Reynolds number and Darcy number on drag and lift coefficients, and the length of circulation region or shedding cycle are investigated.

"Rajani et al. (2009)" have investigated the numerical simulation of laminar flow past a circular cylinder in various laminar flow regimes. In this work implicit pressure based finite volume method is used for time accurate computation of incompressible flow with second order accurate convective flux discretisation scheme. Skin friction coefficients, recirculation wake length at the invariant flow regime, Strouhal frequency of vortex shedding mean and rms value of the oscillating aerodynamic coefficient for cyclical flow regime. The complicated flow structure of the cylinder wake is also fairly captured by the current forecast procedure.

In fig 2.7 the surface pressure and skin friction coefficient is present in three different Reynolds number. For all the Reynolds number the measurement data and simulation results is good agreement to each other in the drive flow zone which is covering the front part of the

cylinder. This differences may be associate usually to the incorrect guess of the location of the variable flow separation point on cylinder surface .The differences may also be attributed to the three-dimensional fluctuation of the wake with the spanwise direction at Reynolds number Re=200 and Re=300.

(a) $Re = 100$

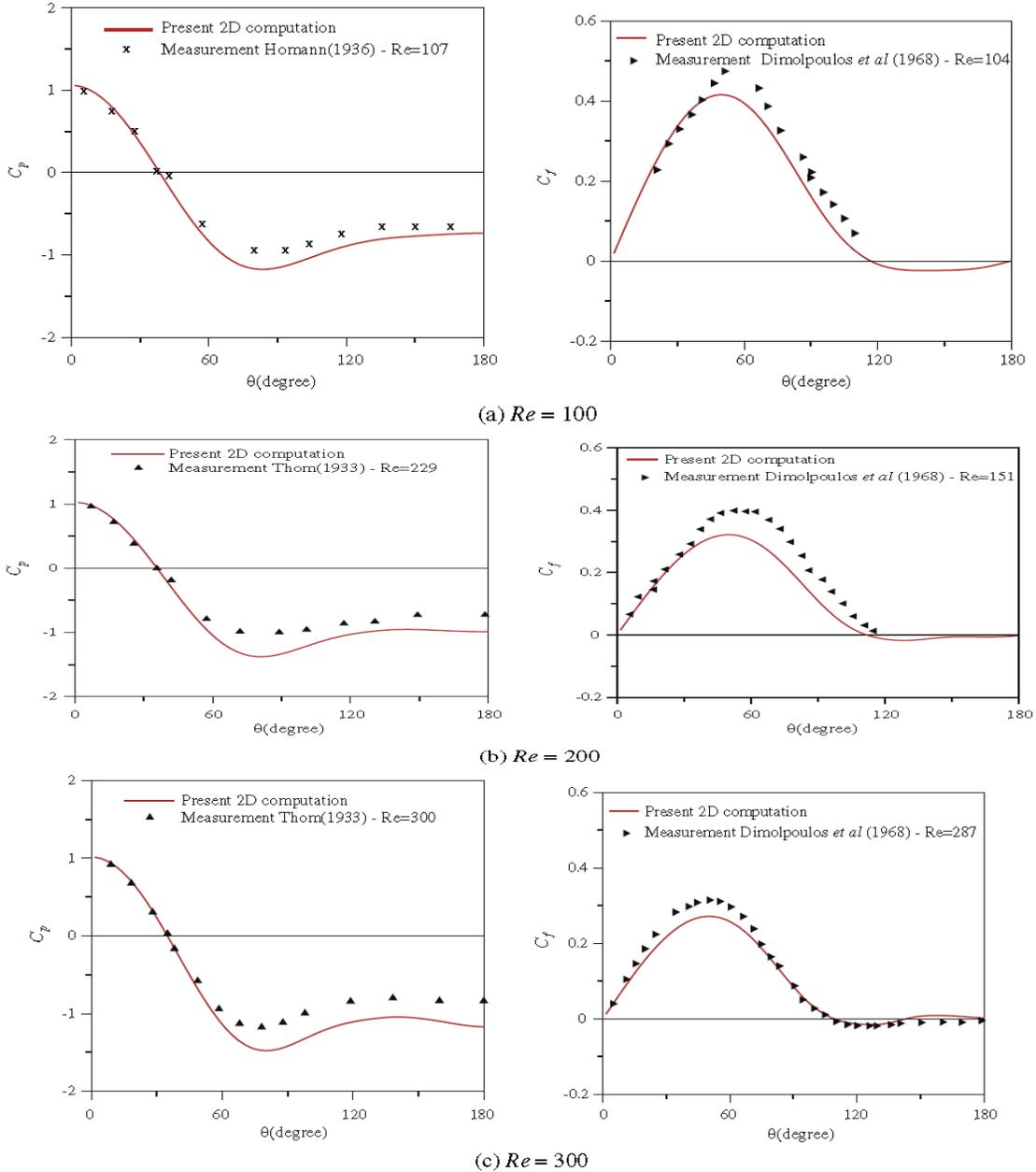(b) $Re = 200$

(c) $Re = 300$

Figure 2.7: Distribution of surface pressure and skin friction around the cylinder at different Reynolds number (Rajani et al., 2009)

The effect of Transitions on flow past a square cylinder at low Reynolds number was investigated by "**Saha (2009)".** The problem is three dimensional and Reynolds number

varying from 100-325.The flow is find out two dimensional at Re 160 and three dimensional at Re 163.5. The transition effect on the instantaneous flow and root mean square fluctuations are quite significant while the time-averaged flow does not show any noticeable variation.

"**Mannini et al.(2010)**" studied the unsteady RANS modeling of flow past a rectangular prism with fineness ratio(cord to thickness) of 5.0.The flow is two dimensional and Unsteady Reynolds-Averaged Navier-Stokes equation are used. The study was done with various Reynolds numbers (from 20×10^3 to $1,850 \times 10^3$), Mach number (0.1), 0^0 and 4^0 and angle of attack. The focus of this work is to judge the capability of the computationally efficient two-dimensional URANS calculations to see the features of complex separated flow around such type of geometry. Another goal is to investigate the Reynolds number effects noticed in wind-tunnel experiments with using numerical simulation.

"**Sen et al. (2010)**" have been analyzing the flow past a square cross section of cylinder at laminar region. A balance finite-element organization is engaged to discretize the equation of incompressible fluid stream. The values of laminar segregation Reynolds number (Re_s) and separation angle (θ_s) are forecast. Further, the change of separation angle with Reynolds number is presented. It is observed that the steady break-up starts at Re=1.15.Opposed to the favourite assumption that break-up originates at the back sharp edge, it is found to emerge from the low specific location, that is $\theta_s = 180^0$ $Re = Re_s$.Separation angle comes nearer the limit of 135^0 at $Re \succ 5$. The length of break-up droplet raise almost linearly with rising Reynolds number. The C_d is changes as $Re^{-0.66}$.Flow nature at $Re \ll 40$ are also conferred for elliptical cylinders of aspect ratios 0.2, 0.5, 0.8 and 1 (circle) having the identical characteristic magnitude as the square and main axis align common to the free-stream.

The developments in enhanced heat transfer with experimentally and theoretically presented by "**Bergles et al. (2011)**". The collect literature includes thousands of references. This study give an outline of the modern state of this essential technology for past ten years representative development in each division of enhancement approach are point out and communicated. The argument is classified into the literature, passive enhancement approach, progressive enhancement techniques, and composite improvement approach. Current modifications of enhancement approach are invariably being advanced and they are being used in modern purpose. Much of the attempt is guided in the direction of micro scale even nanoscale.

"**Berrone et al. (2011)**" studied the numerical simulation of flow past rectangular cylinder by two different numerical methods, a final volume method (FVM) and adjusting final

element method (AFEM). A rectangular and square cylinder with width to height ratio is 5 considered into detail, 2D simulations have been carryout for various Reynolds number in order to taken various flow regimes, namely the steady, the periodic and turbulent flow. Strouhal number, drag coefficient and recirculation length have been distinguished. A reasonable excellent agreement between the FEM and FVM calculations, including with the available literature results, has been establish. Appropriate results of this work are the cross confirmation of an adjusting FE method and famous open source FV code.

The flow nature in the near wake of two exact side-by-side circular cylinders placed close to a perfectly grown turbulent boundary layer are performed by **"Chen et al. (2011)"** with **experimentally** utilizing the particle image velocimetry (PIV) and the pressure sensor. The Reynolds number which based on the diameter of the cylinder (D) is 1,696.The boundary layer thickness is 6.6 D, the cylinder midpoint to midpoint layout (T) is changing from T/D=1 to 1.906,the gap layout between the inferior cylinder and the wall(G) is different from G/D-0 to 1.811.To analyze the effect of varying the gap ratios of T/D and G/D on the wake stream, different wake nature like averaged streamlines, vorticity contours, Reynolds stress and additional crucial flow characteristics as well as Strouhal number and length scale are examined for various ratios T/D and G/D. Grant to these wake features, five key flow arrangement have been analyze.

The convective heat transfer around a triangular cylinder in an air cross flow was analyze by **"Zeitoun et al. (2011)".** The problem is considering two dimensional. Equilateral triangular cylinder of different side dimensions and configurations are examined in laminar conditions.

The effect of adding/opposing buoyancy on the two-dimensional upward flow and heat transfer around a heated/cooled cylinder of square cross section has been numerically studied by **"Chatterjee and Mondal (2012)"**. The influence of adding/opposing buoyancy and the blockage parameters of 2% and 25% is studied for Reynolds and Richardson numbers which ranges of 50 to 150 and -1 to 1**.**

"You and Kwon (2012)" have investigated the performances for the numerical simulation around a circular cylinder using different turbulent models at a critical Reynolds number regime. The Reynolds number and turbulence intensity are taking 8.5×10^5, 0.7% respectively. RANS model (Transition SST Model), Hybrid RANS/LES model (SAS model), a correlation-based transition model are used to simulate the laminar-turbulence transition inside the boundary layer and the unsteady vortex shedding in the wake region.

The flow and heat transfer characteristics inside a rectangular channel enclosed with drop shaped pin fins were experimentally and numerically analyzed by "**Wang et al. (2012)".**Three different shaped pin fin, i.e., circular, elliptical and drop shaped fin accompanying the identical cross sectional area were distinguished in staggered arrangement. The Reynolds number which based on the hydraulic diameter was varied from 4,800 to 8,200. The heat transfer enhancement is less in the case of dropped shaped pin fin compare to the circular pin fins. Figure 2.8 shows the pressure loss coefficient against the different Reynolds number for the channel with various pin fin collection. Even though there was a obvious dissimilarity between experimental and computational results. For the particular performance, the specific friction loss in drop shaped pin fin was inferior than that of elliptical and circular pin fins, which signify that the drop shaped pin fin is more favourable, compare to the other.
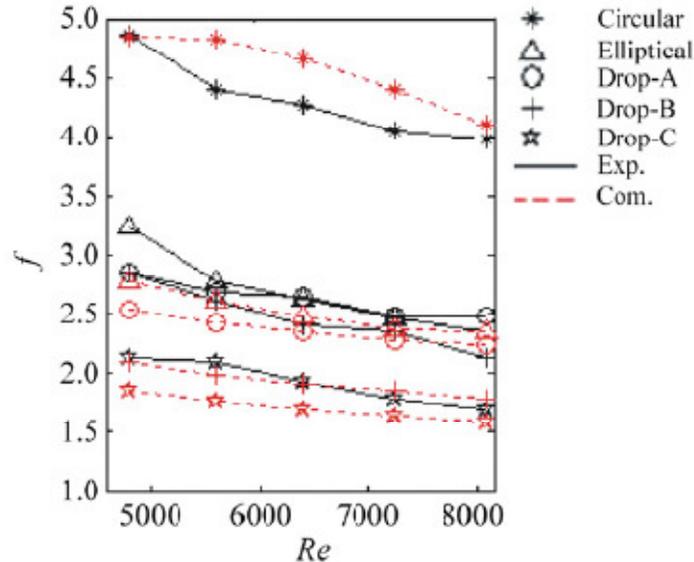
Figure 2.8: Pressure loss coefficient vs Reynolds number [Wang et al.(2012)].

Figure 2.9 show the average Nusselt number against the Reynolds number for the channel with various pin fin bunch. Though there was higher relative error of 10%-20% between the experimental and computational results, the relationship between convective heat transfer capacities to the pin shapes are admit well The elliptical pin fins seemed to decrease the Average Nusselt number by about 20% compare to the circular pin fins at Reynolds number of 4,800-8,200. In the case of drop-shaped pin fins, the reduction of average Nusselt number comparative to circular pin was about 24% for drop A, 26% for drop B, and 27% for drop C.
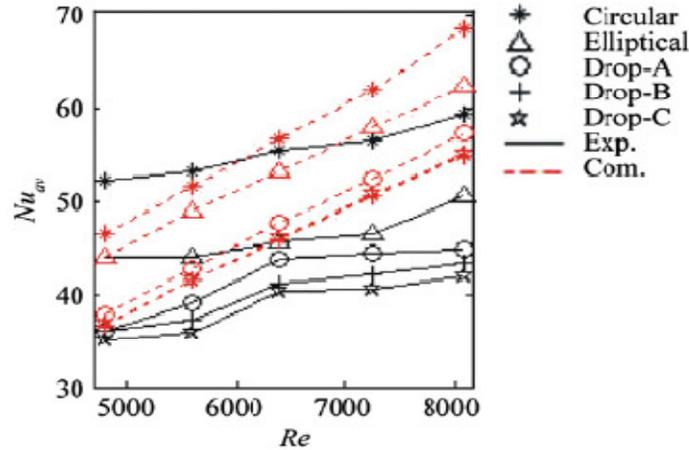
Figure 2.9:Variation of averaged Nuuselt number with Reynolds number [Wang et al.(2012)].

"You and Kwon (2012)" have investigated the performances of various turbulent models for the flow simulation around a circular cylinder at a critical Reynolds number regime. The Reynolds number and turbulence intensity are considering 8.5×10^5, 0.7% respectively. Hybrid RANS/LES model (SAS model), a correlation-based transition model, (γ- Reθ model) and a fully turbulent RANS model (Transition SST model) are utilize to simulate the laminar-turbulence transition inside the boundary layer and the unsteady vortex shedding in the wake region.A vertex-focus finite-volume approach was adopted to discretize the incompressible Navier-Stokes equations and an unorganized mesh method was employ to discretize the calculating territory. The inviscid fluxes were judge by utilizing second-order Roe's FDS and the viscous fluxes were calculated based on the central differencing scheme. A dual-time stepping technique and the Gauss-Seidel iteration were apply for unsteady time integration. To minimize the calculation costs, the parallelization plan employing METIS and MPI libraries was adopted. The unsteady features and time-averaged amount of the flow range were compared between the turbulent models. The computational results have been further compared with experimental results. At the critical regime, turbulent models have exhibit dropout various results owed to the distinct capability of every model to forecast different flow characteristics like laminar-turbulent transition, unsteady vortex shedding.

In this work, the 2-D numerical investigation were perform by **"Ai et al. (2013)"** for unsteady high Reynolds number flows over a soft circular cylinder in the supercritical and upper-transition flow regimes, particularly $8.21 \times 10^4 < Re < 1.54 \times 10^6$. The measurement were carryout by means of resolve the two dimensional Unsteady Reynolds-Averaged Navier-

Stokes (URANS) equations with a k -ε turbulence model. The determined data's formed flow design coefficients of drag and lift, including Strouhal numbers. The judgments were in favourable agreement with earlier written result, which also provide us with a excellent understanding of the flow across cylinders of various high Reynolds numbers. At the same time, an efficient measure was given to regulate the lift force on a cylinder.

"Chatterjeeet al. (2013)" performed to investigate the laminar forced convection heat transfer for flow past a semicircular cylinder in an unconfined medium. The numerical simulation is done for two dimensional unsteady flows. In this study the Reynolds numbers are in the range of 50-150 with a fixed Prandtl number (Pr=0.71).In this work two different configurations of the semicircular cylinder are considered; one when the curved surface facing the flow and the other when the flat surface facing the flow. For the numerical computation a finite volume-based technique is used

The experimental and Numerical analysis of flow around a fixed circular cylinder at Reynolds number 1,00,000 was done by **"Islam and Hassan (2013)"**. The Favre-averaged Navier-Stokes equation are used and solved by finite volume procedure. Numerical surveillance are compared with experimental data's and with research performance of other scientists. Various flow phenomena e.g. flow partition, pressure allocation over the surface, drag, vortex shedding etc. are also calculated at various boundary circumstances. A short comparison between the 2D and 3D numerical studied including the character of vorticity allocation and impacts of surface roughness are broadly considered. In case of polished cylinder, the partition angles for 2D or 3D numerical computation are found to be about 80~90° in one side of the cylinder from the challenging stagnation mark. The drag coefficients for polished surface are 0.771 and 0.533 for 2D and 3D numerical studies respectively and successive variation in drag due to introducing surface coarseness are explain. The critical surface coarseness is begun to be appox 0.004 along drag coefficient 0.43. However, the wake design was unclearly seeable; they are not as regular as in Karman Street.

"Rodríguez et al. (2013)" performed the direct numerical simulations of the flow over a sphere in the wake of turbulence. The numerical simulation have been performed in the sub-critical regime of Re=3,700 and Re=10,000 which is based on the free stream velocity and diameter of sphere. Simulations are done on unstructured grids obtained by the constant step rotation about the axis of a two dimensional grid. With this Poisson equation has been resolve by means of Fourier diagonalization method. The principal features of the flow containing

power spectra of a set of elected monitoring probe at dissimilar positions was describe and explained in clearly. The turbulent enumeration had also been provided clearly.

The fluid flow past an obstruction of circular cross section in the unsteady flow regime has been numerically solved by **"Golani and Dhiman (2014)"**. Here, effect of Reynolds number on Strouhal number, drag and lift coefficients, heat transfer nature of a heated circular cylinder are examined for Reynolds number ranging from Re=50-180 and Prandtl number =0.7(air) in the unstable unsteady mix flow. The numerical computation have been performed with finite volume method(FVM) which based on the commercial CFD solver Fluent(version 6.3).Particularized flow arrangement are conferred by approach of spontaneous stream line, vorticity magnitude, velocity magnitude, and pressure contour. The current results are good agreement with experimental data available for a circular cylinder in the literature. The average Nusselt number rise with raising Reynolds number. When The Reynolds number increases, the vortex shedding frequency, drag value increases, though, the rms lifts and rms drag coefficients are increases with Re.

"**A. Alonzo-García et al. (2014)"** studied the Large Eddy simulation flow around a smooth polished circular cylinder and U-Grooved shape circular cylinder with the Reynolds of 1,40,000.It is nearby transition in the middle of sub critical and critical flow regimes. The numbers of cell were 2.6 million and 20.7 for the case of smooth and U-grooved circular cylinder correspondingly. hexahedral cells were used with extra filtering in close the wall region in order to get y^+ value less than 5.The governing equation of RANS model was solved using commercial CFD software Ansys Fluent V.12.1.In the case of U-grooved cylinder, drag co-efficient ,recirculation length, development of a wake created by secondary vortices were observed reasonably by the LES model.

Numerical analyses of flow around a square cross section cylinder are presented by "**Islam et al. (2014)"** with the multi-relaxation-time lattice Boltzmann methods at low Reynolds numbers. Time-trace study of drag and lift coefficients, vorticity contours visualizations, power spectra study of lift coefficient, phase diagrams and streamlines were reported here. The global quantities like Strouhal number, drag coefficient ,mean drag coefficient, root mean square values of drag and lift coefficients are determined and compared with the strong solve experimental result and numerical data's available in open article. The Reynolds numbers affected the global quantities.

"Saeedi et al. (2014)" studied the direct numerical simulation to perform the turbulent wake behind a surface mounted square cylinder bluff body. The aspect ratio and Reynolds number are considered 4 and 12,000 respectively (based on the free flow velocity and bump side length) in a developing boundary layer. In case of high Reynolds number and high aspect ratio of the cylinder, the wake is broad spread trailing the cylinder and display complicated and dynamic vortex action. The side and travel vortex shedding arrangements at various frequencies, systematic structures downstream of the obstruction, the production rate and transportation of turbulent kinetic energy, the rapid pressure distribution in the wake zone have been carefully examined. In order to justify computational results, the first and second order streams data's achieve from the simulations have been thoroughly compared against accessible wind-tunnel calculation data.

Large eddy simulations of the flow around a circular cylinder with Reynolds number ranging from $2.5 \times 10^5 \; to \; 6.5 \times 10^5$ are carry out by **"Lehmkuhl et al. (2014)".**It is clearly admitted that flow spent a circular cylinder at critical Reynolds number combines flow partition, turbulence transition, reconnection of the flow, and more turbulent partition of the boundary layer. It is exhibit how the pressure allocation changes as the Reynolds number increases in an irregular manner, happen early on one side of the cylinder and next on the alternative side to complete the drop in the drag up to 0.23 at Re=6.5$\times$ 10^5.These difference in the pressure sketch are follow by the presence of a short recirculation droplet, noticed as a little plateau in the pressure, and placed around $\phi = 105^0$ which is measured from the stagnation point. The power spectra for the velocity variation are calculated. The study of the resulting spectrum exhibits the footmark of Kelvin-Helmholtz uncertainty in the entire range. It is found that the ratio of these imbalance frequency to the basic vortex shedding frequency agree well the scaling suggested by Prasad and Williamson ["The instability of the separated shear layer from a bluff body," Phys. Fluids 8, 1347 (1996); "The instability of the shear layer separating from a bluff body," J. Fluid Mech. 333, 375–492 (1997)].

"In this task, Liu et al. (2015)" studied the computational analysis of the effect of particles on the adjacent wake over a circular cross section of cylinder at a moderate Reynolds number with a direct numerical simulation (DNS) technique. High-order finite-deference proposal are used to clarify for the quantity fluid properties, and a Lagrangian method is maintain to record the sole particles The individual-stage flow is resolve and justify with prior experimental result. U and V shaped states are noticed in the adjacent wake, which are

regular with the experimental data's. the drag force from the circular cylinder increases by particles and restrain the circular current shedding frequency.

The effect of a solid wall on the wake dynamics of a square cross section of an infinite cylinder was studied by **"Samani et al. (2015)"** when it is located in closeness to wall. Three various gap value ratio were studied namely g/D=0,0.5 and 1, further to the mention case of a cylinder in a free stream accompanying no wall. The Reynolds number, which based on the cylinder width and free stream velocity was Re=500. Large Eddy simulation was used to predict the determine scale-velocity and pressure fields, and further to produce the input info for the convenient Orthogonal Decomposition studies. When the cylinder was placed to the wall, it imported active asymmetry into the adjacent -wake, which was unmistakable in the readjustment of the upper and lower redistribution cells, including the improvement of a insignificant recirculation region on the base wall itself. For every cut ratio, the systematic structure relate with early three POD approach were analyze and the results which correlated with case of an infinite cylinder in a free flow. For the two minimal gap ratio both the energy allocation between the POD modes and the flow arrangement correlate with the systematic structures for every mode were powerfully influenced by the existence of the wall.

The turbulent flow around a square cylinder using DNS method studied by **Trias et al. (2015).** The results of time averaged flow and statistics of turbulent are discussed together with experimental data which are showing good agreement. Comparison of the turbulent statistics in the wall region which indicates that the transition zone is being well capture.

Experimental and numerical analysis were perform to examine the effect of nozzle shape on unconfined jet impingement heat transfer from a heated circular cylinder by "**Singh et al. (2015)".**Air is considered as a working fluid where prandtl number is fixed 0.71.The surface of heated cylinder are maintained at a constant heat flux. The circular, rectangular and square nozzles are selected with same hydraulic diameter for comparative analysis. The ratio between hydraulic diameters of the nozzle to the diameter of heated cylinder was maintained as 0.2 for the parametric study. The non-dimensional distance between the rear side of nozzle and the cylinder, was varies from 4 to16.Reynolds number was considering ranging from 10,000 to 25,000.For a fixed Reynolds number, the mass flow rate through the various nozzle are different. So a diametric analysis was also carried out to notice the effect of nozzle shape for different constant mass flow rate. The heat transfer rate from the cylinder was higher in the case of rectangular nozzle.

Spanwise correlations in the wake of a circular cylinder and a trapezoid placed inside a circular pipe is studied by **"Venugopal et al. (2015)"** using hotwire anemometer. Results are

considered for Reynolds number 1, 00,000.Three blockage ratio of 0.14, 0.19 and 0.28 are used in present study. Coefficient of correlation is seen to enhance with increase in blockage ratio. Trapezium bluff body holds the high correlation length compared to circular cylinder. It is observed that concurrent effect of curvature, upstream turbulence, and low aspect ratio cut down the correlation co efficient undoubtedly as compared to confined and unconfined flow. Vortex shedding for trapezoid with a blockage ratio of 0.28 was observed to be lower compared to circular cylinder and all other blockage ratios.

"Yagmur et al. (2015)" carried out Experimental and Numerical study of Flow Structures over Cylindrical Bluff Bodies. The major goal of this work is to perform experimentally and numerically the flow field in the wake region of various bluff bodies, like square cylinder, circular cylinder, and triangular cylinder located horizontally perpendicular to the consistent flow. Particle Image Velocimetry method is used for experimental study in an open water tunnel with the Reynolds number range of 5,000 to 10,000.Large eddy simulation model is used and the experimental results are compared with the numerical results. It is observed that the experimental results are good agreement with simulations results in sense of the spontaneous and time-averaged flow field design of vorticity, velocity element stream wise direction and streamline topology. Also, geometries drag coefficients were computationally determined. Profile of the time-averaged stream wise velocity for Re=10000 explain that the stagnation point over the proportion plane shift more upstream for all cylinders in agreement with Re=5000. The highest drag coefficient value was allowed for the square cross-section cylinder as 1.78 due to the sharp-edged geometry.

Experimental and numerical study of heat transfer from a heated whirl horizontal cylinder in pacific air about its axis was investigate by **"Elghnam (2013)".**The rotating cylinder diameter is taken as 50mm.The computation are perform by using finite volume method(FVM) based computational fluid dynamic solver FLUENT. The heat transfer's results are define in terms of non dimensional parameters like Reynolds number, Nusselt number, Grashof number (Gr).The experimental analysis are performed for Re=1880-6220 and Grashof numbers ranges from, Re=14,285-7,14,285, while the computational measurements are performed for Reynolds number ranging from Re=0-1,00,000 and Grashof numbers range of Gr=100-10,00,000.The impact of rotation on heat transfer nature are given in terms of the local and averaged Nusselt number, streamlines, isotherm arrangement. The outcome correlated while: $Nu = 0.022 \, \text{Re}^{0.821}$ which match very strong with the data available for air in published work.

The main focal point of the present investigation was on the computational prediction of the drag crisis which is based on CFD methods. **"Wen et al. (2017)"** investigate the drag crisis phenomena occur between the sub-critical and super critical Reynolds number. In this work, blocked structure meshes with polished grids close the cylinder surface and in the downstream were applied. Both 2D and 3D computation were performed using the different turbulence models, including the SST with LCTM, the DES model, and the LES, the SST k − ω model, the k − ε model. Different Reynolds number between Re=6.31x10^4 and 7.57x10^5 were used for validation studied. The averaged drag force, the RMS of lift force and the Strouhal number were compared with experimental data. The studies marked that standard 2D and 3D RANS methods were weak to capture the drag crisis phenomenon. Though the Large Eddy Simulation method has the possibility to address the doubt.

The Strouhal numbers which are found out in this work are compared with experimental data from de Wilde et al. [6] and the ITTC report [15] in figure2.10. The predicted Strouhal numbers normally follow the similar pattern to that of the experimental results and increase gradually as increasing the Reynolds number. Though, the Strouhal numbers were over-predicted at the sub-critical Reynolds numbers and were under-predicted at the super-critical Reynolds numbers. Strouhal numbers by 2D and 3D RANS with SST k−ω model are smaller.

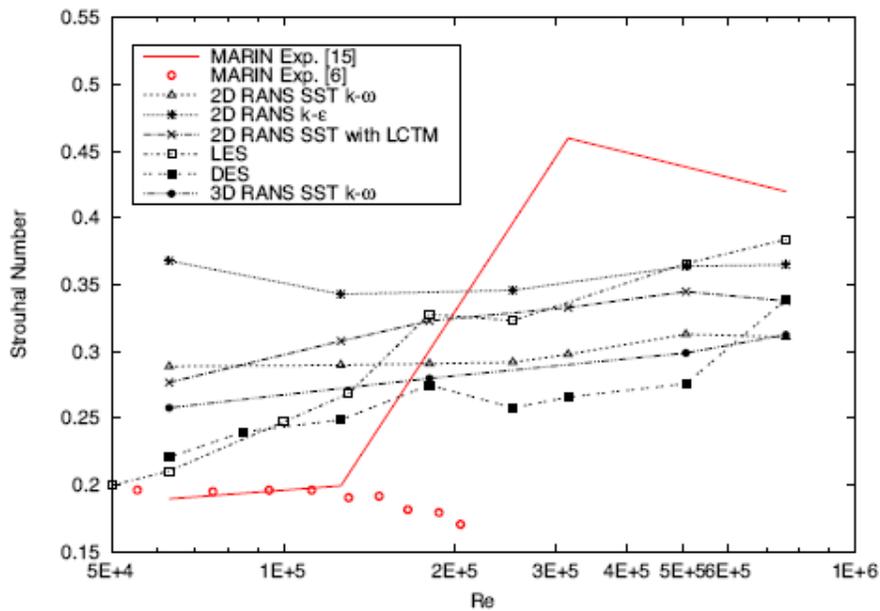Figure 2.10: Variation of Strouhal number with Re. (Wen et al.(2017)

Moreover, figure 2.11 compares the spectra which is achieve from the lift forces predicted by 2D and 3D RANS models with the SST $k - \omega$ turbulence model and by the LES model. The study were carried out for two Reynolds numbers, (a) Re = 6.31×104 and (b)Re = 7.57×105. It is clearly visible that the spectra by the RANS models all have single crest at Re=$6.31x10^4$ and Re=$7.57x10^5$(right). This suggests that the vortices flow predicted by the RANS models thickened at a single frequency at any Reynolds number. The spectrum predicted by LES at Re = 6.31×10^4 has a single narrow crest, where the spectrum is more spreading at Re = 7.57×10^5. The spectra pattern obtained from the LES simulation is consistent with that described in the work of de "Wilde and Huijsmans [6], although that from the RANS solution is not. The variations in the spectra patterns are attention due to the turbulence modelling.
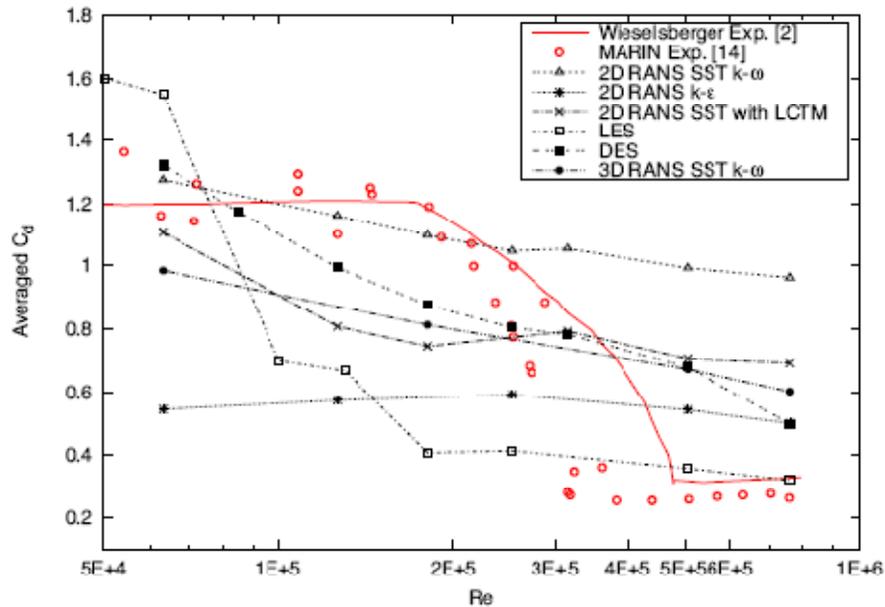
Figure 2.11: Variation of averaged drag coefficients vs Re [Wen et al. (2017)]

Dutta et al.(2004) studied the impact of coordination on the wake of a square cylinder at laminar region. The experimental research of flow past a square cross section of cylinder at Reynolds number range of Re=97-187 is stated. Cylinder coordination of 0^0-60^0 with regard to the mean flow have been treated. Two part hotwire anemometry has been take-up for calculations of velocity. The cylinder's wake has been anticipated with a pulsed laser coat to know the flow formation. Calculations have been performed at the near wake, mid wake and far wake of the cylinder. The impact of coordination and Reynolds number on drag

coefficient, Strouhal number, time average and rms velocity allocation, collapse of velocity oscillations and power spectra are of concern. The drag coefficient and Strouhal number are comparing to the angle of cylinder. A variation in the cylinder adjustment experienced to an initial arrival of quasi-periodicity and therefore, three dimensionality, unpaid to the irregular kind of the wake. The structure of the mean velocity portrait, oscillations and the rate of collapse display a active reliance on the cylinder adjustment in the adjacent wake, however dependency decrease in the far wake. In a group of angle considered, the wake of a cylinder whose orientation is 22.5^0 with regard to the incoming flow is unusually energetic and display powerful three-dimensionality.

2.1.2 Studies on vortex flow around bluff body

One of the universal conditions where computational techniques are of vast support to engineers and scientists is in the design of different fluid stream phenomena. These technique have enhanced to specific an extent that complete airplane construction is presently achievable [(Rogers et al.(2001), Shang et al.(2004), Fujii et al.(2005)].Still, in the territory of wind engineering, computational fluid dynamics (CFD) is alone just start to be used for the construct of aerodynamic design for air effects, like long-span bridges, because of the challenges of complicated design, large- Reynolds numbers and the communication of bluff bodies with the boundary layer of atmosphere. So, modelling is generally based on a important matrix of air channel study which are carry out to support in the assurance of the optimum aerodynamic structure which give the area of realistic restriction for the specific design in inquiry. A specific attention of these analysis is to reduce or check aero flexible inconsistency containing bluff body sparkle and whirlpool-induced fluctuations, including to resolve buffeting loads (look, such as [Davenport(1962), King (2003)].So, the Strouhal number is frequently one of the extreme valuable criterion to be achieve for flows over these bluff bodies.

"**Roshko (1954)"** presents three experiments on the flow past a circular cylinder at very high Reynolds number Re=1,00,0000-10,00,000. The drag value increases from its low hypocritical value to a value 0.7 at $Re = 3.5 \times 10^6$ and then shift constant. Vortex shedding occurs at Reynolds number Re>3.5×10^5 along Strohaul number 0.27.

"Bearman (1968)" studied the vortex shedding around a circular cylinder in the critical regime where the Reynolds number ranging from 10^5 to 7.5×10^5.The Reynolds number which based on diameter of the cylinder. Restricted-band vortex shedding has been noticed up to Re=5.5×10^5, namely strong inside critical regime. Strouhal number arrive the surprisingly high value of 0.6 at this Reynolds number. Spectra of the velocity oscillations calculated in the wake are granted for assorted Re values.

"Hakozaki et al. (1982)" perform an experimental work on the vortex shedding frequency different rectangular cross section cylinder were regulate in an air tunnel and in an water container. The results exhibit that how Strouhal number change with cylinder's width to height ratio within the Reynolds number range of 70 -20,000.There is observed to stay a convinced range of Reynolds number with the width to height ratios of 2 and 3 where flow arrangement unexpectedly varies with a abrupt stop in Strouhal number. The variations in flow design corresponding to the stop of Strouhal number have been prove by way calculation of velocity allocation and flow determinations. These results are correlate with those of alternative researchers. The experimental results show reasonable good agreements with the other simulation results.

"Smyth and Zurita (1994)" has been studied the forced convection heat transfer for considering axial flow of air on the external surface of a whirl cylinder. The study was two dimensional along a grant for a rotating segment of velocity over the cylinder. The outcome exhibit that an exponential law interact the numerical statistics strong with an exponent of 0.8, like is gain for turbulent flow spent a flat plate. The data were correlated with that feasible for mix flow, orbit never turn into dominant sufficient to create the Nusselt number autonomous of the blasting Reynolds number.

A numerical analysis of vortex shedding for two dimensional time dependent flow about rectangles in infinite territory. The numerical approach apply third order upwind divining for convection and Leith kind of temporal differencing. An undertake use of minimize order scheme and its imperfection are further represent. The Reynolds number reign are ranging from 100 to 2800.Another parameter are like angle of attack, upstream velocity profile, rectangle dimension are varied. The introduction and consecutive improvement of the vortex shedding aspect is examined. The equity of vortices are found to be firmly dependent on Reynolds number , while are drag, lift, Strouhal number. Calculated Strouhal numbers

correlated strong with those gain from a wind tunnel analysis for Reynolds numbers less than 1000.

Aerodynamic aspects and flow arrangements over a rectangular cylinder with a portion of different depth/breadth ratios has been study by **Tamura and Itoh (1996).**The arrangement of the cyclic vortex shedding in the wake discharge of cylinders are delicately affected by the form of after body of the cylinder. Sometimes the Strouhal numbers are bounce due to the alteration of the depth/breadth ratio of the cylinder. In this work, the detached flow over a cylinder along different sectional configuration is solved with finite difference method of the incompressible Navier-stokes equations. The mechanism of the changeable and extreme variation in vortex shedding is examined, over the analogy between the numerical simulation and experimental data. Here further take into attention the attitude of the detached shear layers from the cylinder and their following vortex development method in the adjacent wake.

The wake flow fluctuations due to vortex shedding were characterized experimentally for the case of triangular prism of moderate aspect ratio having two different cross-section (equilateral and isosceles with 90°apex angle), placed vertically on a plane by **"Buresti et al.(1998)".** The choice of a triangular shape for the cross sections of the prism was mainly dictated by the low Reynolds number dependence of the geometry (due to the presence of shape edges fixing the boundary layer simulation), and by the possibility of obtaining quite different flow conditions by varying the orientation of the models to the wind; furthermore, a very limited number of data existed in the literature for this body shape.

Two dimensional numerical computations of the Benard-von-Karman fluctuation following trapezoidal shape bluff body has been performed by "**Kahawita and Wang (2000)**" using the spline method of fractional steps. For critical Reynolds number, i.e. $Re/Re_c < 2$, the computational results approve the experimentally noticed action recorded by Goujon Durand et al. (Phys. Rev. E 1994), especially the highest magnitude of the velocity component fluctuate accompanying the crucial frequency follows reasonably strong the scaling laws $A_{max} \sim \left(\text{Re} - \text{Re}_c \right)^{0.5}$ and the location $X_{max} \sim \left(\text{Re} - \text{Re}_c \right)^{-0.5}$.The impact of the trapezoidal body on the critical Reynolds number value and on the vortex shedding is shortly explain. It arrive

that the impact of the trapezoidal height (H) is the commanding impact on the Strouhal number value when distinguished with the effect of shorter trapezoidal base width B.

Flow nature in the adjacent wake of a circular cross section of cylinder placed near to a completely grown turbulent boundary layer are studied experimentally with PIV technique by **"Wang and Tan (2007)".**The Reynolds number which based diameter of the cylinder is 12,000 and circumstance boundary layer thickness is δ=0.4 D. Particularized of vorticity and velocity territory in the wake zone are given for different gap altitude (S) between the circular cylinder and the surface, accompanying S/D varies from 0.1-1.0.The outcome declare that at $S/D \geq 0.3$, the flow is describe through the repeated, Karman-like circular current shedding from the uppermost and under face of the cylinder. For short and transitional cut ratios $(S/D \leq 0.6)$, the wake flow grow definite irregularity around the centerline of the cylinder. Still, few flow batch, like the convection velocity of the discard circular current, Strouhal number, maintain approximately fixed and practically free of S/D.

"Rajani et al. (2009)" have investigated the numerical simulation of laminar flow past a circular cylinder in various laminar flow regimes. In this work implicit pressure based finite volume method is used for time accurate computation of incompressible flow with second order accurate convective flux discretisation scheme. Skin friction coefficients, recirculation wake length at the invariant flow regime, Strouhal frequency of vortex shedding mean and rms value of the oscillating aerodynamic coefficient for cyclical flow regime. The complicated flow structure of the cylinder wake is also fairly captured by the current forecast procedure.

In figure 2.12 the surface pressure and skin friction coefficient is present in three different Reynolds number. For all the Reynolds number the measurement data and simulation results is good agreement to each other in the drive flow zone which is covering the front part of the cylinder. This differences may be associate usually to the incorrect guess of the location of the variable flow separation point on cylinder surface .The differences may also be attributed to the three-dimensional fluctuation of the wake with the spanwise direction at Reynolds number Re=200 and Re=300.
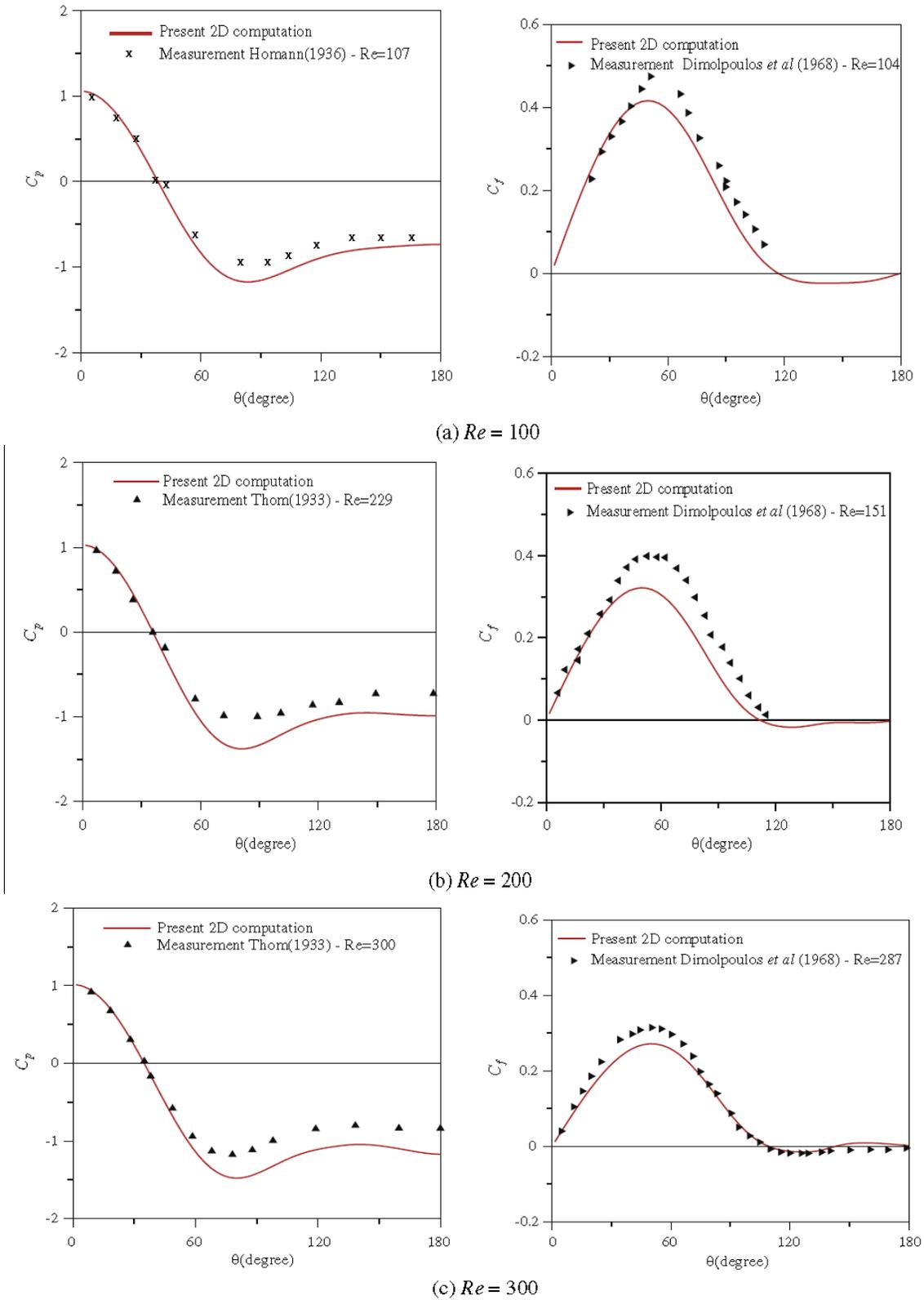
(a) $Re = 100$

(b) $Re = 200$

(c) $Re = 300$

Figure 2.12: Distribution of surface pressure and skin friction around the cylinder at different Reynolds number (Rajani et al., 2009).

The vortex dynamics in the cross section of circular cylinder wake was analyzed by "**Williamson et al. (1996)".**seeing that the analysis of fluctuating flow phenomena by "Berger and Wille (1972)" in this journal past twenty years ago, there had a surge of activity about bluff body wake. New approaches in experiment, laser induced fluorescence and Particle-Image Velocimetry are sincerely being applied to wakes but certain of the new invention have come from concerned use of classical process. These advanced evolution and discoveries of different new approach in wakes are given in this survey.

Figure 2.13 show the transition to three dimensionality in the wake can smoothly be described along reference to the Strouhal -Reynolds number. It is observed that the transition, originally stated by Roshko (1954), in fact associated with two discontinuous changes "(Williamson 1988b)".The first interruption the frequency of Strouhal decrease from the laminar curve to one interrelated to a mode A3-D shedding, at close Re=180-190. The mentioned interruption is most erotic and exact Re_{crit} depends on whether the flow speed is increased or decreased and on the experimental arrangements, as shown below. When Re increased close to 230-260, there is another interruption in Strouhal number, demonstrate a new mode B. This break may be conflict with the first in that it is not most erotic, and rather incorporate a gradual transfer of energy from mode A to mode B, as one enlarged Reynolds number.
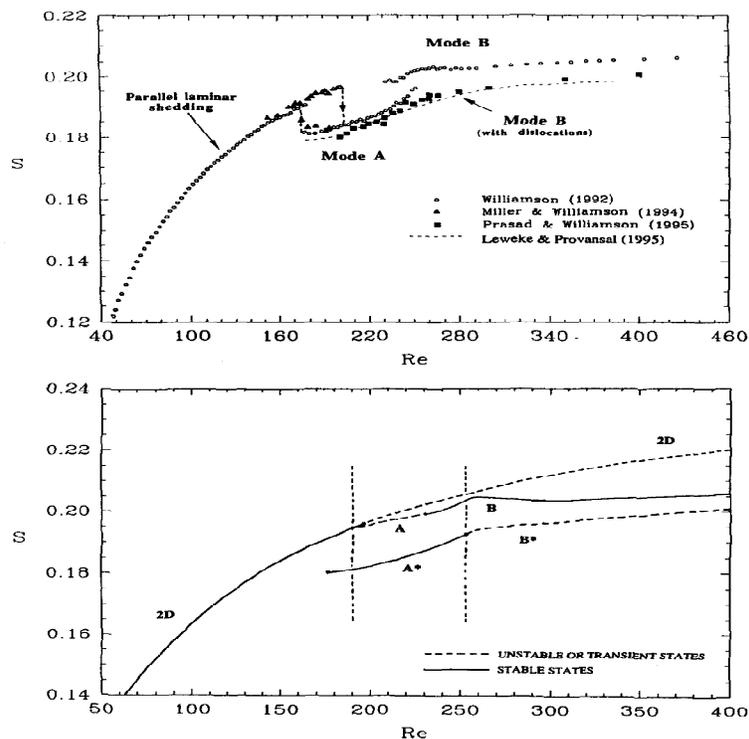
Figure 2.13: Strouhal-Reynolds number relation on laminar and **3-D** transition reign. *(a)*The transition reign is describe by two different stop in the measured wake specification, **as** Re is rise, and possibly cleverly explained with citation to this S-Re plan. *(b)* A fresh analysis of the Strouhal contour; the top contour conform to short scale inconsistency only (like A, B), the bottom one conform to these inconsistency linked with infrequent vortex displacement (like A*, **B***)**. The normal wake transition pursue the order *(2D* + **A*** + B). (plan from **Williamson 1995a.)**

In the transition zone, velocity fluctuation profiles in the wake are distinctly different from those associated with the laminar regime which is shown in figure 2.14. Such as the turbulent flow profile at Re=183, shows a vast proportional peak in the centre plane of the wake as noticeable from the two lower side crest for the Reynolds number Re=52, generally correlate with the two rows of laminar vortices sail downstream. "Williamson (1992a)" exhibit that the presence of vortex disorder produce this large central crest in the profile, in addition to the slow decay of oscillating velocity downstream of the bluff body in fig 6b.the intermittent irregularity which is originally found by Roshko (1954), are shown in figure 2.13(c).
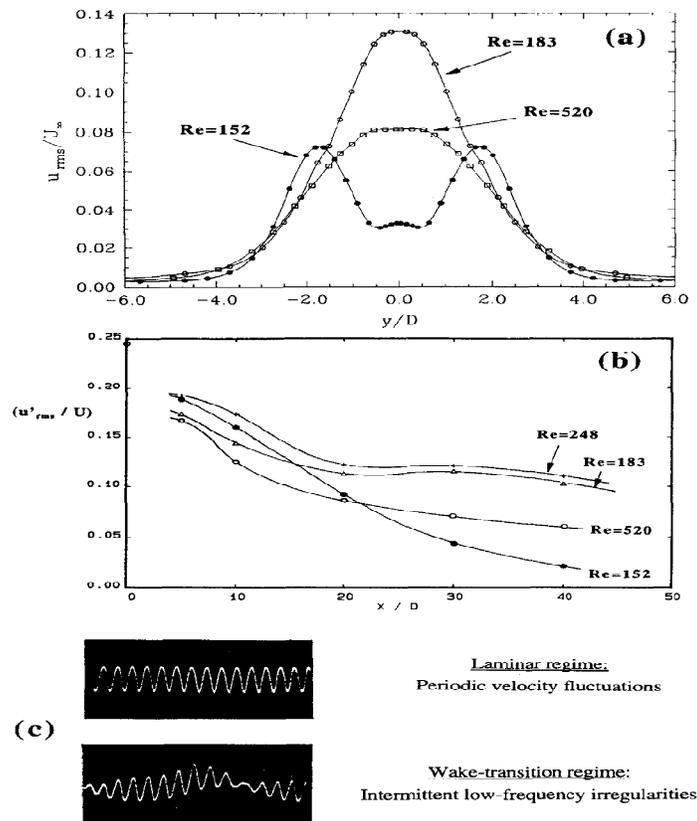
Figure 2.14: Velocity study in the transitional wake. **(a)** The rms velocity oscillation profile measure in both the laminar reign (Re = **152)** and more in the wake-transition reign (Re = 183), at **x / D = 10.** (b) next collapse of normalized rms velocity oscillation, display the exactly various ratio of break-down in the laminar reign (Re = **152)** vs the transition reign

(Re = **1,83,248).** (plan from Williamson 1995a.) **(c)**small-frequency infrequent velocity oscillation sketch and next breakdown plan display in **(a)** and (b). Specific massive variation inconsistencies were initial observed.

The three dimensional inconstancy of the wake of the square cylinder bluff body was investigate by **"Robichaux et al. (1998)"**. Floquet steadiness study is engaged to draw out the various modes of three dimensional inconstancies. It is seen that the three dimensional transition methods for a square cylinder is identical to that of a circular cylinder. Especially the long wavelength(mode A) three dimensional disruption which becomes inconsistent early at Reynolds number of around 161, take the place of by a short wavelength(mode B) three dimensional disruption that becomes inconsistent at a Reynolds number of about Re=190.In adding, a third intervening wavelength mode is also seen to convert into unstable condition at a Reynolds number of about 200.Different mode A and B, the middle wavelength manner is sub-harmonic accompanying a duration of twice the shedding cycle of the two dimensional base condition. The space-time similarities of three models are investigate in detail.

"Thompson et al. (2001)" studied the physical nature of primary transition in bluff body wakes. Based on various suggested mechanism, the probability classification as an elliptical uncertainty is reconstruct in this article. The details of transition Floquet study shows the fair confirmation of the increase elliptic uncertainty in the build vortex centre chased by amplification by the powerful strain field in the hyperbolic zone between the developed and shed vortices. Actually, it arrive that the wake instantly trailing the cylinder display noticeable signs of a coordinated elliptic uncertainty as found long ago for connecting anti-rotating vortices. More downstream, later the vortices have been drop into the wake, the uncertainty again rise in the nucleus.

Dutta et al. (2004) studied the impact of coordination on the wake of a square cylinder at laminar region. The experimental research of flow past a square cross section of cylinder at Reynolds number range of Re=97-187 is stated. Cylinder coordination of 0^0-60^0 with regard to the mean flow have been treated. Two part hotwire anemometry has been take-up for calculations of velocity. The cylinder's wake has been anticipated with a pulsed laser coat to know the flow formation. Calculations have been performed at the near wake, mid wake and far wake of the cylinder. The impact of coordination and Reynolds number on drag coefficient, Strouhal number, time average and rms velocity allocation, collapse of velocity oscillations and power spectra are of concern. The drag coefficient and Strouhal number are

comparing to the angle of cylinder. A variation in the cylinder adjustment experienced to an initial arrival of quasi-periodicity and therefore, three dimensionality, unpaid to the irregular kind of the wake. The structure of the mean velocity portrait, oscillations and the rate of collapse display a active reliance on the cylinder adjustment in the adjacent wake, however dependency decrease in the far wake. In a group of angle considered, the wake of a cylinder whose orientation is 22.5^0 with regard to the incoming flow is unusually energetic and display powerful three-dimensionality.

"Liu et al. (2011)" investigate a two-dimensional (2-D), whirlpool particle technique is carry out, and computation of flows over different bluff bodies are conferred, with a thorough investigation of the flow over rectangular cylinders. Then long-time simulations of flows around square and rectangular cylinders with low to moderate Reynolds numbers are carry out. The arise Strouhal–Reynolds number connection are correlate with experimental and simulation results in the study of literature. For rectangular cylinders, the familiar stepwise difference between   the chord-based Strouhal number and chord-to-thickness ratio is repeat. Then the flow field is survey and compared with experimental investigation. More study with recognize vortices supply fresh judgment inside the shedding method which leads to the stepwise difference of chord-based Strouhal numbers and the frequency vault.

Literature survey suggests that the effects of inlet fluctuation on the transport process over bluff bodies are not covered comprehensively. Only one experimental work "Kondjoyan and Daudin, (1995)"documents the effect of turbulent intensity on circular and elliptic cylinder and no such studies have been performed for square cylinder. Hence investigations of inlet fluctuations in the form of prescribed turbulent intensity are undertaken in this work covering both the laminar and turbulent regimes.

2.2 Studies on augmentation of heat transfer in a channel wall in presence of bluff body

Augmentation of heat transfer is a subject of considerable interest to researchers as it leads to savings in energy and cost. A bluff body can be defined as a body that as a result of it shape has separated flow over a substantial part of its surface. An important

feature of a bluff body flow is that there is a very strong interaction between the viscous and inviscous regions. If we consider that at the moment of starting the flow is attached then the adverse pressure gradient that this flow imposes on the boundary layer will be too great to sustain the attachment.

"Edwards and Alker (1974)" find that the delta winglets provided a higher overall heat transfer enhancement, compare to cube placed on a plate'. Experimental investigation of Doi et al. (1977) shows that the heat transfer is locally enhanced in the region where to neighbouring vortices impose a flow toward the surface and heat transfer locally decreases where the vortices impose flow away from the surface.

The incompressible laminar flow and heat transfer in a 2-D channel with a built in triangular prism was computationally analysed by **"Abbasi et al.(2002)"**. They showed that the use a triangular prism could enhance the heat transfer to the channel walls. Heat exchangers have several industrial and engineering applications. The design procedure of heat exchangers is quite complicated, as it needs exact analysis of heat transfer rate and pressure drop estimations apart from issues such as long term performance and the economic aspect of the equipment. The major challenge in designing a heat exchanger is to make the equipment compact and achieve a high heat transfer rate using minimum pumping power.

"Chattopadhyay (2007)" have numerically carried out the turbulent flow and heat transfer around a triangular prism in a channel in the turbulent flow regime up to the Reynolds 40,000.The aspect ratio between the channel wall to the prism element is 4.0.The Navier–Stokes equation along with the energy equation has been resolved applying SIMPLE method and the standard k–ε model was preferred for turbulence stoppage. Structured grid was used at the entrance and exit domain, the area close to the prism element was discretized by using an unstructured triangular mesh. The results show that in presence of a triangular prism, heat transfer in a channel is enhanced by around 15%. The augmentation in heat transfer is connected to the vortex development downstream of the prism element.

The numerical solutions of a viscous uniform approach flow past square and diamond cylinders, with and without rounded corners was carried out by **"Dalton et al.(2003)"**. The Reynolds number range is 250-1,000. This unsteady viscous flow problem is solved by the 2-D Navier–Stokes equations in vorticity and stream-function form on body-fitted coordinates. The finite difference method is used. Central-difference schemes, Second-order Adams-Bash forth and are used to discretize the vorticity transport equation and a third-order upwinding

scheme is used to represent the nonlinear convective terms. For an efficient mesh system for the flow a grid generation technique is use. The average in-line force coefficients and Strouhal number and agree well with previous numerical and the experimental value. The evolutions of vortex shedding and vortex structures are illustrated by vorticity contours. Rounding the corners of the diamond and square cylinders produced a noticeable decrease on the lift and drag coefficients.

Techniques for heat transfer augmentation are relevant to several engineering applications. These studies demonstrated heat transfer enhancement and can be conveniently categorized in passive and active techniques by "Webb et al. (2005)" and 'Bergeles (1983)" which either harness flow energy or utilize external source of energy to augmentation the heat transfer respectively. The flow pass bluff, rigid bodies such as, rectangular cylinder studied by "Valencia (1995)", inclined square cylinder by "Yoon et al.(2009)", triangular cylinder by "Chatterjee et al.(2012)". Biswas et al. (1992)" and "Hiravennavar et al. (2007)" in a channel.

"Benim et al. (2011)" have been investigated computational analysis of turbulent forced convection in a channel with a triangular prism using cascade of modelling strategies Reynolds Averaged Numerical Simulations (RANS) and two-dimensional Unsteady RANS (2D URANS) are used for the Reynolds numbers (Re) 2,500, 5,000 and 25,000.and the Prandtl number is equal to 0.7 in all computations'. For Re ¼ 2500 and Re ¼ 5000 three-dimensional URANS (3D URANS) and Large Eddy Simulations (LES) are also performed. For the RANS and URANS computations, the Shear Stress Transport (SST) model is used as the turbulence model.

The confined flow and heat transfer across a triangular cylinder in a channel was thoroughly investigated by **"Srikanta et al. (2010)"**. Reynolds number is taken 1-80 and prandtl number of 0.71 for a fixed blockage ratio of 0.25. The governing Navier-Stokes and energy equations along are solved by using a commercial CFD solver FLUENT (6.3). the temperature and flow field are shown by isotherm and streamline, respectively. Average Nusselt number, mean drag coefficient, wake length/recirculation length, etc. are reported here. The transition to transient is found to lie between Re=58 and Re=59. The average Nusselt number and the wake length increase with increasing the value of Reynolds number, though, the mean drag coefficient decreases with increasing the value of Reynolds number. Also, simple correlations for average Nusselt number, wake length, mean drag coefficient are obtained for the range of above Reynolds number.

"Zheng and Zhang (2011)" have been investigated the flow fields in vortex flow sensors with circular cylinder and trapezoidal cylinder bluff bodies'. Also the characteristics of two flow fields are compared by numerical simulations while the mechanism of vortex shedding is analyzed in detail.

Finally, the reason, which leads to different vortex shedding frequency and affects the relationship between Reynolds number and Strouhal number, has been specified as the size of wake flow region behind bluff body where the vortex generated. Steady and unsteady forced convection flow and heat transfer past a long expanded trapezoidal bluff body are investigated for the air as working fluid for Re = 1–150. The wake length increases as the Reynolds number increases in the steady flow regime ($1 \le$ Re ≤ 47). However, heat transfer as well as Strouhal number increases with the increasing value of the Reynolds number.

The maximum augmentation in heat transfer for the expanded trapezoidal cylinder with respect to the tapered trapezoidal cylinder is found to be approximately 146% by **"Dhiman and Ghosh (2013)".**Heat transfer enhancement in duct flow by using an inclined vortex generator has been numerically investigated for the air as working fluid for Reynolds number, Re = 1–150. The wake length rises when the Reynolds number rises in the steady flow regime ($1 \le$ Re ≤ 47). The changeover from steady regime to unsteady regime happen between Re = 47 and 48. The total drag coefficient reduce with the rising the value of Reynolds number up to Re = 90 and then it rise along Reynolds number. Though, heat transfer including Strouhal number rise with the rising value of the Reynolds number. The highest enhancement in heat transfer for the enlarge trapezoidal cylinder with honour to the tapered trapezoidal cylinder is found to be almost 146%. On the alternative side, pressure decline display an augmentation of nearly 97% for the enlarge trapezoidal cylinder when compared with the tapered cylinder. Simple correlations of wake length, average Nusselt number and Strouhal number, drag, with Reynolds number have further been entrenched.

"Torii et al.(2000)" is only study, have found for a diamond shaped cylinder(or a square cylinder with the flow at a 45° angle'.

"Yoon et al. (2009)" has investigated a square cylinder is located on the centreline of laminar channel flow, which is subject to a constant heat flux on the lower channel wall'. As the cylinder is inclined with some angle of attack with respect to the main flow direction, flow characteristics change downstream of the cylinder, and significantly affect heat transfer on the channel wall.
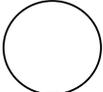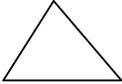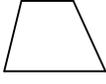
2.3 Objective of the Thesis

After comprehensive survey of literature on above mentioned turbulent promoters of investigations, objective of this thesis has been set to address certain unexplored issues. This work is mainly concerned about the following points:

    i.   To study transport phenomena around bluff bodies at all flow regimes with varying turbulent intensity at the inlet.

    ii.   To compare performance of different bluff bodies e.g. circular cylinder, square cylinder, triangular prism, diamond in heat transfer enhancement in a channel.

    iii.   To study effect of Turbulence Intensity on heat transfer around bluff bodies and also enhancement on channel walls.

    iv.   To study the heat transfer at different confinement ratio and also without confinement.

In this work different shapes of bluff bodies have been considered. They are (1) Square cylinder, (2) Circular cylinder, (3) Triangular prism, (4) Diamond, 5(a) Large edge facing Trapezium,(b) Small edge facing Trapezium,(c) Symmetrically placed which are shown in below .

Some of bluff body are given with the geometry. These are as follows:

Square cylinder	Circular cylinder	Triangular prism	Diamond
Large edge facing trapezium	Small edge facing trapezium	Symmetrically placed	

Chapter

3

Mathematical Methodology

CHAPTER- 3

MATHEMATICAL METHODOLOGY
_____

3.1 Introduction

This work address numerical review of heat transfer enhancement using different shapes bluff body.

This chapter describes the technique with which the solutions were achieve. In most of the literature explain in chapter 2, the flow regime has been independently demonstrated based on whether the flow is laminar or turbulent. Here in this work Reynolds-averaged Navier–Stokes equation (RANS) based approach is used to analysis flow construction of laminar, turbulent and also while in transition from laminar to turbulent.

Since the working fluid, air, is assumed to be Newtonian, the flow of the fluid can be described by the Navier-Stokes equations. Therefore, the heat transfer and fluid flow under consideration are governed by the Navier-Stokes and energy transport equations. The working fluid is considered to be incompressible, and thermal radiation, chemical reaction and compression work are negligible. The Navier-Stokes equations, developed by Stokes and Navier, represent the general behaviour of the fluid. They are continuity, momentum and energy equations.

3.2 Transition Shear Stress Transport (SST) turbulence model

The predictions of turbulent flows can be based on the time-averaged properties of turbulence. The process of time-averaging gives rise to fluctuating temperature and velocities in the conservation equations. These small-scale turbulent fluctuations do not have to be directly simulated. To achieve this, the Navier-Stokes equations are rendered tractable by employing the Reynolds Averaged Navier-Stokes (RANS) equations.

Within the frame work of a RANS approach, the momentum and energy equations are closed by a turbulent viscosity hypothesis, where the turbulent viscosity is obtained via the Transitional SST model of ("Menter et. al. 2002"), allowing a seamless modelling of all three flow regimes by a single formulation. The turbulence model requires the solution of the transport equations of three quantities, namely the turbulence kinetic energy (κ), the specific dissipation rate (ω), the intermittency (γ) and the momentum thickness Reynolds number ($Re_{\theta t}$). Thus, with the three components of the momentum equation, the pressure correction equation (replacing the continuity equation) and the energy equation, the total number of field equations to be solved results in nine.

"Abraham et. al. (2009)" used transition SST model to predict the heat transfer characteristics in all flow regimes i.e., laminar, intermittent and turbulent. The authors used one set of Reynolds averaged conservation equations for mass, momentum and energy with two supplementary equations for turbulent viscosity and effective thermal conductivity and another set for turbulence containing equations to solve turbulent kinetic energy, specific rate of turbulence dissipation and intermittency. This intermittency will help in predicting laminar to turbulent transition. The same Transition-SST model was used for predicting heat transfer in all flow regimes for various heat transfer problems effectively, namely parallel plate channels ("Minkowycz et. al. 2009"), Internal flows ("Abraham et. al., 2010 "and "Abraham et. al., 2011"), diverging conical ducts ("Sparrow et. al., 2009"), and synthetic jets ("Abraham and Thomas 2009").

As the pressure correction scheme, the SIMPLE scheme is used. For the discretization of the convective terms, the Second Order Upwind scheme is used for the momentum and energy equations, and the second Order Upwind scheme for the transport equations of the turbulence quantities. The convergence criteria for continuity, momentum and energy are set at 10^{-4}, 10^{-5}, and 10^{-7} respectively. The convergence criterion for the four turbulence quantities was also fixed at 10^{-4}.

3.3 Governing Equations

The three dimensional governing equations of continuity, momentum and energy equations are solved using transition SST model modified and proposed by **"Abraham et. al. (2009**)". The flow is steady, incompressible Ansys Fluent 16.2 is used to solve the following governing equations.

Continuity equation

$$\frac{\partial u_i}{\partial x_i} = 0 \qquad i=1,2$$

(3.1)

Momentum equation

$$\rho\left(u_i \frac{\partial u_j}{\partial x_i}\right) = -\frac{\partial p}{\partial x_i} + \frac{\partial}{\partial x_i}\left((\mu + \mu_{turb})\frac{\partial u_i}{\partial x_i}\right) \qquad j=1.2$$

(3.2)

Energy equation

$$\left(u_i \frac{\partial \Theta}{\partial x_i}\right) = \frac{\partial}{\partial x_i}\left(\left(\alpha + \frac{v_{turb}}{\text{Pr}_{turb}}\right)\frac{\partial \Theta}{\partial x_i}\right)$$

(3.3)

The values of turbulent Prandtl number (Pr_{turb}) are taken from "Abraham et. al. (2009)". The laminar to turbulent modelling provided by the following equations for K and ω.

$$\frac{\partial(\rho u_i \kappa)}{\partial x_i} = \gamma . P_\kappa - \beta_1 \rho \kappa \omega + \frac{\partial}{\partial x_i}\left(\left(\mu + \frac{\mu_{turb}}{\sigma_\kappa}\right)\frac{\partial \kappa}{\partial x_i}\right)$$

(3.4)

$$\frac{\partial(\rho u_i \omega)}{\partial x_i} = A\rho S^2 - \beta_2 \rho \omega^2 + \frac{\partial}{\partial x_i}\left(\left(\mu + \frac{\mu_{turb}}{\sigma_\omega}\right)\frac{\partial \omega}{\partial x_i}\right) + 2(1-F_1)\rho\frac{1}{\sigma_{\omega 2}\omega}\frac{\partial \kappa}{\partial x_i}\frac{\partial \omega}{\partial x_i}$$

(3.5)

where $\mu_{turb} = \dfrac{a\rho\kappa}{\max(a\omega, SF_2)}$

(3.6)

The working equations for the intermittency and intermittency adjunct function Π adopted [2002, 2009] are given below.

$$\frac{\partial(\rho\gamma)}{\partial t} + \frac{\partial(\rho u_i \gamma)}{\partial x_i} = P_{\gamma,1} - E_{\gamma,1} + P_{\gamma,2} - E_{\gamma,2} + \frac{\partial}{\partial x_i}\left(\left(\mu + \frac{\mu_{turb}}{\sigma_\gamma}\right)\frac{\partial \gamma}{\partial x_i}\right)$$

(3.7)

$$\frac{\partial(\rho\Pi)}{\partial t} + \frac{\partial(\rho u_i \Pi)}{\partial x_i} = P_{\Pi,t} + \frac{\partial}{\partial x_i}\left(\sigma_{\Pi,t}\left(\mu + \mu_{turb}\right)\frac{\partial\Pi}{\partial x_i}\right) \tag{3.8}$$

The equations (3.4), (3.5), (3.7) and (3.8) are the additional equations which are solved along with regular equations of continuity (3.1), momentum (3.2) and energy (3.3) for calculating velocities, pressure, temperature, turbulent kinetic energy, specific turbulent dissipation and intermittency (γ). The state of transition will depend on intermittency parameter (γ) which varies from 0 to 1. Near 0 value of γ determines the state as laminar, while the value near 1 determines the flow as turbulent. The term Π is again required for calculation of term F_1 in eqn. (3.5). The details are available in "Menter et al (2002)".

In equation (3.7) the transition sources are describe as follows:

$$P_{\gamma 1} = C_{a1}F_{length}\rho S\left[\gamma F_{onset}\right]^{c_{\gamma 3}} \tag{3.9}$$

$$E_{\gamma 1} = C_{e1}P_{\gamma 1}\gamma \tag{3.10}$$

Where S is the absolute value of shear strain rate, F_{length} is an empirical correlation which supervision the length of the transition zone, and C_{a1} and C_{e1} grasp the values of 2 and 1, accordingly. The desvastation/relaminarization sources are described as follows:

$$P_{\gamma 2} = C_{a2}\rho\Omega\gamma F_{turb} \tag{3.11}$$

$$E_{\gamma 2} = C_{e2}P_{\gamma 2}\gamma \tag{3.12}$$

Where Ω is the vorticity magnitude. The transition onset is regulated by the following functions:

$$\text{Re}_V = \frac{\rho y^2 S}{\mu} \tag{3.13}$$

$$R_T = \frac{\rho k}{\mu\omega} \tag{3.14}$$

$$F_{onset1} = \frac{\text{Re}_V}{2.193\,\text{Re}_{\theta c}} \tag{3.15}$$

$$F_{onset2} = \min\left(\max\left(F_{onset1}, F_{onset1}^4\right), 2.0\right) \tag{3.16}$$

$$F_{onset3} = \max\left(1 - \left(\frac{R_T}{2.5}\right)^3, 0\right) \tag{3.17}$$

$$F_{onset} = \max\left(F_{onset2} - F_{onset3}, 0\right) \tag{3.18}$$

$$F_{turb} = e^{-\left(\frac{R_T}{4}\right)^4}$$ (3.19)

$Re_{\theta c}$ is the critical Reynolds number where the intermittency first starts to raise in the boundary layer. This happen upstream of the transition Reynolds number $\overline{Re}_{\theta t}$ and the difference between the two must be achieve from an empirical correlation. Both the F_{length} and $Re_{\theta c}$ interrelationship are tasks of $\overline{Re}_{\theta t}$.

The constants for the intermittency equation are:

$C_{a1} = 2; \quad C_{e1} = 1; \quad C_{a2} = 0.06; \quad C_{e2} = 50; \quad C_{\gamma 3} = 0.5; \quad \sigma_{\gamma} = 1.0$

Previous work on slot jet impingement (Kadiyala and Chattopadhyay, 2017, Pal et al., 2018) and duct flow (Bhattacharya et al., 2017) has reported successful deployment of the method employed here.

Skin friction coefficient is also an important parameter, which is a non-dimensional form of wall shear stress and visualizes the type of flow adjacent to the wall.

$$C_f = \left(\frac{\tau}{\frac{1}{2} \times \rho \times U^2}\right)$$ (3.20)

The governing equations along with appropriate closures were solved to obtain time-averaged flow and temperature fields. The solution procedure of Patankar and Spalding (1972) implemented in Ansys Fluent 16.2 was adopted. The details of solution procedure including choice of discretization schemes and convergence criterion are discussed in the following chapters.

For all the computation carried out, special attention was paid to the Y^+ value. The Y^+ parameter were controlled in addition to grid independency check. The value of Y^+ was kept within 1 - 4. For achieving this, sufficiently fine grids were employed. Y^+ is a non-dimensional wall distance obtained by non-dimensionalizing the distance to the wall via the wall shear stress, viscosity and density. Figure 3.1 show the variation of Y^+ values around bluff body wall.
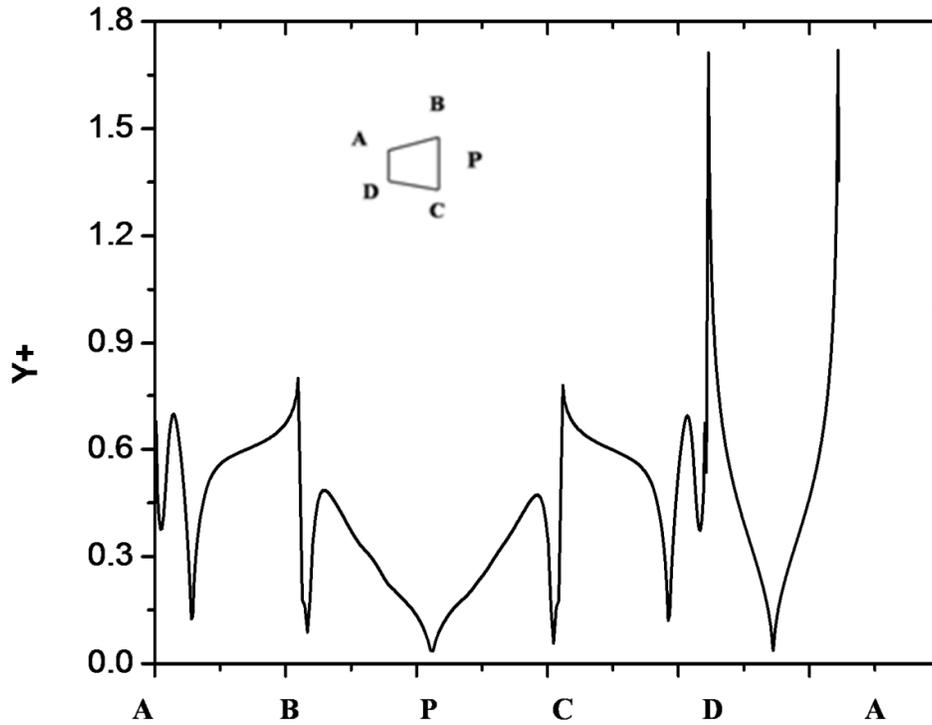
Fig.3.1:Variation of Y$^+$ values

The Nusselt number was calculated according to the following way,

$$Nu = \frac{hD_i}{K}$$
(3.21)

Where, k is the thermal conductivity of air and h is the convective heat transfer coefficient

The Reynolds number based on the hydraulic diameter of the object is given by,

$$Re = \frac{\rho v D_i}{\mu}$$
(3.22)

The friction factor is evaluated by,

$$f = \frac{2}{\frac{L}{D}} \frac{\Delta P}{\rho u_\infty{}^2}$$
(3.23)

Where, ΔP is the pressure drop across the test section and v is the mean air velocity of the duct channel.

"Fan et al. (2012)" defined the thermal enhancement factor, η, as the ratio of the heat transfer coefficient of an augmented surface, f to that of a smooth surface, f_0, at an equal pumping power:

$$\eta = \frac{Nu}{Nu_0} / (\frac{f}{f_0})^{0.33} \tag{3.24}$$

The viscous and pressure forces acting on the both cylinder are used to calculate the drag coefficients. The drag coefficient is given by:

$$C_d = \frac{F_d}{\frac{1}{2}\rho U_\infty^2 d} \tag{3.25}$$

Where F_d is the drag force acting on the cylinder.

Average Nusselt number is obtained by integrating this value over the surface of the cylinder, which is defined as (for circular cylinder):

$$Nu = \frac{1}{\pi}\int_0^\pi Nu(\theta)d\theta \tag{3.26}$$

The Nusselt number which can be found by the local temperature gradient:

$$Nu = \frac{\partial T}{\partial z} \tag{3.27}$$

The pressure co-efficient is defining as:

$$C_P = \frac{P - P_\infty}{\frac{1}{2}\rho U_\infty^2} \tag{3.28}$$

Chapter

4

Transport phenomena over different shapes bluff body

4.1 Introduction

This chapter explains simulation of series of transport phenomena around bluff body. The research was performing to address the effect of turbulence intensity on different shapes bluff body. The results are validated with correlation findings of "Zukauskas (1978)" and "Whitaker (1976)" and with computational results of "Dhiman and Shyam (2011)" and "Dalal et al. (2008)".Among the more discovery of this study, pressure coefficient and surface Nusselt number distribution on different bluff body surface, effect of TI on drag coefficient and intermittency at the exit plane are reported here.

4.2 Computational domain

The first work considers the forced convection cross flow around two bluff bodies, an infinite circular and square cylinder as shown in figure 4.1. While the diameter of circular cylinder is D, for square cylinder D is one side of the square leading to same hydraulic diameter. The non-dimensional distance between the inlet plane and the front surface of the cylinder is 15D and the non-dimensional distance between the rear surface of the cylinder and exit plane is 35D with the total non-dimensional length of the computational domain 50D. The ratio of the width of the cylinder to the vertical distance between the upper and lower walls, H=10D has been used in this work. The problem is considered to be two-dimensional. Air is considered as working fluid for which Prandtl number of 0.71.
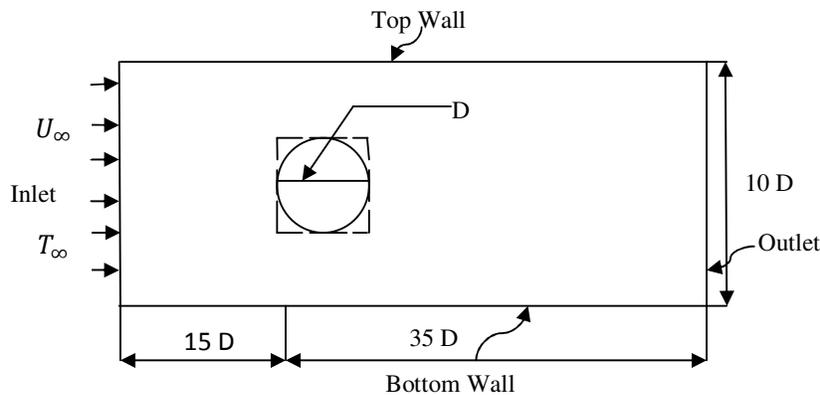

Figure 4.1: Computational domain for flow around a bluff body

4.3 Boundary condition

Fluid approaches to the cylinder with inlet velocity of U_∞ and temperature of the inlet fluid is T_∞ where the cylinder constant surface temperature is maintained about T_s =398 K. The fluid is defined to be air with constant physical properties (Pr=0.71) with an inlet temperature of 298 K. The top and bottom walls are assumed symmetrical where the first derivative vanishes. The domain size is fixed and the fluid properties are also consider to be constant thus the variation of Reynolds number are done by changing the inlet velocity.

4.4 Solution procedure

The three dimensional governing equations of continuity, momentum and energy equations are solved using Transient SST model proposed by Abraham et. al. (2009) were discussed in chapter 3. The governing equations are discretized on a non-uniform structured grid using finite volume method. The governing equations were solved using commercial CFD software ANSYSFLUENT 16.2. The momentum equation was discretized with second order accurate QUICK scheme by "Leonard (1990)" for achieving desired level of accuracy and the energy equation was solved using third-order MUSCL by "Van Leer (1979)" The solutions were assumed to converge when the scaled residual was below 10^{-5} for momentum , 10^{-5} for continuity and 10^{-8} for energy equations. The interpolation of the gradients of and temperature used the third-order accurate scheme and the gradients for intermittency (γ), turbulent kinetic energy, specific dissipation rate, and momentum thickness was done second order accurate upwind scheme**.**

After performing rigorous check for grid independence, adequate numbers of cells were used. The number of cells for the square cylinder case is 210 x 325 and for the circular cylinder a triangular mesh with 55,000 cells was used. It was found that further refinement of grids do not lead appreciable change in results such as drag coefficient and Nusselt number distribution. In proceeding section, validation with experimental and available data from literature is also discussed. A part of the grid is shown in figure 4.2.
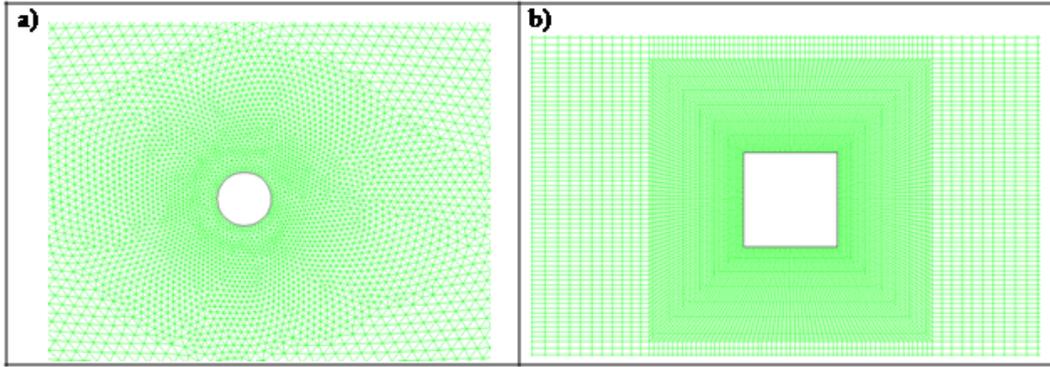
Figure 4.2: Close up view of grids (a) circular cylinder (b) square cylinder

4.5 Results and Discussion

Simulation results obtained for different Reynolds numbers are discussed in this section. The simulations are conducted for Reynolds numbers upto to 200,000. The variation of average Nusselt number with the increase of Reynolds number at particular turbulence intensity is investigated and the increase in heat transfer coefficient with the increase in turbulence intensity is reported. The turbulence intensity varies from 5% to 40%.

4.5.1 Circular Cylinder

Average Nusselt number is obtained by integrating this value over the surface of the cylinder, which is define as

$$\text{Nu} = \frac{1}{\pi}\int_0^\pi Nu(\theta)d\theta \tag{3.29}$$

"Sparrow et al (2004)" had summarized correlations for both circular and non-circular cylinders in cross-flow. In this work, "Zukauskas, (1978)" and "Whitaker, (1976)" correlation for the external flow have been used in this study for verification of SST model simulation results for heat transfer coefficient calculation over the circular cylinders.

$$\overline{Nu}_D = 0.25 + \left(0.4Re^{\frac{1}{2}} + 0.06Re^{2/3}\right)Pr^{0.37} * \left(\frac{\mu}{\mu_w}\right)^{\frac{1}{4}} \tag{3.30}$$

Where μ is the dynamic viscosity of the air and μ_w is the dynamic viscosity at the wall.

Figure 4.3 shows variation of Nusselt number for a fixed value of turbulence intensity of 5%.The CFD simulation is performed for Reynolds number of 500 to 200,000 and the results shows good agreements with the correlation mentioned above.
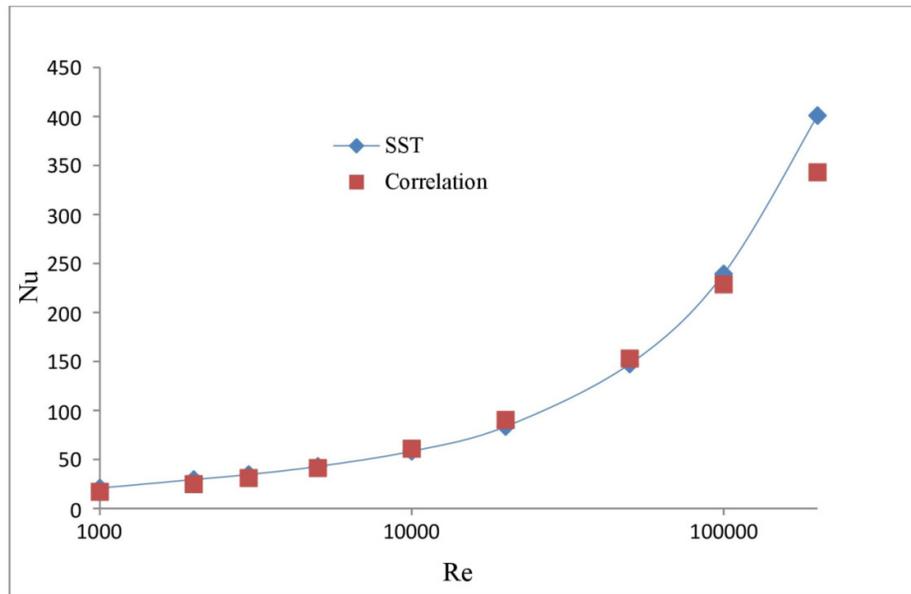
68

Figure 4.3: Validation of average Nusselt number with correlation

The predicted heat transfer rate is in good agreements with the experimental correlation prediction with a quantitative error of not more than 10% up to Reynolds number of 5,000.whereas at so higher value of Reynolds numbers the results shows less error with experimental correlation prediction and almost merge with the data from experimental correlation prediction.

Influence of turbulence intensity on Nu

The influence of turbulence intensity on Nusselt number had been studied by "Kondjoyan and Daudin (1995)", who worked out the dependence of Nusselt number on turbulence intensity for a lower range of Reynolds number albeit for circular cylinder. In this present work the increase in Nusselt number has been recorded with increase in Reynolds number for the turbulence intensity levels of 5%, 10%, 15%, 20% and 40%. From figure 4.4 it is clear that for low value of Reynolds number the turbulence intensity is not affecting significantly the heat transfer rate but when the value of Reynolds number is more than 20,000 there is noticeable increase in heat transfer coefficient .The Nusselt number is more or less same up to Reynolds number 8,000. But beyond this value of Re, Nusselt number increases prominently with increasing turbulence intensity. For example, at Re= 20,000 Nu increases from 75 to 100 when TI changes to 40% from 5% respectively. However at Re = 100, 000, Nu changed from 220 to 420 when TI changes from 5% to 40%. Thus the level of

enhancement can be as high as 80% with imposition of high turbulent intensity. This is in agreement with the results of "Kondjoyan and Daudin (1995)" though they have worked till Re of up to 50,000.
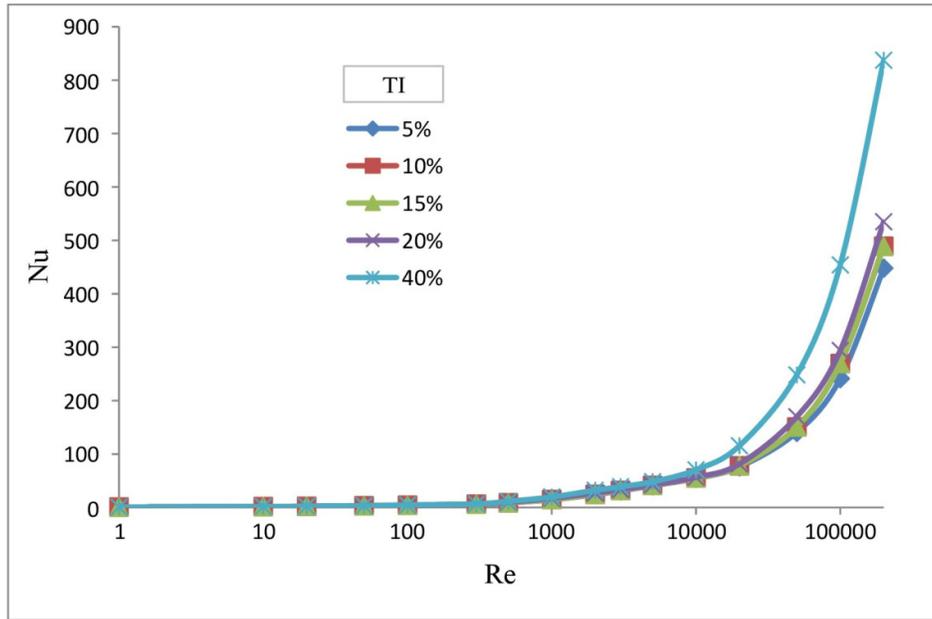

Figure 4.4: Effect of turbulence intensity on Nu

Variation of local Nusselt number over the cylinder surface

Figure 4.5 shows the variation of local Nusselt number over the cylinder for the value of Reynolds number 1,000 to 100,000 with turbulence intensity of 5%. The distribution is plotted for the one half of the cylinder. For all levels of Reynolds number, the stagnation Nusselt number has local minima (Θ=0) though it increase slightly nearer to 60^0 to 90^0 but beyond that this value very sharply drop. It is also seen that with increasing Reynolds number the separation point observed by looking at the local minima is shifting towards the rear side of the cylinder.
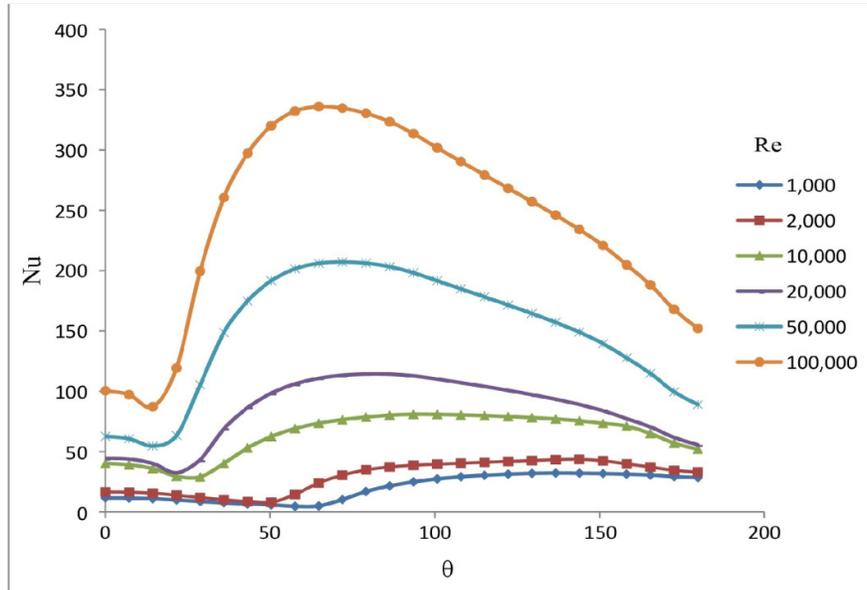
Figure 4.5: Variation of local Nusselt number over the cylinder surface at TI = 5%

Variation of local Nusselt number with turbulence intensity

The variation of local Nusselt number over the cylinder at a particular Reynolds number with the increase in turbulence intensity has been shown in the figure 4.6. Figure 4.6 (a) shows the variation of local Nusselt number at a Reynolds number of 10,000 with turbulence intensity of between 5% to 40%. From figure it is observed that with the increase in turbulence intensity the point of separation does not change much but the value of local Nusselt number at stagnation point increases rapidly. Same type of graphical agreement found for all Reynolds number simulated. To see this result whether the same pattern followed or not for higher Reynolds number, authors have plotted to show the variation of local Nusselt number at Reynolds number equals to 100,000. The effect of increasing turbulent intensity is found to particularly affect the rear half of the cylinder ($90 - 270^0$) where the magnitude of Nu increases significantly with increase in inlet turbulence. The highest change is noticed at the rear stagnation point.
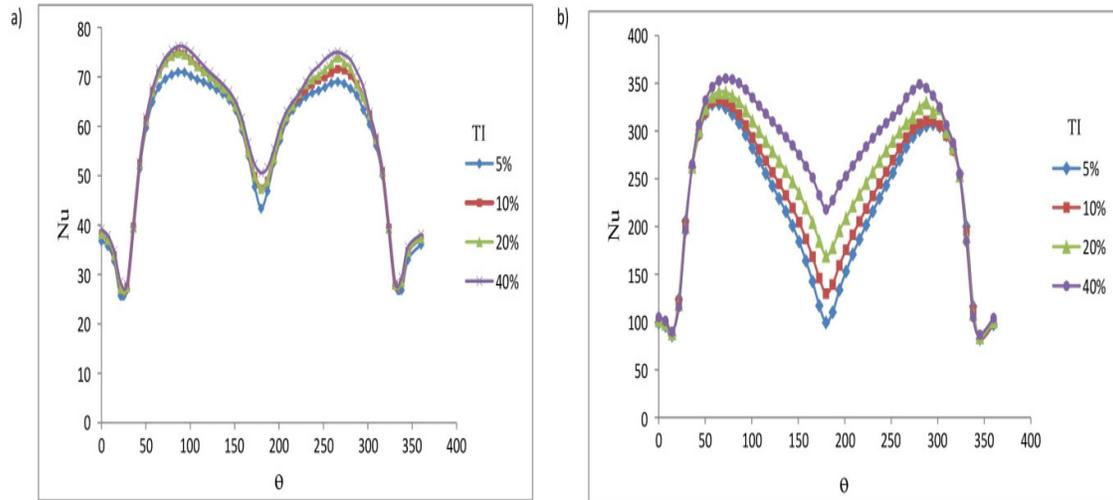
71

Figure 4.6: Local Nusselt number over the cylinder surface (a) Re=10,000 and (b) Re = 10^5

Azimuthal variation of C_p at different Reynolds number

Figure 4.7 shows the validation at low Re with the work of "Park et al. (1998)" which shows reasonably good agreement with the present computation for Re between 10 - 40. where pressure coefficient is given by $C_P = \frac{(p-p_\infty)}{\frac{1}{2}\rho u_\infty^2}$. In figure 4.8, C_p is presented for higher levels of Re upto 2 x 10^5. At large Re about 50,000 to 200,000, C_p value over -2 can be observed at about 90^0.
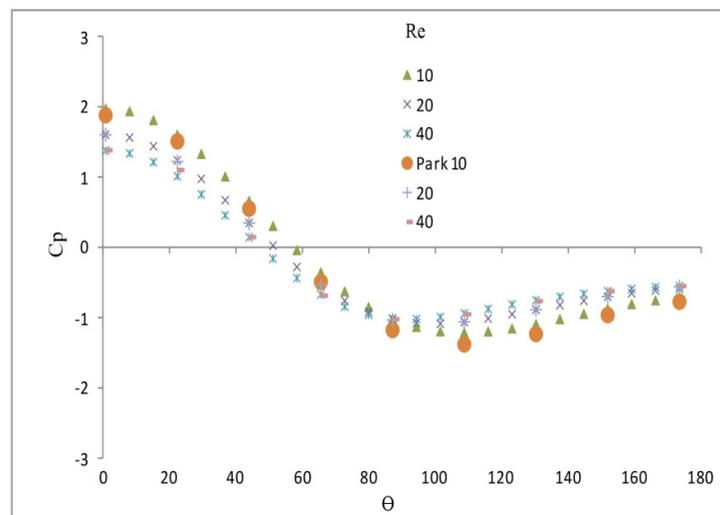
Figure 4.7: Validation of C_p
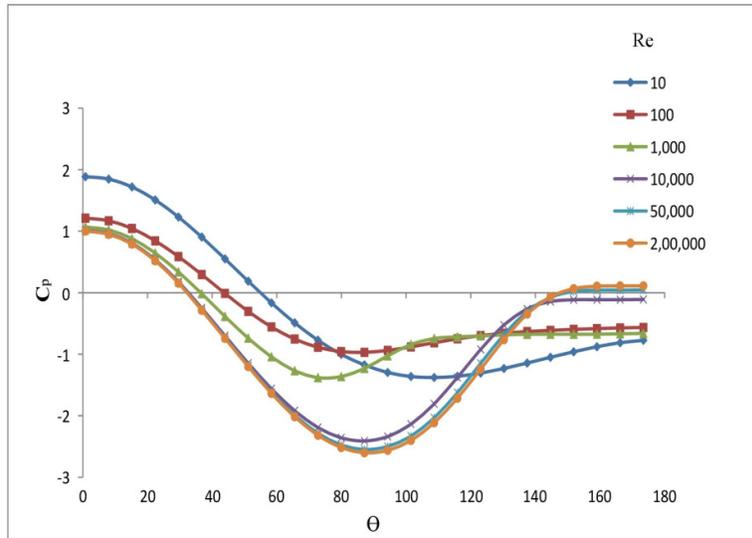
Figure 4.8: Variation of C_p over the cylinder at different Reynolds number

Effect of turbulent intensity over pressure coefficient

Looking at figure 4.9, it can be observed that C_p is about 1 at the stagnation point which gradually goes on reducing and at 90^0 its show maximum negative magnitude of around 2.5. After the topmost part i.e. 90^0 , the C_p value starts increasing and reaches zero at about 150^0. On increasing the value of TI there is insignificant changes in the local distribution of pressure coefficient.
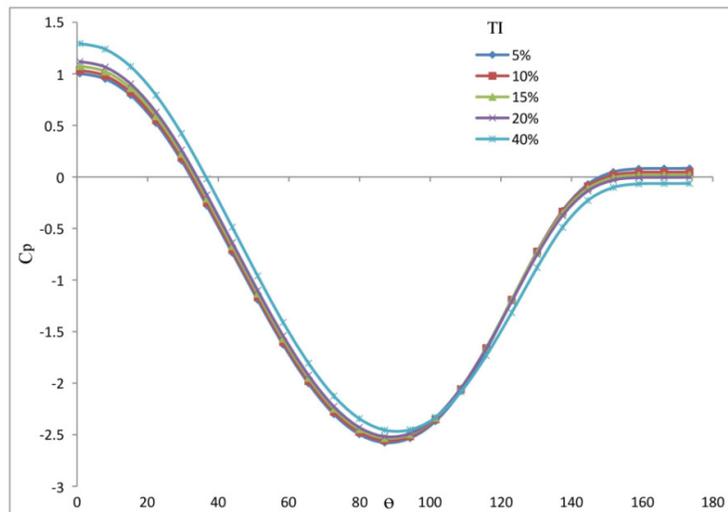
Figure 4.9: Azimuthal variation of C_p at different TI

Drag coefficient

The overall drag coefficient for the circular cylinder for various Reynolds number is shown in figure 4.10 which shows that for lower value of Reynolds number the drag coefficient decrease up to Re=100. Further on increasing Re value beyond 100, again C_d values reduces up to Re 1,000 but with a lower slope. For Reynolds number beyond 10,000, C_d value is almost same up to 100,000. For example while Re changes from 1 to100, the C_d value decrease from 5.698 to 1.498. However C_d values are 0.581 to 0.167 for Re 2,000 and 100,000 respectively. It is also seen that the present result is slightly higher compared to that of "Park et al. (1998)" up to Re 80 beyond which C_d is almost constant at about 1.7.
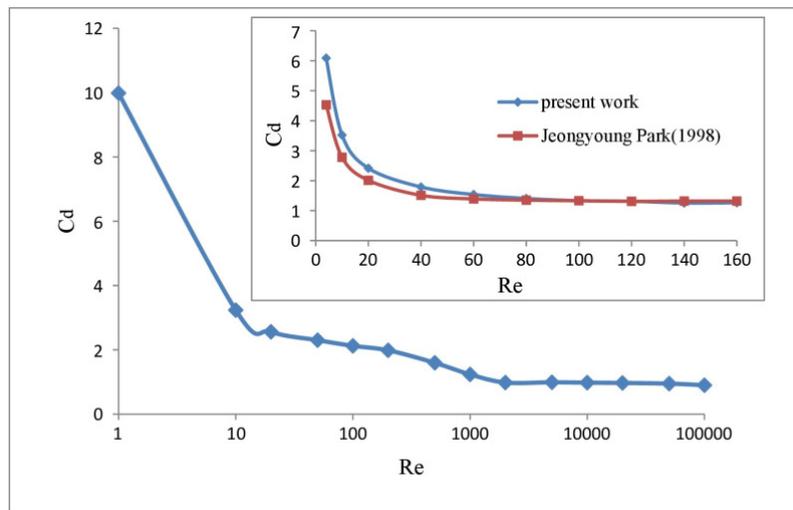

Figure 4.10: Effect of Reynolds number on C_d for circular cylinder

4.5.2 Square Cylinder

Influence of turbulence intensity on the heat transfer coefficient

The influence of turbulence intensity on Nusselt number had been studied by "Kondjoyan and Daudin (1995)" for circular cylinders only. In this present work the increase in Nusselt number has been recorded with increase in Reynolds number for the turbulence intensity of upto 40% for a square cylinder. From the figure 4.11 it is clear that for low value of Reynolds number the turbulence intensity is not much increasing the heat transfer rate but when the value of Reynolds number is more than 20,000 there is higher increasing rate in heat transfer coefficient .The Nusselt number is more or less same up to Reynolds number 10,000. But beyond this value of Re, Nusselt number increases prominently with increasing turbulence

intensity. For example, at Re= 20,000 Nu increases from 77 to 110 for TI of 5% and 40% respectively. However at Re = 1 00, 000, Nu changed from 248 to 450 when TI changes from 5% to 40%.
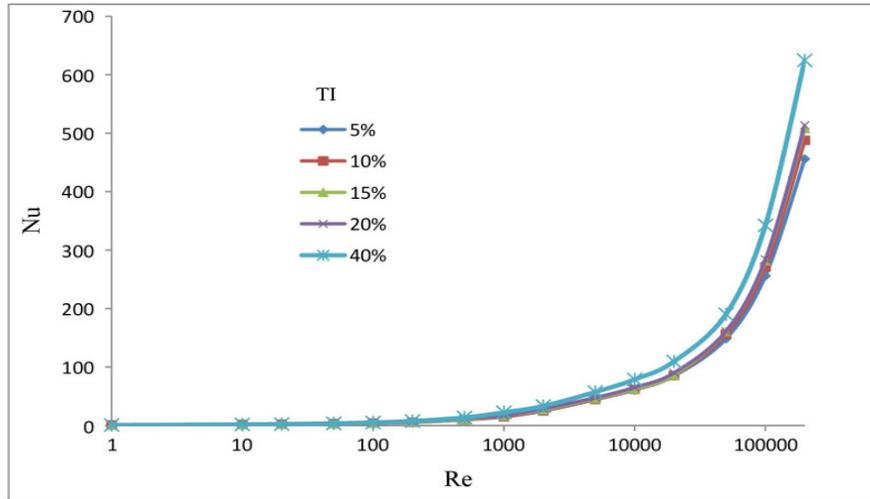

Figure 4.11: Effect of turbulence intensity on overall heat transfer

Variation of local Nusselt number with Reynolds number

Figure 4.12 shows the variation of local Nusselt number over the cylinder surface for the value of Reynolds number 100 to 200,000 with turbulence intensity of 5%. At low turbulence intensity Nusselt number is increasing gradually and it is maximum at rear surface of the cylinder which can be attributed to the strong vertical flow structure at the rear wake. As such at low levels of Re (e.g. 100) heat transfer at the rear surface is rather marginal.
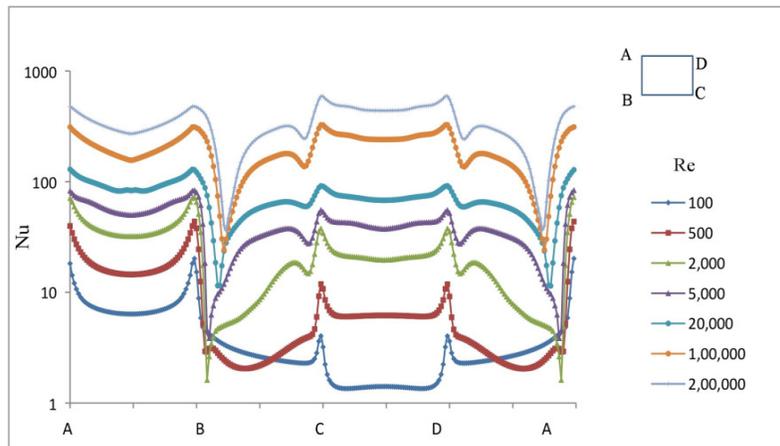

Figure 4.12: Variation of local Nusselt number over the square cylinder at TI = 5%

75

Variation of drag co-efficient with Reynolds number

The overall drag coefficient for the square cylinder for various Reynolds number is shown in figure 4.13 which shows that for lower value of Reynolds number the drag coefficient decrease up to Re=100. Further on increasing Re value beyond 100, again C_d values gradually increases up to Re 1,000 .But beyond that Reynolds number C_d values is almost same up to Re=200,000. For example .Re=1-100, the C_d value decrease from 5.698 to 1.498. However C_d values from 1.614 to 1.757 for Re 2,000 and 200,000 respectively.

The inset figure here shows the variation of drag coefficient with Re in the low range of Re upto 40. It is observed that drag coefficient obtained in the present work is slightly upper up to Re 15 compared to "Sharma (2004)" and "Okajima (1997)" after that for all the Re value the C_d value is almost same. The capability of the model is thus demonstrated for laminar regime.
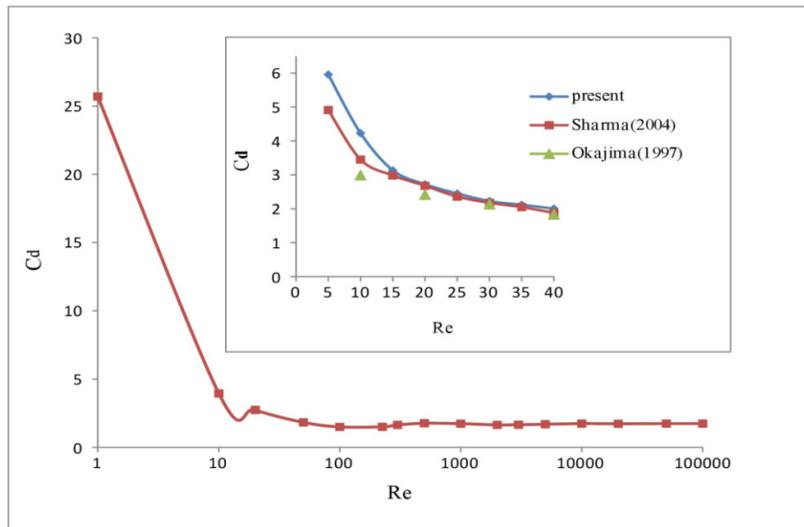

Figure 4.13: Variation of drag co-efficient with Reynolds number for square cylinder

Variation of local Nusselt number over the cylinder length with turbulence intensity

The variation of local Nusselt number around the cylinder at a particular Reynolds number with the increase in turbulence intensity has been shown in the figure given below. Figure 4.14(a) shows the variation of local Nusselt number at a Reynolds number of 10,000 with turbulence intensity of 10%, 15%, 20%, and 40%.The local values of the Nusselt numbers are the highest on the front surface (with respect to the incoming flow) of the cylinder for all turbulence intensity, indicating the highest heat transfer on the front surface compared to other surfaces of the cylinder. A symmetric Nu number distribution is observed on the top(BC) and bottom (DA) surfaces of the cylinders The corresponding Nu is minimum at the midpoint and maximum close to the corners. Since the heat transfer rate is closely related to the flow field, the local heat transfer rate is minimum where the velocity magnitudes are relatively small.
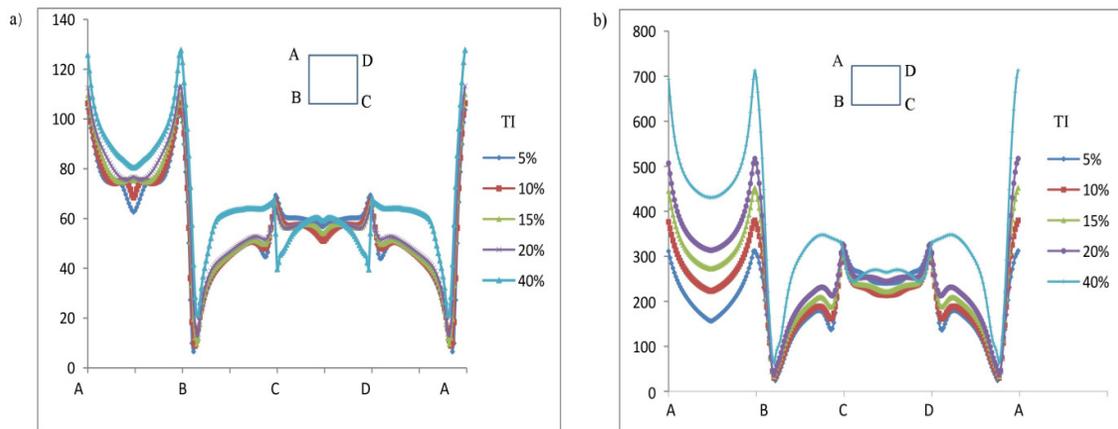

Figure 4.14: Variation of local Nusselt number over the cylinder with turbulence intensity at (a) Re=10,000 and (b) Re=100,000

Same type of graphical agreement found for all Reynolds number simulated. Another curve showing the variation of local Nusselt number over the entire cylinder at Reynolds number equals to 100,000 which is shown in figure 4.14(b) above.

Variation of drag coefficient with Re at different turbulence intensity

The drag coefficient C_d vs. Re is plotted in figure 4.15 which shows that initially there is strong descent in C_d value upto Re about 10. Thereafter there is a gradual decrease in drag coefficient while moving up to around Re 100 and on further increase in Re value there is no such commendable variation of C_d value, i.e. C_d value becomes more or less constant. It is

also observed that with varying percentage of TI there is no appreciable changes in C_d value at all Re as observed for the case of pressure coefficient of circular cylinder also.
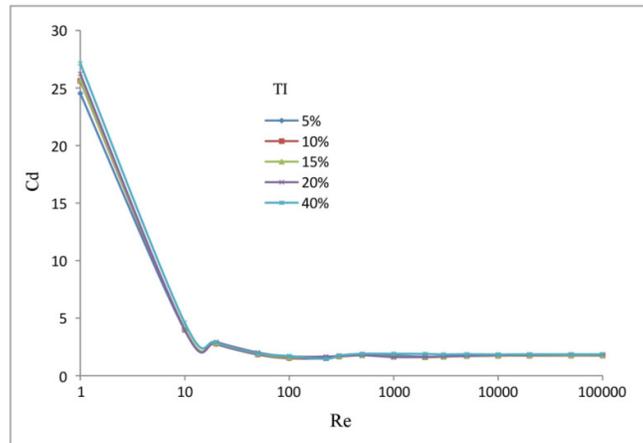

Figure 4.15: Variation of C_d vs. Re at different TI for square cylinder

Variation of C_p over the cylinder

The C_p value as seen in figure 4.16 shows a parabolic curve for flow over surface AB which depicts a gradual symmetrical rise in C_p value from its minimum range around -1.5 to its maximum magnitude of about 1.2 in the positive x-y plane. After reaching this maximum, the C_p value again decreases gradually. it has been observed that the C_p value pattern is similar while flow takes place over the surface AD and BC. In the rear surface CD, the variation is not strong as it has low level of local velocity.
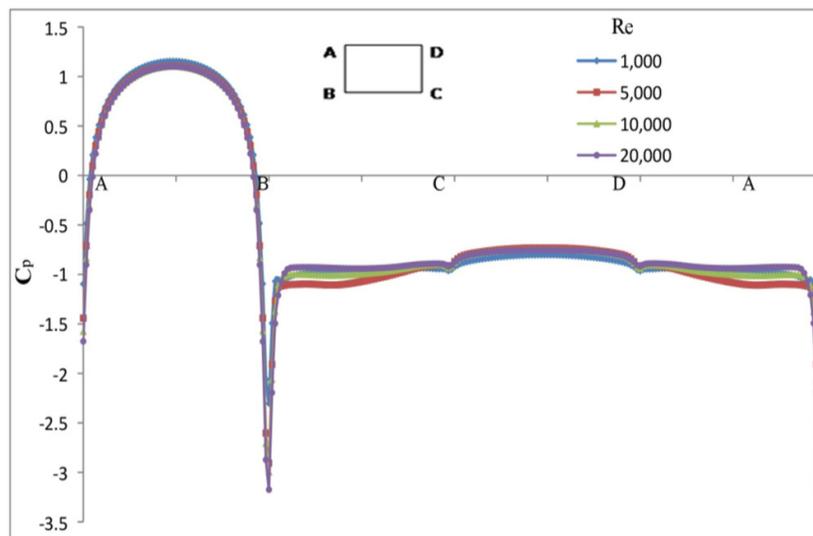

Figure 4.16: Variation of C_p over the cylinder at different Re

Variation of intermittency at outlet boundary

It has been mentioned that the present methodology of "Menter (2013)" can cover all flow regimes seamlessly. For this an intermittency value at inlet is prescribed which is dampened to near-zero value for predominantly laminar flows and approaches unity for turbulent flow. In figure 4.17 intermittency value at the central point of the exit plane is monitored. It can be seen that the intermittency value gradually increasing and value of intermittency is 1.0 for Re above 10,000.
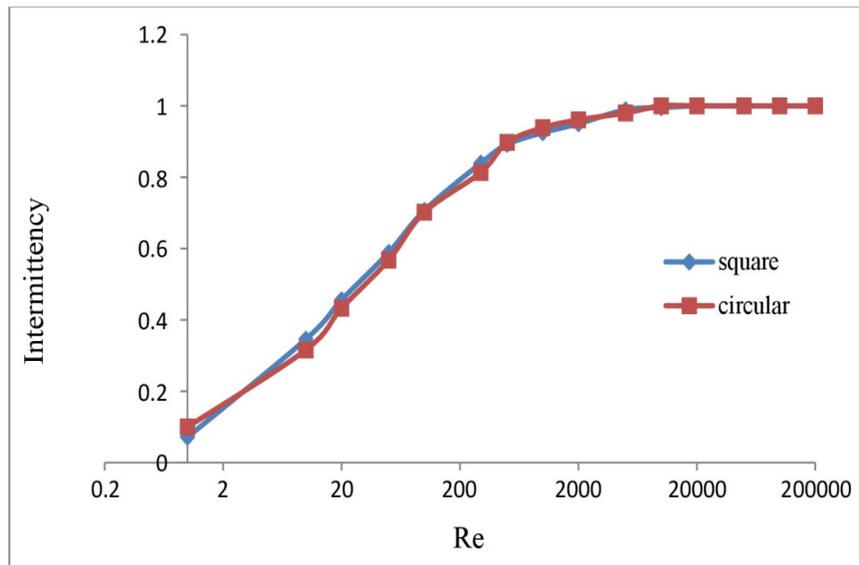

Figure 4.17: Variation of intermittency with Re

Effect of confinement

We have performed simulation for unconfined cases by using vanishing derivatives on top and bottom surfaces. However, the effect of confinement sometimes may be important particularly when the H/D is low. In the present case of H/D = 10, as seen in figure 4.18, confinement does not change the result. To simulate confinement, on top and bottom no slip condition was e prescribed. Figure 18 shows variation of Nusselt number for a fixed value of turbulence intensity of 5%.. The CFD simulation is performed for Reynolds number of 1 to 200,000 and the curve shows perfect agreement between the case of confined flow and unconfined flow. Thus for the given blockage ratio of 10.0, confinement has no effect.
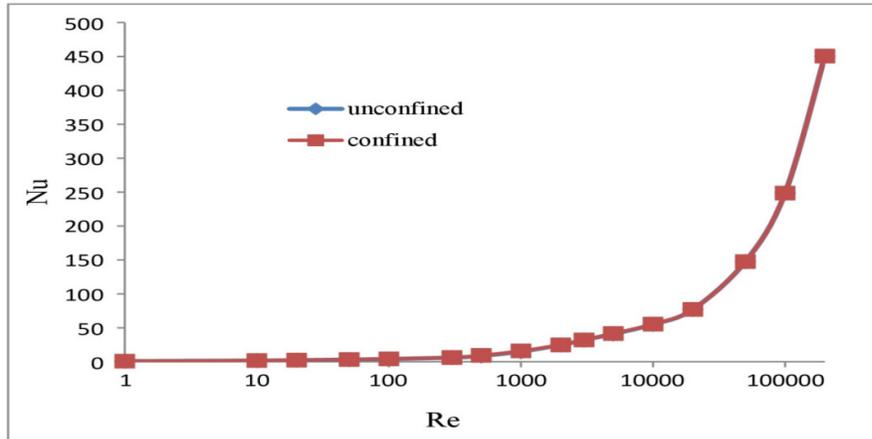
Figure 4.18: Effect of confinement on Nu-Re curve

4.6 Summary

A transition-SST model which yielded promising results in predicting heat transfer under all conditions namely laminar, intermittent and turbulent conditions proposed by Abraham et. al. (2009) is used for the present study. The heat transfer prediction is achieved seamlessly from, laminar to turbulent using the same model. Heat transfer over bluff bodies in the form of circular and square cylinder are studied in this work in a wide range of Reynolds number. The study quantifies the effect of turbulent intensity on local Nusselt number as well as the averaged. The drag coefficient and pressure coefficient are not significantly affected by inlet turbulent intensity.

4.7 Introduction

Another work is performed using different shape bluff body like, equilateral triangular prism, diamond shape bluff body and three orientation of trapezium shape bluff body.

4.8 Computational domain

The present work considers the forced convection cross flow over triangular cylinder prism (TP), diamond and trapezoidal cylinder as shown in figure 4.19 (a), (b). The hydraulic diameter D of the triangular cylinder is the non-dimensional length. The total non-dimensional length of the computational domain is 50D. The ratio of the width of the cylinder to the vertical distance between the upper and lower walls, H=10D has been used in this work.
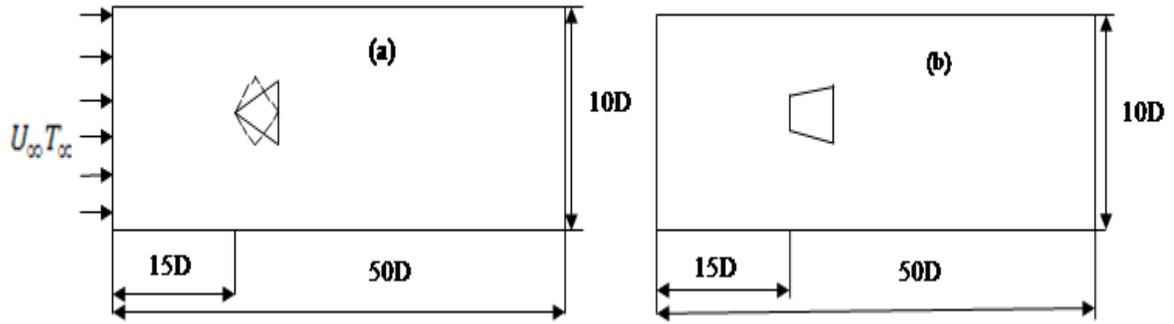
Figure 4.19: Computational domain (a) Triangular prism and diamond (b) small edge facing trapezium (all bluff bodies have the same hydraulic diameter)

The boundary condition and solution procedure are same which discussed in section 4.3 and 4.4.

Figure 4.20 shows the grid layouts close to different bluff body. After performing rigorous check for grid independence, adequate numbers of cells were used. The number of nodes is 157,368 for the case of TP. Structured meshes are used throughout the domain. The number of nodes is 348,080 and 502,200 for the case of diamond and trapezium respectively. Wall y^+ of the surface of the bluff bodies varies from 0.1 to 5 which are within the recommended limit.

Rigorous grid independence studies were conducted for all the bluff bodies. The profiles of parameters like Nusselt number and skin friction coefficient were calculated and compared for three levels of grids and finally a grid size is taken which results in a profile where the values are within 1-2% of the extrapolated profile obtained from three grid levels.
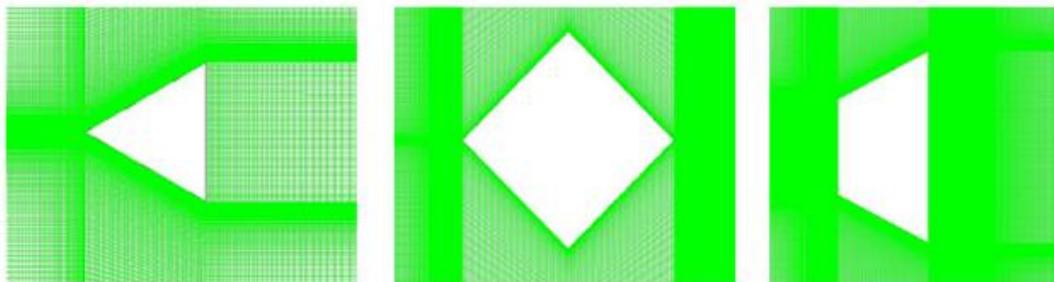

Figure 4.20: Close up view of grids (a) Triangle prism, (b) Diamond, and(c) Trapezoidal shape bluff body

4.9 Results and Discussion

The results that obtained after the simulation performed with the several Reynolds numbers are discussed in this section. The simulations are control for Reynolds numbers upto to 200,000. The difference of average Nusselt number with the rise of Reynolds number at specific turbulence intensity is examined and the rise in heat transfer coefficient with the rise in turbulence intensity is stated. The turbulence intensity alters from 5% to 40%.

4.9.1 Triangular prism

Figure 4.21 provides the validation of Nu with respect to Re that ranges from 50-150.From earlier literatures it has been observed that the Nu of the present work is in accordance with "Dhiman, Shyam (2011)" and "Dalal (2006)".It shows a gradual increasing Nu as Re increased.
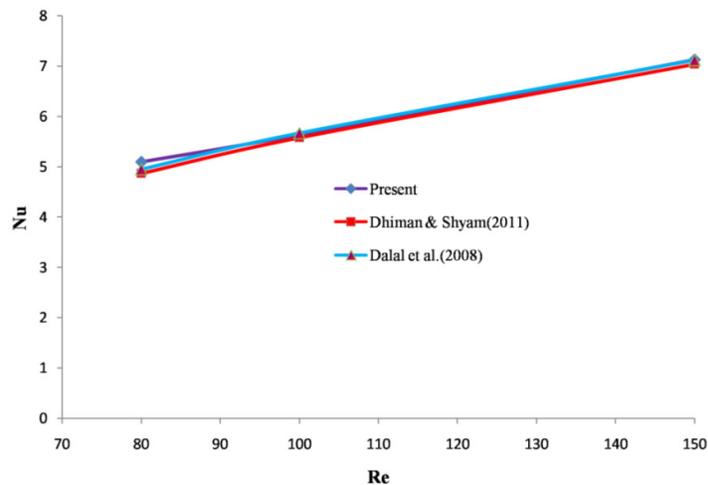

Figure 4.21: Validation of Nusselt number

The influence of turbulence intensity on Nusselt number had been studied by "Kondjoyan and Daudin (1995)", who worked out the dependence of Nusselt number on turbulence intensity for a lower range of Reynolds number. In this present work the increase in Nusselt number has been recorded with increase in Reynolds number for the turbulence intensity levels of 5%, 10%, 15%, 20% and 40%. From figure 4.22 it is clear that for low value of Reynolds number the turbulence intensity is not affecting significantly the heat transfer rate but when

the value of Reynolds number is more than 10,000 there is noticeable increase in heat transfer coefficient. The Nusselt number is more or less same up to Reynolds number 8,000 at all levels of inlet turbulent intensity. But beyond this value of Re, Nusselt number increases prominently with increasing turbulence intensity.
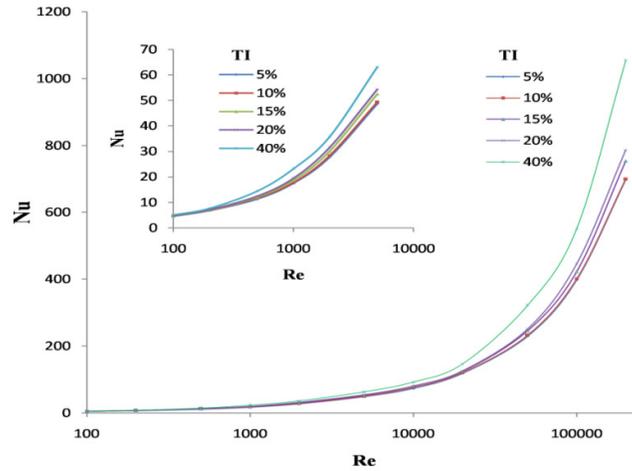

Figure 4.22: Effect of turbulence intensity on Nu

Figure 4.23 depicts variation of local Nu over the triangular cylinder for lower Reynolds number. At point A Nu has been observed to be maximum. In the face BC the Nu falls sharply and then again rises parabolically and gradually falls upto point C. From C to A it has been observed that there is in steep rise in Nu then again the pattern of variation follows the reverse path as A to B point. It has been also observed that the Nu shows higher value at each corner of the triangle relative to their adjacent sides. On considering different values of Re the Nu for each case increases slightly.
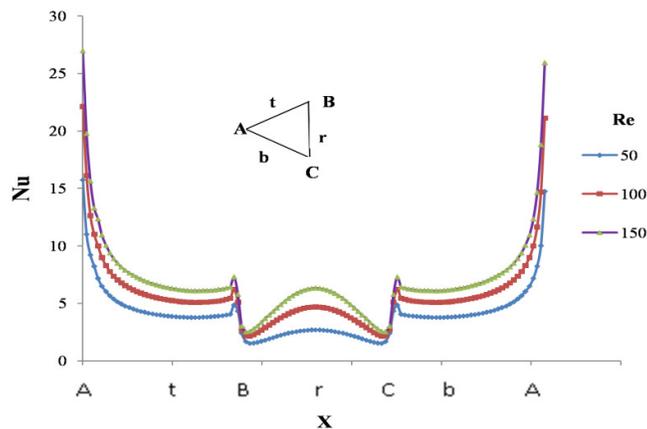
Figure 4.23: Variation of local Nusselt number over the triangular cylinder at low Reynolds number

In fig 4.24. the variation of Nu of the flow across the triangular cylinder has been plotted for range of Re from 500-100,000.As increasing the Re the Nu also increases. As the flow moves A to B there is a gradual fall of Nu and same pattern of the plot has been observed when moving from C to A. As the flow reaches closer to B. There is a steep rise in Nu and it more or less remain unchanged from B to C likewise as the flow comes closer to point C there is again symmetrical steep fall in Nu as seen in the case of point B. It has been documented that heat transfer rate is higher of rare face BC due to vortex formation.
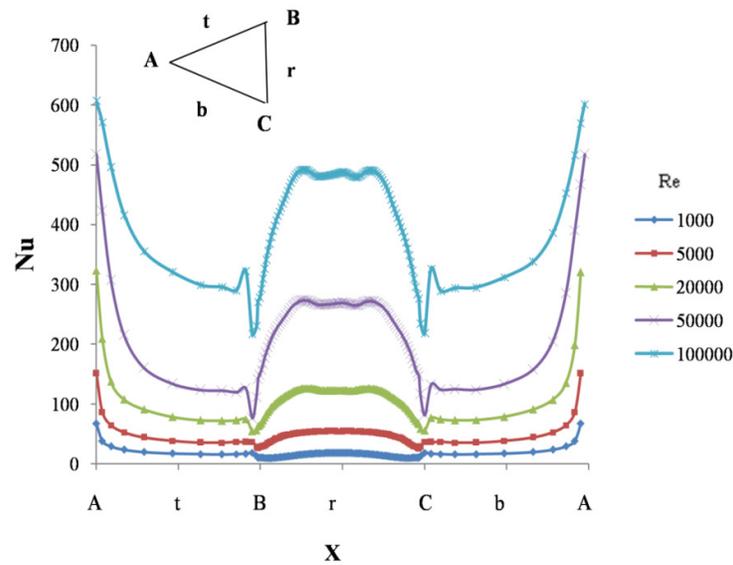

Figure 4.24: Variation of local Nusselt number over the triangular cylinder at TI = 5% with different Re

Figure 4.25 depicts variation of surface Nusselt number along the prism surface of different TI at low Reynolds number. It is observed that heat transfer increased in the entire TP surface as turbulence intensity increases. The rate of enhancement is similar through upper and lower slant sides (i.e. AB and AC) but maximum change is observed at the rear side of the TP.
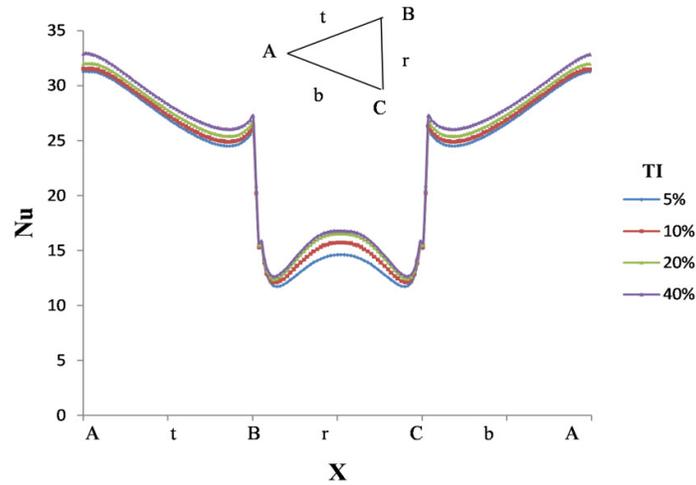
Figure 4.25: Variation of local Nusselt number over the triangular cylinder of different TI at Re=1,000

Fig. 4.26 show the Nusselt number distribution over the triangular prism with different turbulence intensity at fixed Re=20,000.The Nu value gradually decreases before point B, after that heat transfer suddenly decrease close to the point B. It is very interesting to note that unlike the case at Low Re, now at the slant surface BC the Nu value decreases with increasing turbulence intensity. The similar pattern is observed in the face CA being a symmetric surface. It is also seen that Re is proportionally varies with turbulence intensity in the face AB and AC.
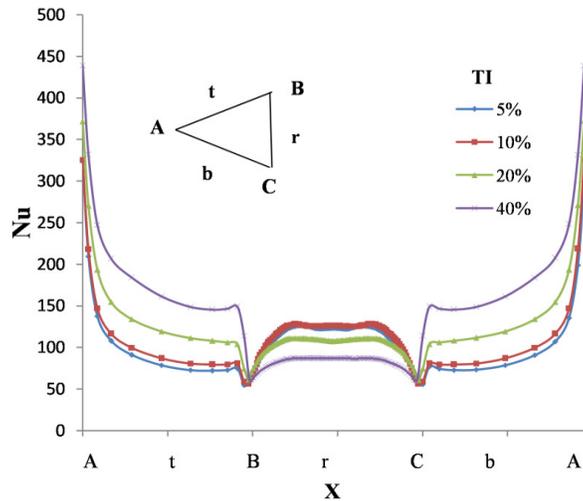

Figure 4.26: Variation of local Nusselt number over the triangular cylinder of different TI at Re=20,000

The plots at Fig. 4.27 show the surface Nusselt number distribution over the triangular prism at different turbulence intensity at high Reynolds number (Re=200,000).The curves show the high heat transfer on rare face BC due to vortex interaction. Heat transfer increases with increasing Re at all the surfaces.
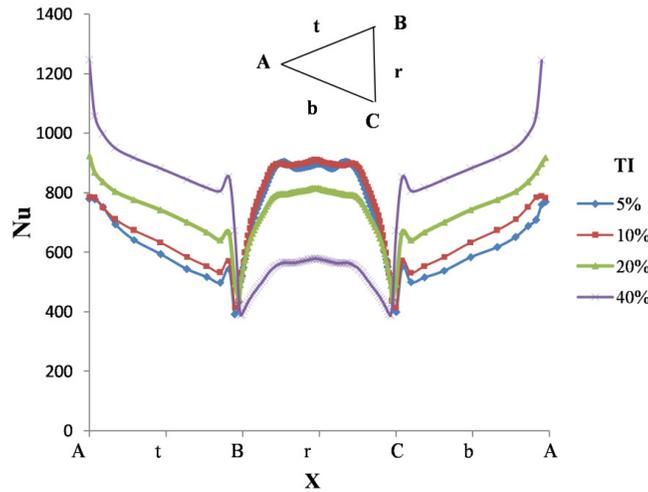

Figure 4.27: Variation of local Nusselt number over the triangular cylinder at different TI with Re=200,000

The drag coefficient C_d vs. Re is plotted in figure 4.28 which shows for different turbulent intensity. It is also observed that with varying percentage of TI there is appreciable changes in C_d value at all Re observed.
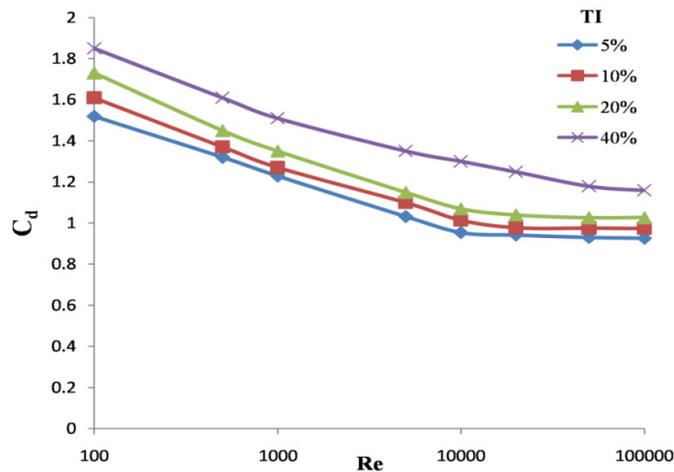

86

Figure 4.28: Variation of drag coefficient with Re at different turbulence intensity for triangular prism

4.9.2 Diamond

In fig. 4.29 show the effect of turbulence intensity on Nusselt number at different range of turbulence intensity. The value of Reynolds number is more than 10,000 there is a noticeable increase in heat transfer coefficient. The Nusselt number is more or less same up to Reynolds number 5,000. But beyond this value of Re, Nusselt number increases significantly with increasing turbulence intensity.
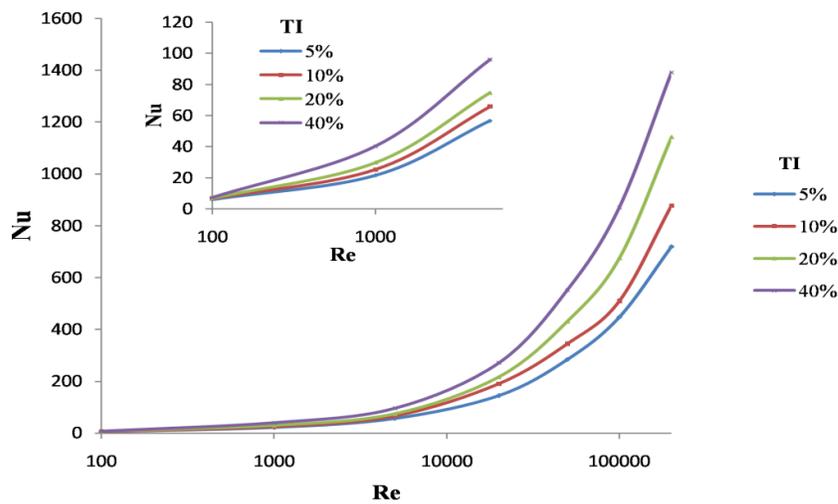
Figure 4.29: Effect of turbulence intensity on Nu

In fig Figure 4.30 the variation of Nu of the flow across the diamond cylinder has been plotted for range of Re from 500-100,000.As increasing the Re the Nu also increases. As the flow moves A to B there is a gradual rise of the Nu. The same pattern of the entire plot has been observed when moving from D to A. As the flow reaches closer to B, there is a steep rise in Nu which again slightly decreases and gradually fall closer to C, likewise as the flow comes to point C there is again steep rise in Nu. The entire plot of the upper half is symmetric with the lower half. Beyond the point B and D, there is a higher heat transfer due to vortex formation.
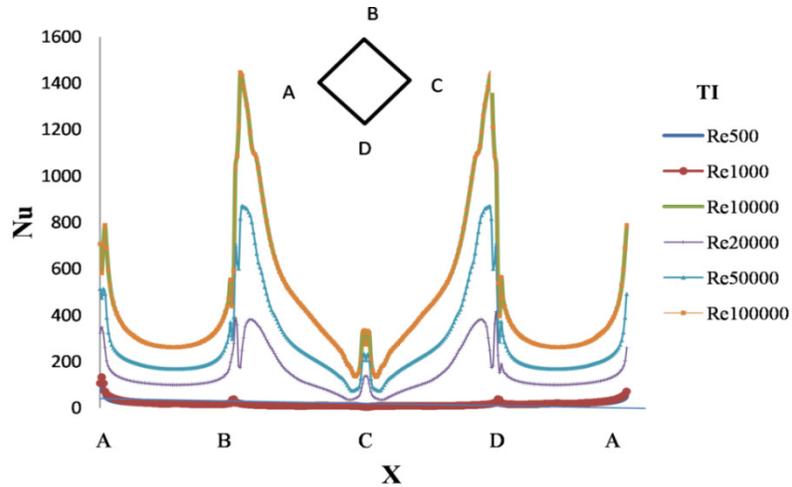
Figure 4.30: Distribution of Nu along channel in presence of diamond shape bluff body at different Re.

In fig 4.31 shows the variation of Nu with changing TI, keeping Re constant at 100,000. With increasing TI from 5-40% it has been accentuated that the Nu value for the face A-B increases, while completely reverse happens for D to A. In face A to B there is a steep negative slope of Nu value and again rises gradually up to point B. After the point B there are sudden decreases in the value and while gradually moving from B to C, It again rises close the point D. The plot of B to C would show completely reverse nature of the plot as C to D and would coincide with this plot thus implying symmetry.
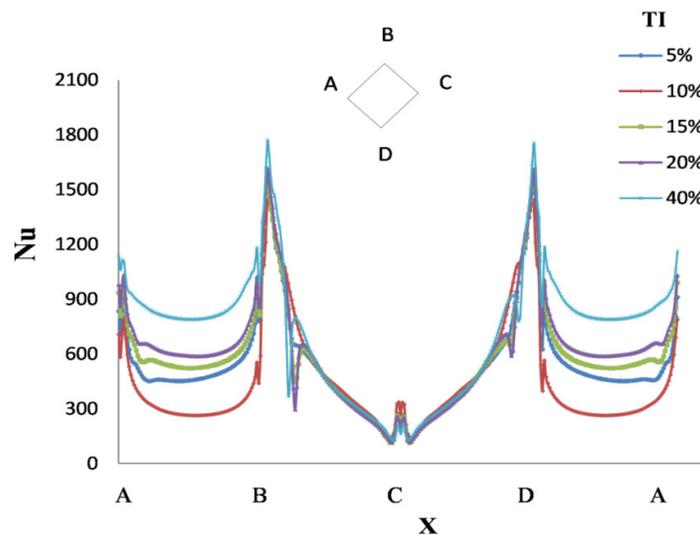
Figure 4.31: Variation of local Nusselt number over the curve length with turbulence intensity at Re=100,000.

Figure 4.32 depicts the relationship of average intermittency at the outlet plane at different Reynolds number. A fully turbulent flow has unit intermittency. In our case the flow becomes completely turbulent at approximately 8,000 Reynolds number.
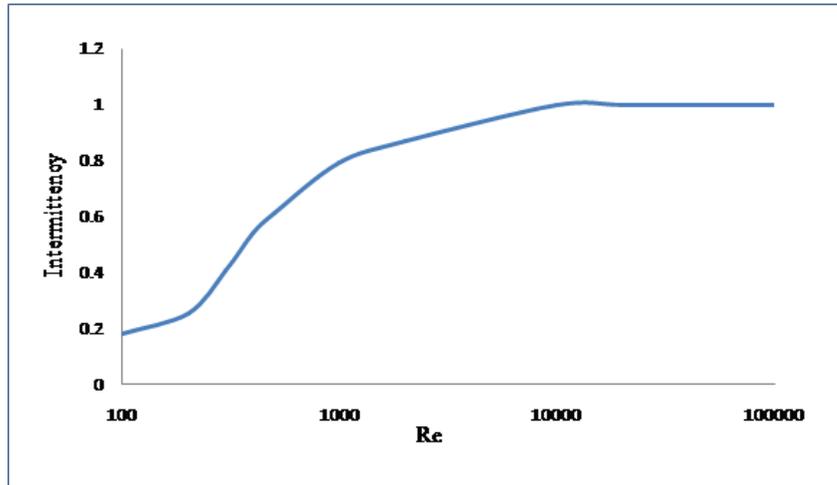
Figure 4.32: Intermittency at exit.

In figure 4.33 drag coefficient has been depicted. As in the case of circular or square cylinder, the drag coefficient is decreases, here also the drag coefficient is inversely related to Re.

Figure 4.33: Variation of drag coefficient with Re for diamond

4.9.3 Small edge facing Trapezium

Figure 4.34 shows distribution of heat transfer around the trapezium surface. While ABCD is the surface of the trapezium, R is at the middle of surface BC. As AB and CD are symmetrically placed and should show similar distribution. Ad and BC surfaces should exhibit different natures of distribution as the former is the frontal side and the latter is the rear surface. From fig. below it could be observed that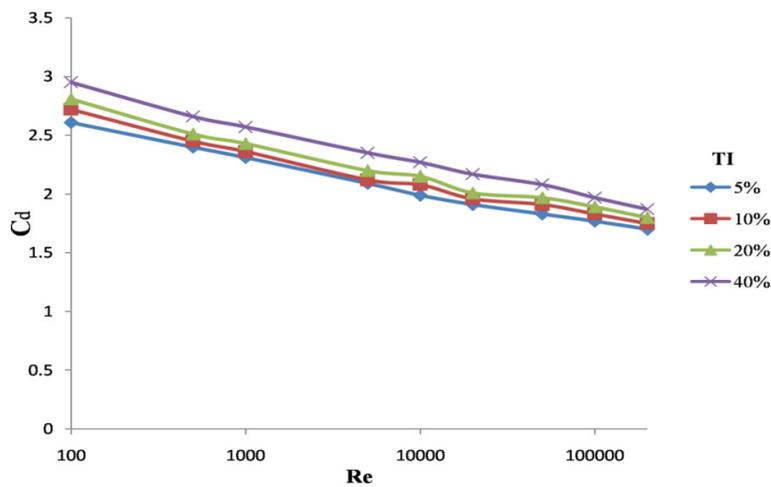 there is a gradual fall in Nu while the flow is moving from A to B except in the case of Re 1,000 where there is a sudden rise in Nu and it gradually drops. As the flow reaches near to B there is steep rise of Nu due to sudden increase in pressure and the value of Nu steeply drop and reaches near to zero while the flow reaches point R the same symmetrical behavior of Nu is observed for the symmetrical part RCD of the trapezium. On surface DA the Nu shows an inverse parabolic pattern for all sets of Re with lowest heat transfer at the stagnation point. Nu depends strongly on Re.
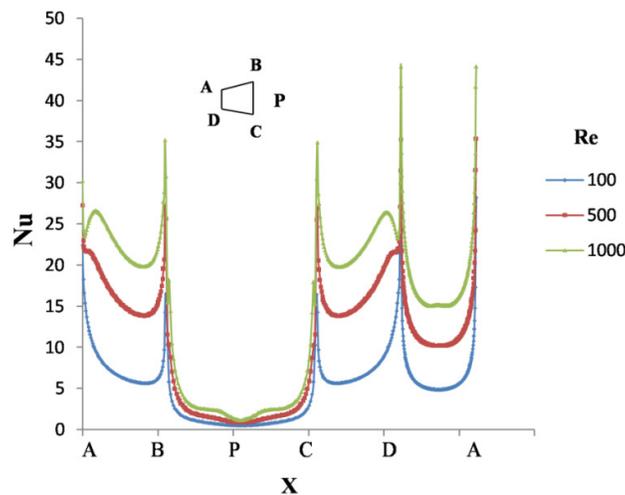
Figure 4.34: Distribution of local Nusselt number along the short side trapezoidal surface at laminar region at 5% TI

Figure 4.35 is a plot of Nu for various regions of bluff body at relatively higher Re at 5% TI. As the flow moves A to B there is sudden rise and fall of Nu due to proportional pressure variation. As the flow reaches toward B there is a slight increase in Nu but a steep drop in Nu value is noticed. For three lower values of Re, the Nu is gradually decreasing as it reaches the midpoint R of surface BC but for Re=200,000 the pattern is just the reverse due to strong vertical interaction of the flow. The symmetrical pattern of Nu plot is observed for the

symmetrical part of bluff body. The nature of Nu on the surface DA is similar as that is observed in fig.16.
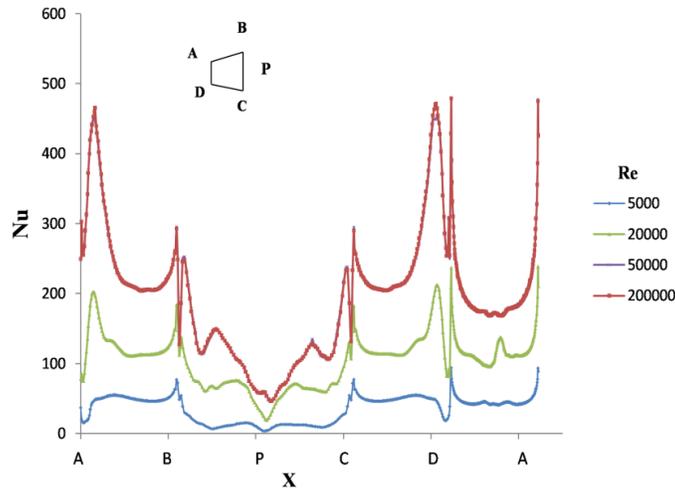
Figure 4.35: Distribution of local Nusselt number along the short side trapezoidal surface at different Reynolds number at 5%TI

Figure. 4.36 below shows the distribution of Nu along the trapezoidal surface at fixed Re=20,000 at different TI varying within 5 -40% TI. The graph show steep rise in Re at the vicinity of corner (A, B, C, D).This nature is observed due to increase in pressure of the flow. The surfaces of the bluff body show much lower values of Nu as the pressure in these regions is considerably low. It is also been observed that TI percentage positively affect the Nu value. Presence of bluff body introduce higher vorticity level/prevents fluid mixing/increases turbulence. Thereby enhancing heat transfer is more.
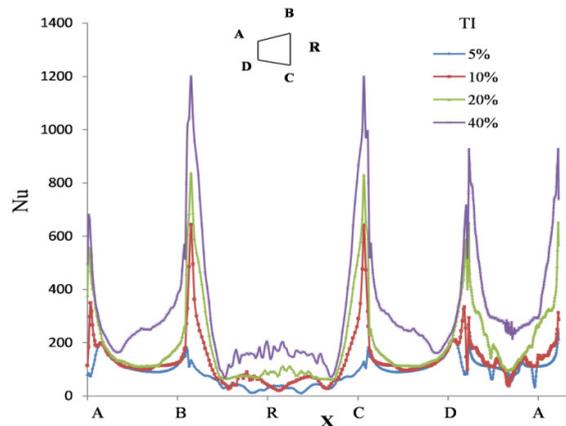
Figure 4.36: Distribution of local Nusselt number along the short side trapezoidal surface at different TI(Re=20,000)

Figure 4.37 shows the distribution of Nu along the trapezoidal surface at fixed higher Re=50,000 at different TI 5 -40% TI. The plot shows that The curve is almost similar to that curve in fig.5.3.16 above. But for the higher TI of 40% the Nu value steeply increases and gradually drops while the flow reaches R from B due to fully development of the at higher TI.
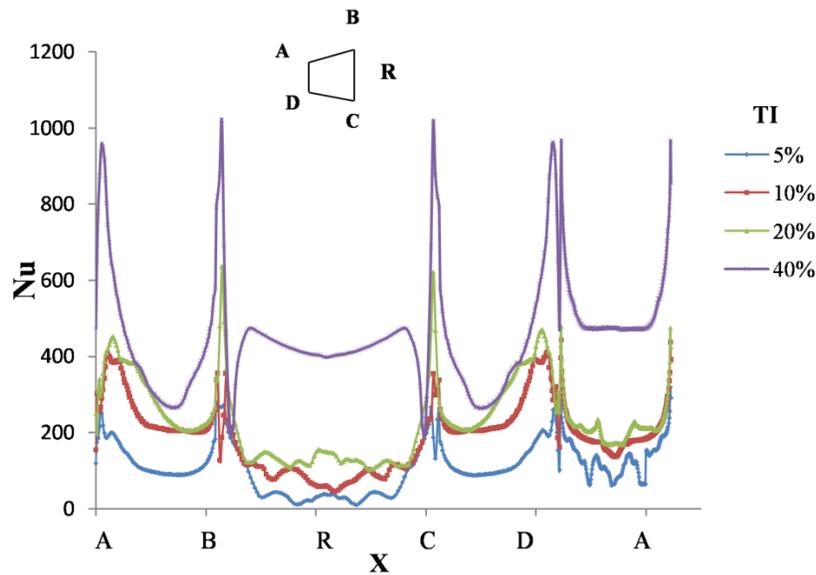
Figure. 4.37: Distribution of local Nusselt number along the short side trapezoidal surface at different TI(Re=50,000)

Heat transfer around the trapezium surface is presented now. The influence of turbulence intensity on Nusselt number had been studied by "Kondjoyan and Daudin (1995)", who worked out the dependence of Nusselt number on turbulence intensity for a lower range of Reynolds number. In this present work the increase in Nusselt number has been recorded with increase in Reynolds number for the turbulence intensity levels of 5%, 10%, 15%, 20% and 40%. From figure 4.38 it is clear that for low value of Reynolds number the turbulence intensity is not affecting significantly the heat transfer rate but when the value of Reynolds number is more than 9,000 there is noticeable increase in heat transfer coefficient.
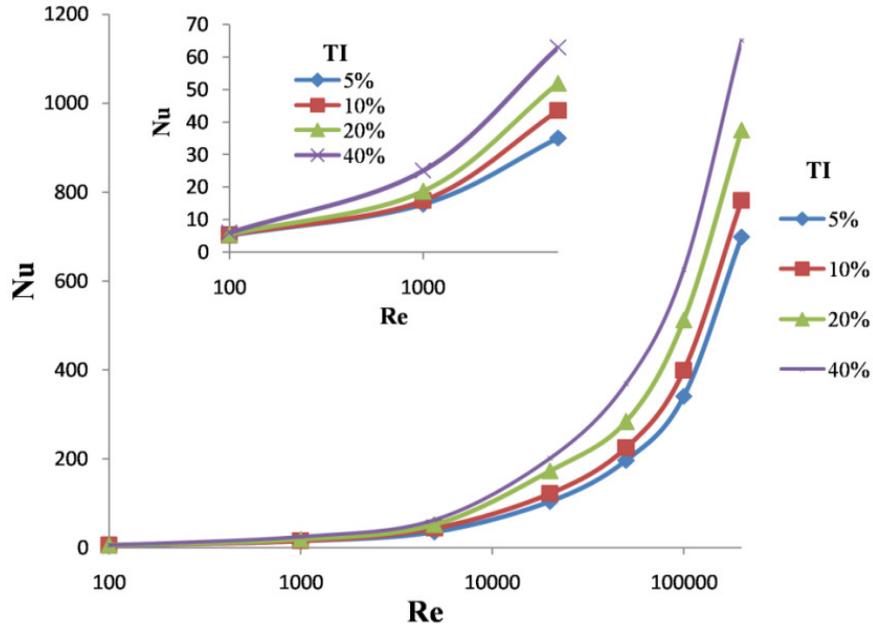
Figure 4.38: Effect of turbulence intensity on Nu

The drag coefficient C_d vs. Re is plot is shown in figure 4.39 which shows that initially there is strong descent in C_d value upto Re about 1,000. Thereafter there is a gradual increase in drag coefficient while moving up to around Re 8,000 and on further increase in Re value there is also gradual decrease of C_d value. It is also observed that with varying percentage of TI there is an appreciable change in C_d value at all Re as observed.

Figure 4.39: Variation of C_d vs. Re at different TI for small edge facing trapezium cylinder

Table 1 show the heat transfer distribution for three different shape geometry at different turbulent intensity and compare with correlation values. It is seen that for diamond het transfer is higher compare to the other two bluff bodies.

Table 3: **Averaged Nusselt number for different bluff body**

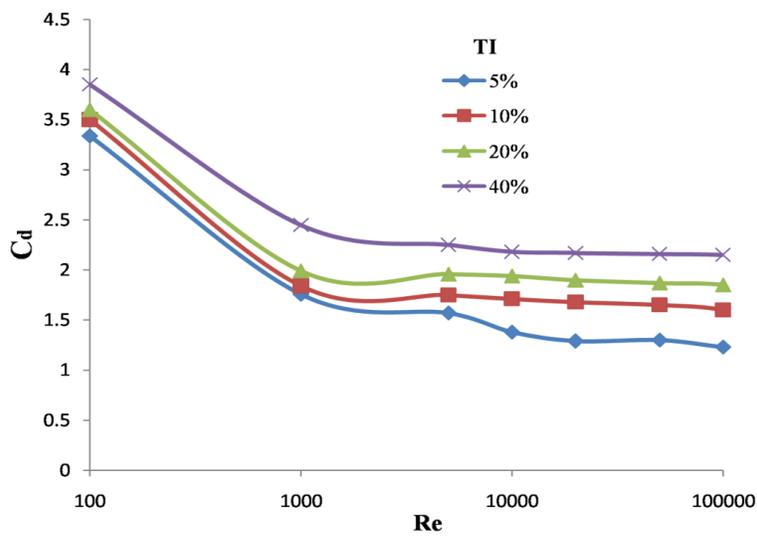| Re	Triangular prism				Small edge facing trapezium				Diamond				Correlation values
	TI				TI				TI				
	5%	10%	20%	40%	5%	10%	20%	40%	5%	10%	20%	40%	
100	4.50	4.54	4.64	4.99	5.25	5.35	5.55	6.1	6.1	6.7	6.94	7.33	4.99
1,000	17.5	17.7	19.4	23.1	14.8	15.8	18.7	25.1	21	25	29.8	40.3	16.94
5,000	48.6	49.3	54.3	63.1	35.1	43.5	52.1	62.9	56	65	74.6	96.1	41.23
20,000	118	119	125	146	104.	122	190	321	144	190	216	271	90.32
50,000	210	231	250	321	196	216	283	477	284	345	430.8	551	152.89
100,000	298	401	446	550	375	512	473	518	447	510	675.	871	228.61
200,000	499	698	787	1055	530	722	810	1141	720	878	1142	1391	343.47

4.10 Summary

Convective heat transfer around different bluff bodies in the design of triangular prism, diamond and trapezoidal cylinder are studied in this work in a large range of Reynolds number The transition SST model has been apply for simulation which provide excellent results in predicting heat transfer under all situation i.e., laminar, transition and turbulent conditions suggested by Abraham et. al. (2009) was used for the current investigation. The heat transfer forecast was obtained smoothly from, laminar to turbulent using the identical model. The investigation evaluates the effect of turbulent intensity on local surface Nusselt

number including the averaged. The present simulation averaged Nusselt number is good agreed with other paper simulation results. The drag coefficient value is decreases with increasing the Reynolds number. The drag coefficients are significantly affected by increasing inlet turbulent intensity for all bluff bodies.

Chapter

5

Augmentation Heat Transfer In Presence Of Triangular Prism, Diamond And Trapezoidal Bluff Body

5.1 Introduction

The primary area of the work is to show the augmentation of heat transfer in a channel due to the insertion of a bluff body. The fundamental governing equations of continuity, momentum and energy are solved along with the transition SST model. The variation of the Nusselt number along the length of the channel is plotted with varying Reynolds numbers from Re 2,500-2,00,000. The Augmentation is also expressed as a percentage increased of heat transfer from a similar system without the bluff body.

5.2 Computational domain

The present work considers the forced convection cross flow around three bluff bodies, an equilateral triangle prism, diamond shaped and trapezoidal shaped shown in figure 5.1 for all the cases. The hydraulic diameter D of the prism, diamond, trapezoidal cylinder is the non-dimensional length. The trapezium can here three different orientations-(i) the larger base at the upstream(ii) the small base at the upstream and (iii) symmetrical placed as depicted through figure 5.1(c)-(e). The non-dimensional distance between the inlet plane and the front surface of the cylinder is 15D and the non-dimensional distance between the rear surface of the cylinder and exit plane is 35D with the total non-dimensional length of the computational domain 50D. The ratio of the width of the cylinder to the vertical distance between the upper and lower walls, H=4D has been used in this work. The problem is considered to be two-dimensional. Air is considered as working fluid for which Prandtl number of 0.71.
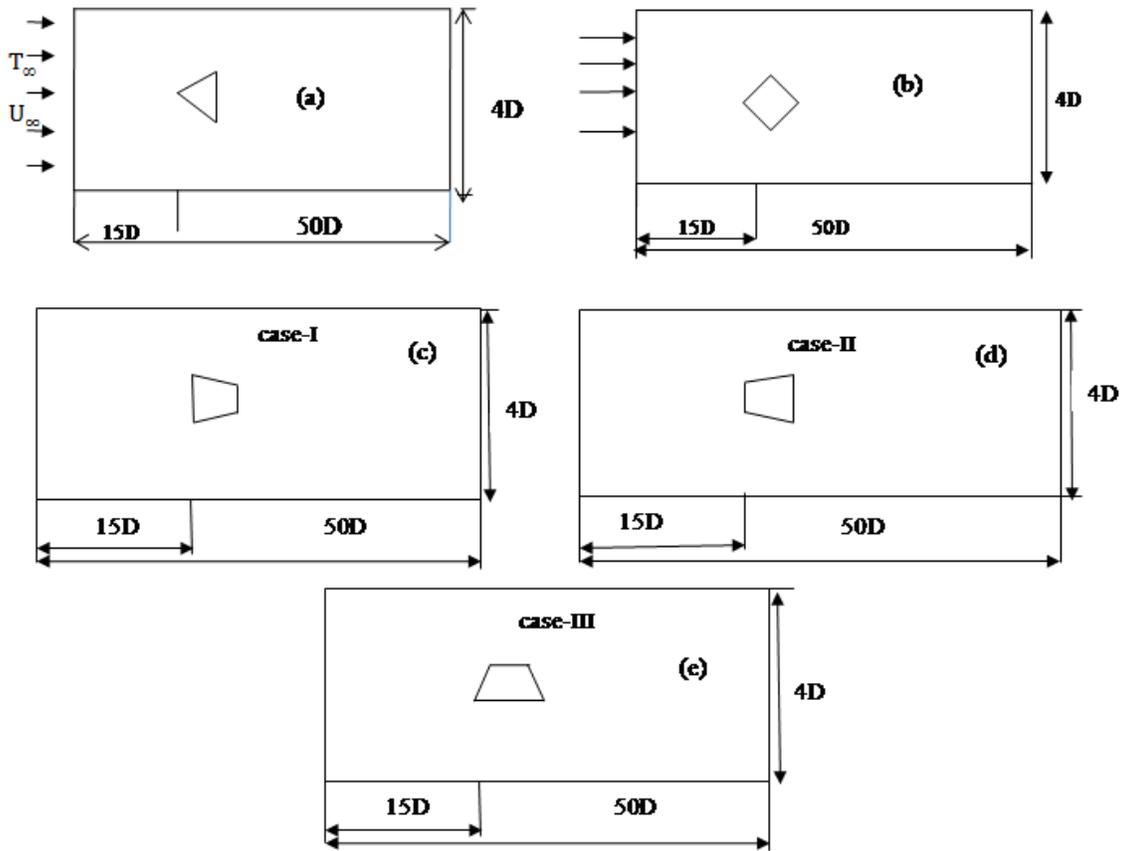
Figure 5.1: Computational domain for flow around bluff body (a) Triangular Prism (b) Diamond (c) Trapezium large facing (d) small facing (e) symmetry

5.3 Boundary conditions

Fluid approaches to the bluff body with uniform inlet velocity of U_∞ and uniform temperature of the inlet fluid is T_∞. The fluid is decide to be air with fixed physical properties (Pr=0.71) with an inlet temperature of 298 K. The bluff bodies are kept at adiabatic condition so that $\frac{\partial T}{\partial n}$=o where n is the normal to the TP surface. The top and bottom walls are heated up. The domain size is fixed and the fluid properties are also considered to be constant thus the variation of Reynolds number are done by changing the inlet velocity.

98
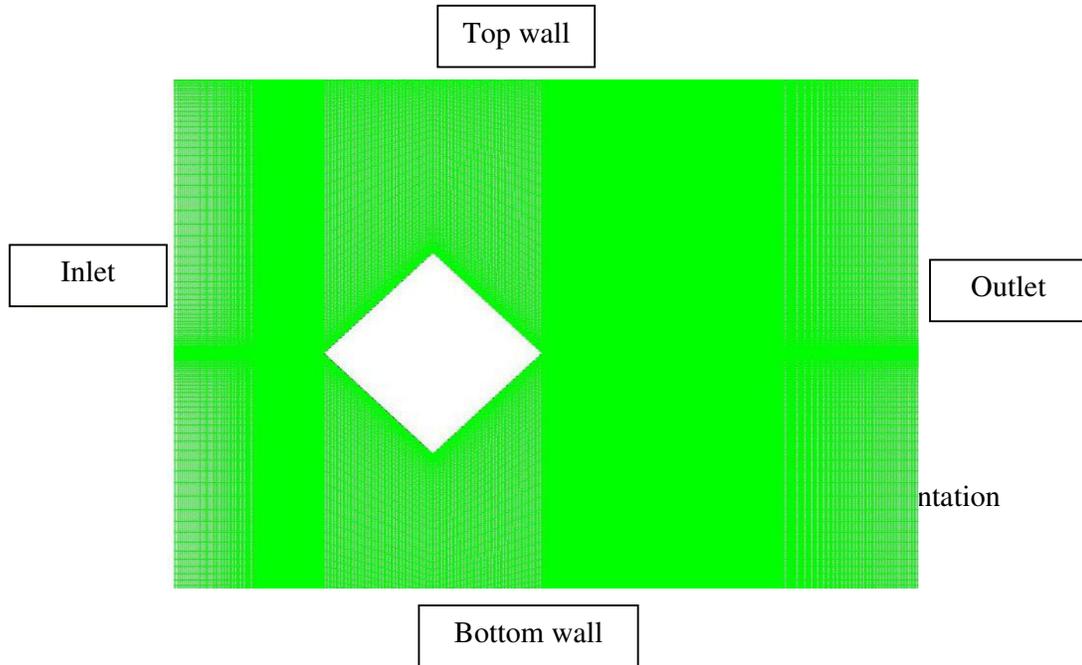
Fig.5.2: Closed up view of boundary condition for heat transfer augmentation

5.4 Solution procedure

The two dimensional governing equations of continuity, momentum and energy equations are solved using Transition SST model proposed by "Abraham et. al. (2009)" were discussed in chapter 3. The governing equations are discretized on a non-uniform structured grid using finite volume method. The velocities and pressures were predicted using semi implicit pressure linked equations (SIMPLE) scheme ("Patankar, 1978"). The interpolation of the gradients of velocities and temperature used the third-order accurate MUSCL scheme ("Van Leer, 1979"), while the gradients for intermittency (γ), turbulent kinetic energy, specific dissipation rate, and momentum thickness used second order accurate upwind scheme. The discretized equations are then linearized using an implicit scheme and solved iteratively using Ansys Fluent 16.2, 2d double precision solver. The convergence criteria for energy, momentum and continuity are 10^{-6}, 10^{-4} and 10^{-4} respectively.

The fig.5.3 show the some close view of different bluff body. After performing rigorous check for grid independence, adequate numbers of cells were used. The number of nodes is 57,368 and40,311 for the case with TP and without TP respectively. Both cases structure meshes are used throughout the domain. The number of nodes is 3,48,080 and 5,02,200 for the case of diamond and trapezium respectively. A part of the grid is shown in figure 5.3.
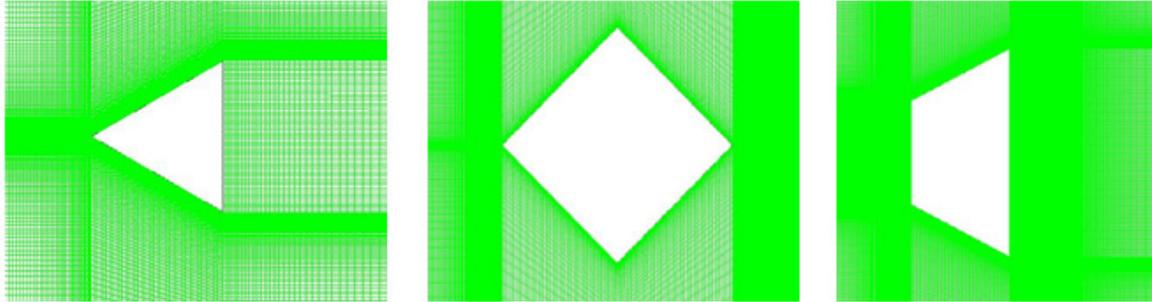
Figure5.3: Close up view of grids (a) Triangle prism, (b) Diamond, and(c) trapezoidal shape bluff body

5.5 Results and discussions

The results that obtained after the simulation performed with the several Reynolds numbers with different turbulence intensity are discussed in this section. The simulations are conducted for Reynolds numbers ranging from 2,500- 2,00,000. The variation of Nusselt number with the increase of turbulence intensity at particular Reynolds number is investigated. The turbulence intensity varies from 5% to 40%.

5.5.1 Triangular Prism

Figure 5.4 shows the validation at high Re with the work of "Benim (2011)" which shows reasonably good agreement with the present computation for Re between 2,500 - 25,000. It is seen that present Nu_{avg} which is find out by RANS model and Without TP is in good agreement with 'Benim et al.(2011)'.
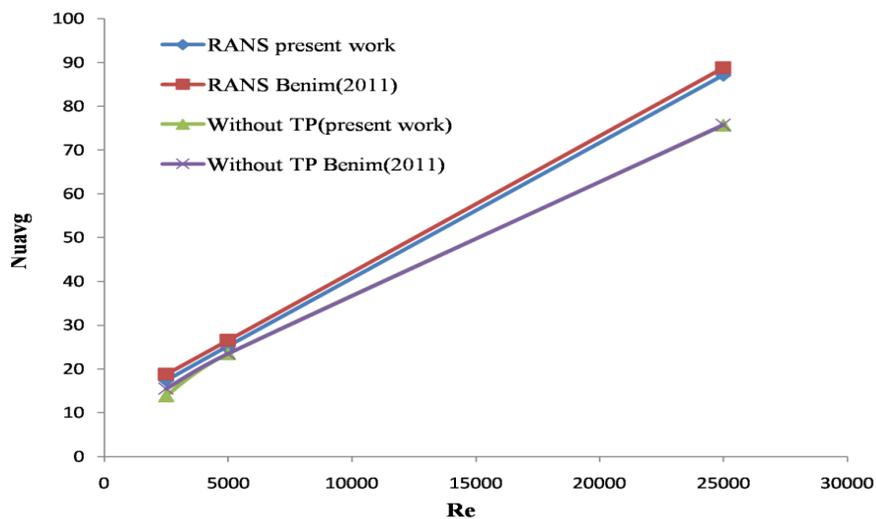
Figure 5.4: Validation of Averaged Nusselt number

Table 4 has shown the heat transfer data for the case with triangular prism. The table shows the avg. value in the channel as well as asymptotic value. It can be observed that averaged Nusselt number as well as Nu_{asy} increases by about 10% in the channel when TP is present. The asymptotic values are almost same with all the Reynolds number. The heat transfer enhanced is about 10-14% which is higher at high Re.

Table.4 Heat transfer data for triangular prism

| Re_D	Nu_{avg}	$Nu_{avg,TP}$	Enhancement (%)	Nu_{asy}	$Nu_{asy,TP}$	Enhancement (%)
10,000	23.89	26.55	11.13	20.53	22.69	10.52
20,000	43.20	48.52	12.31	32.13	35.70	11.12
40,000	78.09	86.47	10.73	64.26	71.46	11.20
1,00,000	170.75	192.59	12.79	131.196	146.69	11.80
2,00,000	306.92	345.14	12.45	242.45	276.48	14.03

Figure .5.5 shows the Nu for the case with TP is compared with case of plane channel at Re-20,000 with fixed 10% turbulence intensity. The plot show that Nu value increases immediately after the location of TP. When the TP is present the asymptotic Nu value are found to be higher at the exit region.
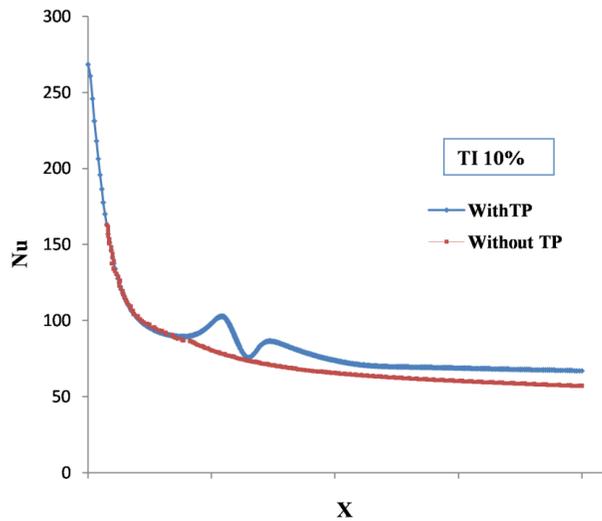
Figure 5.5: Nusselt number distribution at Reynolds number 20,000

Nusselt number distribution at different Re in presence of TP at turbulence intensity 10% is shown in Figure 5.6. From the graph it can be observed those Nusselt number distribution patterns are similar. Though magnitude of heat transfer is increases with increasing the

Reynolds number. First peak is higher in magnitude compared to the second peak following the TP at Reynolds number 10,000, 20,000 and 40,000.
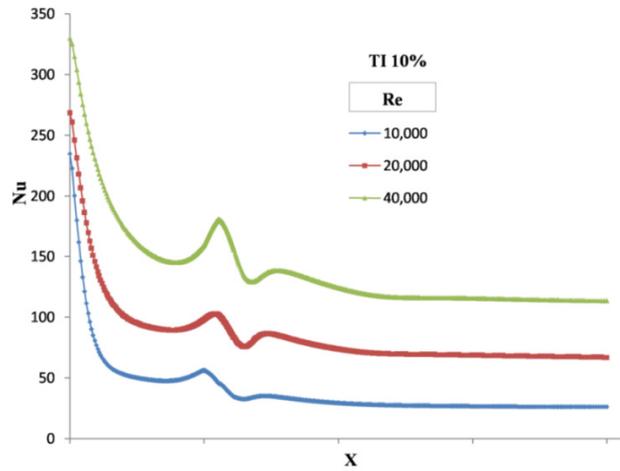
Figure 5.6: Nusselt number distribution along the channel wall

Earlier work by 'Kodjoan et al.(1995)' shows the variation of turbulent intensity can lead to increase in heat transfer. Accordingly we calculated for different TI at inlet. In figure 5.7, the Nu for the case with TP is compared with the case of plane channel at Re 2,00,000 with different turbulence intensity. It can be seen that Nu increases immediately after the location of the TP with increasing the inlet turbulent intensity. There occur a primary peak and crest further downstream. There is a change of 480-580 in average Nusselt number when TI changes from 5%-40%.
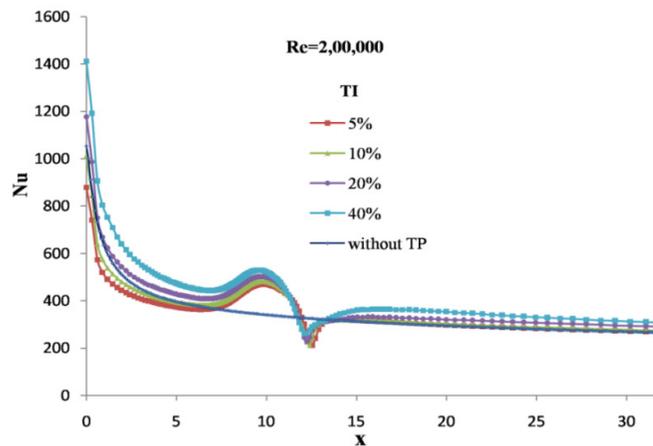
Figure 5.7: Nusselt number distribution along the channel wall at difference turbulence intensity

It is well known that the enhancement in heat transfer is associated with penalty in terms if increase skin friction coefficient reading to higher pressure drop. The figure 5.8 present the distributions of C_fRe, where it is evident that the presence of the TP involves increased the value of surface friction on the channel wall. Also the rise of C_f following the TP persists even at far downstream location.
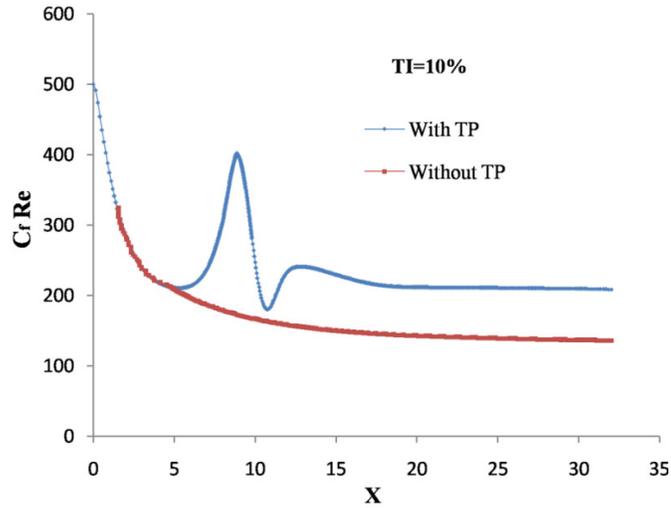
Figure 5.8: Distribution of skin friction coefficient at Reynolds number 20,000

In table 5 effect of TI is present. The average Nu value is increases with increasing the TI for the case of prism. For example in case of TP the Nu value increases from 480 to 580 (as 20%) So it is quantify the TI effect on TP shape bluff body is effective.

Table.5 Effect of turbulence intensity for triangular prism

Re_D	$Nu_{avg,TP}$		
	5% TI	40% TI	% increase
10,000	24.16	33.34	37
20,000	44.05	64.83	47
50,000	99.30	129.55	30
1,00,000	182.92	233.06	27
2,00,000	480	580	20

5.5.2 Diamond

The Nusselt number distributions at different Reynolds number in presence of diamond is shown in figure 5.9. It is shown that that the patterns are almost similar. However the

magnitude of heat transfer increases with increasing Re. The magnitude of the heat transfer is shifted towards downstream of the diamond. The second peak is higher compare to the first peak.
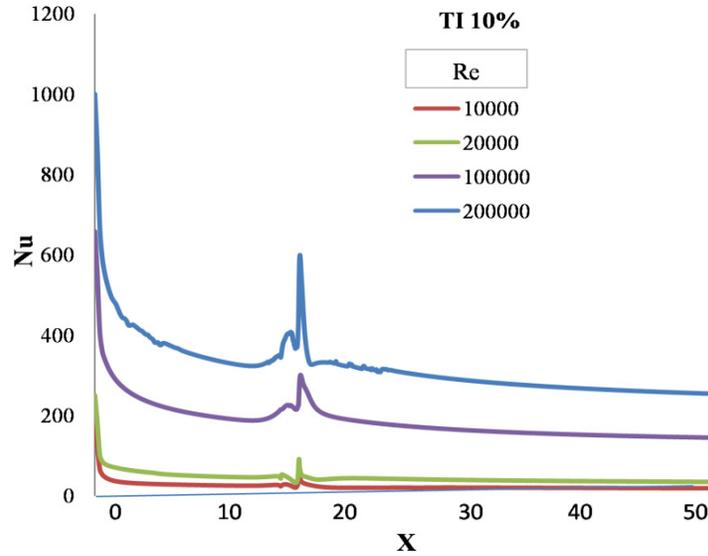
Figure 5.9: Distribution of Nu along channel in presence of diamond shape bluff body

Table 6 summarizes the heat transfer data. It can be observed from the table that average Nu increases by about 4.6% in the duct when a diamond shaped bluff body is present.

Table.6 Comparison of Heat Transfer for diamond

Re_D	Nu_{avg_plane}	$Nu_{avg\_diamond}$	Enhancement(%)	Nu_{asy}	$Nu_{asy,diamond}$	Enhancement(%)
10,000	23.89	24.69	3.24	18.21	19.63	7.79
20,000	43.20	45.03	4.06	34.25	36.05	5.25
1,00,000	172.15	188.26	8.57	143.60	148.30	3.27
2,00,000	306.32	322.40	4.89	249.20	255.99	2.72

5.5.3. Trapezium

Figure 5.10 shows three different orientations of the trapezium .In first case2(a) the short side is facing the flow, in case 1 (b) large side is facing flow and in case of 3 (c) the trapezium is symmetrically placed.

Figure 5.10: (a) small facing (case2) (b) large facing (case1) (c) symmetric (case3)

Nu number distribution at Re 2,00,000 with 10% turbulent intensity is shown in figure 5.11. It shows that the placement of trapezium affect the heat transfer pattern. Largest peak of heat transfer is seen for short side facing the flow. For the vertically symmetric trapezium present the enhancement is least.
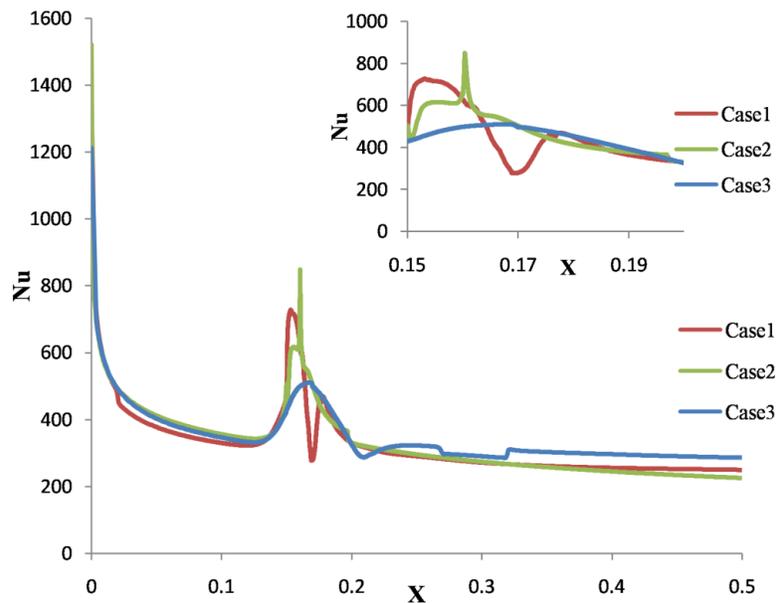
Figure 5.11: Distribution of Nu along channel wall in presence of trapezoidal shape bluffs body

In table 7 summaries of results is present. The average Nu number values are summarized for Re 20,000, 1,00,000, 2,00,000. Nu number value is higher in case of TP compare to the

diamond and trapezium. For example Nu value is 345.14 for TP compare to that diamond is 337.40 for fixed Re 2,00,000.

Table.7 Comparison of Heat Transfer for different shape bluff body

Re_D	$Nu_{avg,trapezium}$			$Nu_{avg,TP}$	$Nu_{avg,diamond}$
	Case1	Case2	Case3		
20,000	44.09	45.50	43.43	48.52	45.67
1,00,000	96.73	99.14	95.23	192.59	188.26
2,00,000	330.04	332.02	327.66	345.14	337.40

Figure 5.12 shows the distribution of friction factor vs. Reynolds number for three different shape bluff body. The curve show that the friction factor is gradually decreasing up to Reynolds number approx 8,000.Beyond this point the friction factor is almost same. It is also seen that the friction factor is higher for the case of triangular prism compared to the other two bluff bodies.
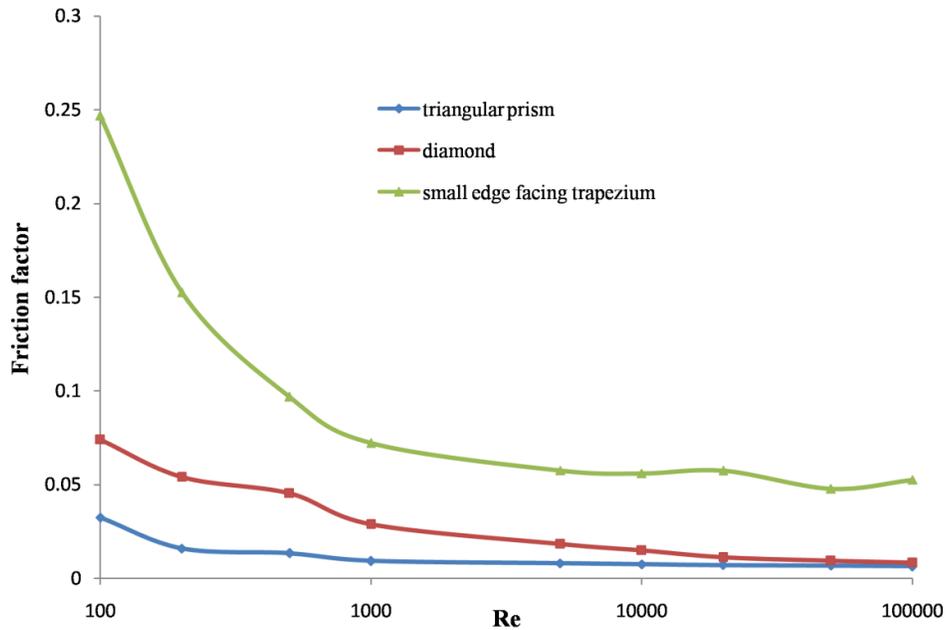
Figure 5.12: Distribution of friction factor against the Re in presence of different shape bluffs body

In figure 5.13, distribution of the thermo hydraulic efficiency is shown against the Re. Here three orientation of trapezoidal shape bluff body is compared. The cases are a) small edge facing flow, b) large edge facing flow and c) symmetrical placed trapezium. When increasing the Reynolds number the thermo hydraulic performance steeply fall upto Re 1,000 for the symmetrically placed trapezium and Re=approx. 500 for large edge facing flow. Beyond that point the thermo hydraulic efficiency gradually fall upto Re=about. 8000 and after that the η is almost same for the symmetrical placed trapezium. Beyond the Re of 500,in the case of large edge facing flow the thermo hydraulic efficiency is gradually fall up to Re= 800,beyond that point the term hydraulic efficiency is almost same.
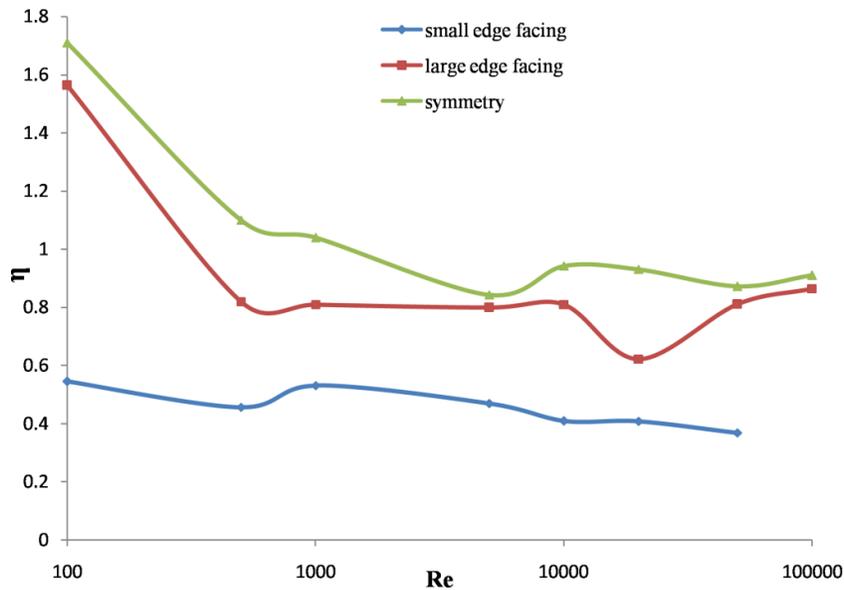
Figure 5.13: Distribution of thermo hydraulic efficiency vs. Re in three orientation of trapezoidal shape bluff body

It has been already mentioned that heat transfer is accompanied with increase in pressure drop and hence a performance parameter (η) which combines heat transfer with pressure drop has been defined (see eq. 3.14, in chapter 3).A value over unity indicates that the pressure drop penalty does not overshadow the enhancement in heat transfer. In figure 5.14 an improvement of the thermo-hydraulic performance is only observed for very small Reynolds numbers upto about 1000 in the laminar region. With increasing Reynolds number, the thermo-hydraulic performance deteriorates rapidly upto Re = around1000. Thereafter, a mild increase up to Re = approx. 1200 is observed. Beyond this point, the curve is almost

same upto Re=1,00,000. For this case the frictional effects seem to play a dominant role and lead to a generally inferior thermal performance. It is of course obvious that for bluff bodies pressure drop penalty is always high. The results indicate that among the bluff bodies used, triangular prism provides better performance.
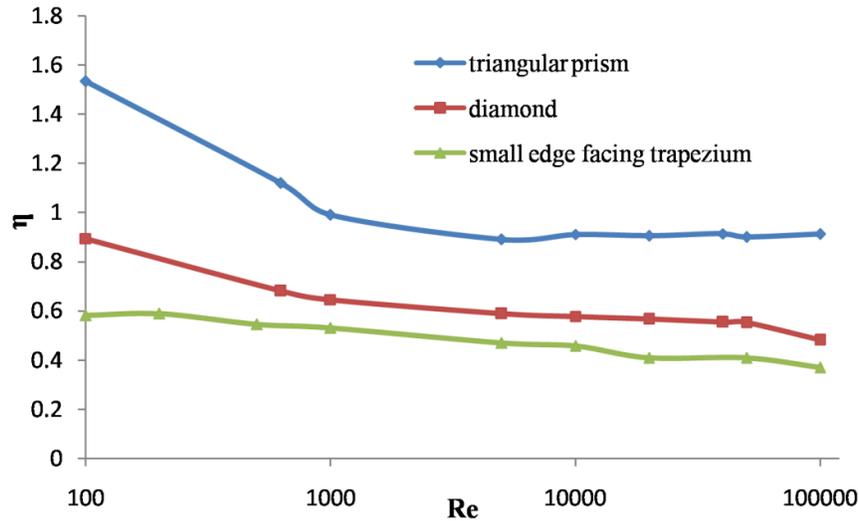
Figure 5.14: Distribution of thermo hydraulic efficiency vs. Re in three different shape bluff body

5.6 Summary

Heat transfer enhancement is estimate in a channel due to the presence different type of bluff bodies using numerical simulation. The order of enhancement is higher (about 10%) in case of triangular prism compare to the diamond and trapezoidal shape bluff body. Though augmentation is associated with enhanced skin friction co-efficient, a comparative study using performance parameter combining friction and heat transfer shows triangular prism provided best performance.

Chapter

6

Conclusions And Future Prospects

CHAPTER- 6

CONCLUSIONS AND FUTURE PROSPETCS

_____

In the present work, heat transfer and fluid flow over bluff bodies of differentshapes in a channel is investigated. Heat transfer augmentation on wall due topresence of bluff bodies are also investigated. The investigation was carried out for all three regimes encompassing laminar, transitional and turbulent flows. Particular focus of the work is the effect of inlet turbulent intensity on transport performance.

The entire research work has been sum up in this thesis which consists of seven chapters including the current one.

Chapter1 is containing the introductory comments about the difference between streamlined body and bluff body. The chapter discusses thedetails of wake, flow separation, external flow, internal flow, vortex flow which are mostly important to design heat exchanger, electronics cooling device etc.

In chapter 2 a comprehensive state-of-art is presented. In *chapter 3* the numerical scheme is described. Transition SST Model has been used as turbulent closure in this work.

In *Chapter 4*, the transport phenomena around bluff body (circular cylinder, square cylinder) and in *Chapter 5*, transport phenomena over triangular prism, diamond and trapezoidal shape bluff body were numerically investigated over two dimensional domain of air.

In *Chapter 4,* the study quantifies the effect of turbulent intensity on local Nusselt number as well as the averaged value. The local and averaged Nusselt number increases with increasing the turbulence intensity. The drag coefficient and pressure coefficient are not significantly affected by inlet turbulent intensity.

In *Chapter 5*, the present simulation averaged Nusselt number is good agreed with other paper simulation results. The drag coefficient value is decreases with increasing the Reynolds number. Local Nusselt number on the diamond from stagnation decreases along the chord length initially. After that it increases slightly as laminar boundary layer starts separating. Finally turbulent boundary layer starts growing and local Nusselt number again decreases. Turbulence intensity has an effect on local Nusselt number, with

the increasing in turbulence intensity local Nusselt number increases specially at stagnation point. The entire part is symmetrical of the upper and lower part.

For trapezoidalbodies, three different orientations are examined, they are large edge facing trapezoidal, small edge facing trapezoidal and symmetrical placed. In presence of small edge facing trapezoidal bluff body Nu value is higher than other two orientations of trapezoidal bluff bodies.

In *Chapter 6,* heat transfer and fluid flow through channel induced with variousshapes of bluff body (triangular prism, diamond and short side facing flow trapezoidal cylinders) numerically and investigated.

Heat transfer enhancement is estimate in a channel due to the presenceof different type of bluff bodies using numerical simulation. The order of enhancement is higher (about 10%) in case of triangular prism compare to the diamond and trapezoidal shape bluff body. Though augmentation is associated with enhanced skin friction co-efficient, a comparative study usingperformance parameter combining friction and heat transfer shows triangular prism provided best performance.

6.3 Future prospects

The research work is anprimary attempt to analysiscomprehensive transport phenomena around the bluff bodies in cross flow. Additional works may involve the following

➢ Future extension of the work involves computation of three dimensional flow fieldas the present work is done in two dimensional only.

➢ The extension of work can be carried out for alternativemodel of bluff bodies will different orientations.

➢ Effect of Prandtl number is not performing in this work. So, more study of various fluids like water, poly butane, etc may be employ.

➢ In this study, RANS is utilizing for turbulent flow. Advanced simulations may be carried out which can shed light on the turbulent structures and detailed turbulent statistics.

References

Abdollah, S., Mahdi, A., Noorallah, R., (2008), Experimental study of near wake flow behind a rectangular cylinder, American J. Applied Sciences, vol.5, pp. 917-926.

Abraham, A.P., Sparrow, E.M. and Tong, J.C.K., (2009), Heat transfer in all pipe flow regimes: laminar, transitional/ intermittent, and turbulent, Int. J. Heat and Mass Transfer, vol. 52, pp. 557–563.

Achenbach, E., (1968), Distribution of local pressure and skin friction around a circular cylinder in cross-flow up to Re $=5\times10^6$, J. fluid mech.,vol.34, part 4, pp. 625-639.

Ahmadi Motlagh, A.H. and Hashemabadi, S.H., (2008), CFD based evaluation of heat transfer coefficient from cylindrical particles, International Communications in Heat and Mass Transfer , vol. 12(35), pp. 674–680.

Ai, Y., Feng, D., Ye, H., Li, L., (2013), Unsteady numerical simulation of flow around 2-D circular cylinder for high Reynolds numbers, Application, vol. 12, pp. 2,180–184.

Bearman, P.W., Trueman, D.M., (1972), Aeronautical Quarterly, vol.23, pp. 229.

Bearman, P.W., Morel T., (1983), Effect of free stream turbulence on the flow around bluff bodies, Prog. Aerospace Sci. vol. 20, pp. 97-123.

Bearman, P.W., (1969), On vortex shedding from a circular cylinder in the critical Reynolds number regime, J. Fluid Mech, vol. 37, pp. 577–585.

Bearman, P.W., Trueman, D.M., (1972), An investigation of the flow around rectangular cylinders, Aeronaut. Quart., vol. 23, pp. 229-237.

Benim, A.C., Chattopadhyay, H. and Navahandi, A., (2011), Computational analysis of turbulent forced convection in a channel with a triangular prism, Int. J. Thermal Science, vol. 50, pp. 1973-1983.

Benim, A.C., Cagan M., Nahavandi, A., Pasqualotto, E., August 25-27., (2007), RANS Predictions of Turbulent Flow Past a Circular Cylinder over the Critical Regime, 5th IASME / WSEAS international Conference on Fluid Mechanics and Aerodynamics, Athens, Greece.

Benim, A.C., Pasqualotto, E. and Suh, S.H., (2008), Modelling of turbulent flow past a circular cylinder by RANS, URANS, LES and DES', Progress in Computational Dynamics, vol. 8(5), pp. 299-307.

Bergles, A.E., (1983), Techniques to augment heat transfer, in: Handbook of Heat Transfer Applications, McGraw-Hill, New York, pp. 31-80.

Bergles, A.E., (2011), Recent developments in enhanced heat transfer, Heat Mass Transfer, vol. 47(8), pp. 1001–1008.

Berger, E., Wille, R., (1972) Periodic flow phenomena. Annu. Rev. Fluid Mech. vol.4, pp. 313.

Berrone, S., Garbero, V., Marro, M., (2011), Numerical simulation of low-Reynolds number flows past rectangular cylinders based on adaptive finite element and finite volume methods. Comput. Fluids vol. 40, pp. 92–112.

Bhattacharyya, S., Chattopadhyay, H., Benim, A.C., 2017, Simulation of heat transfer enhancement in duct flow with twisted tape insert, Progress in Computational Fluid Dynamics, an International Journal, vol. 17, no. 3, pp. 193-197.

Biswas, G. and Chattopadhyay, H., (1992), Heat-transfer in a channel with built-in wing-type vortex generators, Int. J. Heat Mass Transfer, vol.35, no.4, pp. 803–814.

Breuer, M., Bernsdorf, J., Zeiser, T., and Durst. F., (2000), Accurate computations of the laminar flow past a square cylinder based on two different methods: Lattice-Boltzmann and finite volume, Int. J. Heat Fluid Flow, vol. 21, pp. 186–196.

Buresti, G., Lombardi,G. and Talamelli, A., (1998), Low aspect-ratio triangular prisms in cross-flow: measurements of the wake fluctuating velocity field, J. Wind Eng. Ind. Aerodynamic, vol. 74–76 , pp. 463–473.

Buresti, G. and Lombardi, G., (1998), Experimental analysis of the free-end and upper wake flow fields of finite triangular prisms, in: G. Diana, F. Cheli, A. Zasso (Eds.), Proceedings of the Seventh National Congress on Wind.

Camarri, S., Salvetti, M., Buresti, G., (2006), Large-eddy simulation of the flow around a triangular prism with moderate aspect ratio, vol. 94(5), PP. 309-322.

Cantwel, L. B., Coles, D., (1983), An experimental study of entrainment and transport in the turbulent near wake of a circular cylinder, J. Fluid Mech., vol. 136, pp. 321-374.

Catalona, P., Wang, Laccarina, P., Moin, P G., (2003), Numerical simulation of the flow around a circular cylinder at high Reynolds numbers, Int. J. of Heat and Fluid Flow, vol. 24, Issue 4, pp. 463–469.

Chaterjee, D. and Mondal, B., (2012), Effect of thermal buoyancy on the two-dimensional upward flow and heat transfer around a square cylinder, Heat Transfer Engineering, vol.33(12), pp. 1063-1074.

Chatterjee, D. Mondal, B. and Halder, P., (2013), Unsteady forced convection heat transfer over a semicircular cylinder at low Reynolds numbers, Int. J. Computation and Methodology, vol. 6(63), pp. 411-429.

Chattopadhyay, H., (2007), Augmentation of heat transfer in a channel using a triangular prism, Int. J. Thermal Sciences, vol.46, pp. 501-505.

Chen, O. M., Utnes, T., Holmedel, L. E., Pettersen, D. M. B., (2009), Numerical simulation of flow around a smooth circular cylinder at very high Reynolds numbers, marine structures, vol. 22, pp. 142-153.

Chen, Z., Li, Q., Meier, D., Warnecke, H. J., (1997), Convective heat transfer and pressure loss in rectangular ducts with drop-shaped pin fins, Heat and Mass Transfer, vol. 33 (3) , pp. 219–224.

Chen, X.B., Yu, P., Winoto, S.H., (2009), Numerical analysis for the flow past a porous trapezoidal-cylinder based on the stress-jump interfacial-conditions, International Journal of Numerical Methods for Heat and Fluid Flow, vol.19(2), pp. 223-241.

Dalal, A., Eswaran, V., Biswas, G., (2008), A Finite-Volume Method for Navier-Stokes Equations on Unstructured Meshes, Numerical Heat Transfer, Part B, pp. 54238–259.

Dalton, C. and Zheng, W., (2003), Numerical solutions of a viscous uniform approach flow past square and diamond cylinders, J. of Fluids and Structures, vol. 18, pp. 455-465.

Courchesne, J., Leneville, A., (1997), J. of Fluid Eng., Trans. ASME 101, vol. 101, pp. 506.

Davis, R. W., and Moore, E F., (1982), A numerical study of vortex shedding from rectangles, J. Fluid Mech., vol. 116, pp. 475–506.

Dhiman. A., Ghosh. R., (2013), Computer simulation of momentum and heat transfer across an expanded trapezoidal bluff body, Int. J. Heat and Mass Transfer, vol.59, pp. pp. 338–352.

Dhiman, A. Radhe, S., (2011), Unsteady Heat Transfer from an Equilateral Triangular Cylinder in the Unconfined Flow Regime, International Scholarly Research Network , ISRN Mechanical Engineering, Article ID 932738, 13pages.

Davenport, AG., (1962), Buffeting of a suspension bridge by storm winds. J Struct Div ASCE vol. 88(ST3), pp. 233–68.

Djeridi, H.,Braza, M., Perrin, R., Harran, G., Cid, E., Cazin, S., (2003), Near-Wake Turbulence Properties around a Circular Cylinder at High Reynolds Number, Flow,vol.71(1), pp. 19–34.

Ding, H., Shu, C., Yeo, K. S and Xu, D., (2004), Simulation of incompressible viscous flow past a circular cylinder by hybrid FD scheme and meshless least square-based finite difference method, Computer Methods in Applied Mechanics and Engineering, vol.193, pp. 727-744.

Doi, K. and Komai, H. T., (1977), Heat/mass transfer in Taylor vortex flow with constant axial flow rates. Int. J. Heat and Mass Transfer, vol. 20, pp. 57–63.

Dutta, S., Panigrahi, P. K., Muralidhar, K., (2004), Effect of orientation on the wake of a square cylinder at low Reynolds numbers, Indian J. of Engineering & Materials Sciences, vol. 11, 447-459, Steady and unsteady regimes, Asia-Pac. J. Chem. Eng., in press.

Edwards, F.J. and Alker, G.J.R., (1974), The improvement of forced convection surface heat transfer using surface protrusions in the form of (a) cubes and (b) vortex generators. Proceedings of the Fifth International Heat Transfer Conference Tokyo , pp. 2,2244–2248.

Elghnam, R. I., (2014), Experimental and numerical investigation of heat transfer from a heated horizontal cylinder rotating in still air around its axis, Ain Shams Eng., vol. 5, pp. 177-185.

Farouk, B., Guceri, S. I., (1982), Natural and Mixed Convection Heat Transfer Around a Horizontal Cylinder Within Confining Walls, Num. Heat Transfer , vol. 5, pp. 329–341.

Fan, A.W., Deng, J.J., Nakayama, A. and Liu, W., (2012), Parametric study on turbulent heat transfer and flow characteristics in a circular tube fitted with louvered strip inserts, Int. J. Heat and Mass Transfer, September, vol. 55, no. 19–20, pp.5205–5213.

Fujii, K., (2005), Progress and future prospects of CFD in aerospace – wind tunnel and beyond. Progr Aero Sci , vol.41: pp. 455–70.

Gartshore, I, S., (1973), The effects of free stream turbulence on the drag of rectangular two-dimensionalprisms, Boundary Layer Wind Tunnel Laboratory 4-73, The University of Western Ontario.

Garcia, A. A., Gutiérrez-Torres, C., Del, C., Jiménez-Bernal, J. A., Barbosa-Saldaña, J G., Mollinedo-Ponce de León, H. R., Martínez-Delgadillo, S. A., (2013), Numerical simulation of

the subcritical flow over a circular cylinder with u and v grooves, Proceedings of the ASME 2013 Int. Mechanical Engineering Congress and ExpositionIMECE2013,San Diego, California, USA.

Gupta, A.K, Sharma, A, Chhabra, R.P, Eswaran, V.B., (2003), Two-dimensional steady flow of a power-law fluid past a square cylinder in a plane channel: momentum and heat-transfer characteristics, Industrial and Engineering Chemistry Research, vol. 42, pp. 5674–5686.

Golani, R., Dhiman, A. K., (2014), Fluid flow and heat transfer across a circular cylinder in the unsteady flow regime, Int. J. Eng. And Science, vol. 3, pp. 08-19.

Goujan-Durand, S., Renffer, K., Wesfried, JE., (1994), Downstream evolution of the Benard-von-Karman instability, Phys Rev E, vol.50, pp. 308.

Haan, Jr. F. L., Kareem, A., Szewczyk, A. A., (1998), The effects of turbulence on the pressure distribution around a rectangular prism, J. of Wind Eng. and Industrial Aerodyn., vol. 77 and 78, pp. 381-392.

Hasan, M., Dhiman, A., (2010), Flow and heat transfer over a trapezoidal cylinder, 37th National & 4th International Conference on Fluid Mechanics and Fluid Power, At IIT Madras, India.

Hiravennavar, S.R., Tulapurkara, E.G. and Biswas, G., (2007), A note on the flow and heat transfer enhancement in a channel with built-in winglet pair, Int. J. Heat Fluid Flow, vol. 28, no. 2, pp. 299–300.

Igarashi, T., (1987), Int. J. Heat Mass Transfer, vol.30, pp. 893.

Isaev, S. A., Leontiev, A. I., Kudryavtsev, N. A., Baranova, T. A., Lysenko, D. A., (2005) , Numerical simulation of unsteady state heat transfer under conditions of laminar transverse flow past a circular cylinder, High Temperature, vol. 43 , pp. 746 – 759.
.
Islam, T., Hassan R.M.S., (2013), Experimental and Numerical Investigation of Flow over a Cylinder at Reynolds Number 105, J. Modern Science and Technology vol. 1, pp. 52-60.

Islam, U.S., Abbasi, S.W., Rahman, H., (2014), Force Statistics and Wake Structure Mechanism of Flow around a Square Cylinder at Low Reynolds Numbers International Journal of Mechanical, Aerospace, Industrial, Mechatronic and Manufacturing Eng., vol. 8, pp. 1405-1410.

Islam, U.S., Zhou, C.Y., Shah, A., Xie , P., (2012), Numerical simulation of flow past rectangular cylinders with different aspect ratios using the incompressible lattice Boltzmann method, J. of Mechanical Science and Technology, vol. 26 (4), pp. 1027-1041.

Kahawita, R., Wang, P., (2002), Numerical simulation of the wake flow behind the trapezoidal bluff bodies, Computers and fluids, vol. 31, pp. 99-112.

Kato, M., Launder, B. E., (1993), The modeling of turbulent flow around stationary and vibrating square cylinders. Ninth Symposium on Turbulent Shear Flows, Paper 10-4, Kyoto, Japan.

Kawamura, T., Kuwahara, K., (1984), Computation of high Reynolds number flow around circular cylinder with surface roughness, AIAA Paper 84-0340, vol. 4, pp. 450-480.

Kelkar, K.M., Patankar, S.V., (1992), Numerical prediction of vortex shedding behind a square cylinder, Int. J. Numerical Methods for Fluids, vol. 14, pp. 327–341.

Kadiyala, P.K., Chattopadhyay, H., 2017, Numerical Analysis of Heat Transfer from a Moving Surface Due to Impingement of Slot Jets, Heat Transfer Engineering, pp. 1-7.

Kim, D.H., Yang, K.S., Senda, M., (2004), Large-Eddy Simulation of Turbulent Flow Past a Square Cylinder Confined in a Channel, Comput. Fluids, vol. 33(1), pp. 81–96.

King, JPC., (2003), The aerodynamics of long-span bridges. Ph.D. Thesis, Faculty of Engineering, University of Western Ontario.

Kondjoyan, A., and Daudin, J.D., (1995), Effects of free stream turbulence intensity on heat and mass transfers at the surface of a circular cylinder and an elliptical cylinder, axis ratio 4, Int. J. Heat Mass Transfer, vol. 10(38), pp. 1735- 1749.

Knisely, C.W., J. of Fluid and Structures, (1990), vol.4, pp. 371.

Lehmkuhl, O., Rodríguez, I., Borrell, R., Chiva, J., Oliva, A., (2014), Unsteady forces on a circular cylinder at critical Reynolds numbers, physics of fluids, vol. 26, pp. 110-125.

Leonard, B.P., Mokhtari, (1990), S.ULTRA-SHARP Nonoscillatory Convection Schemes for High-Speed Steady Multidimensional Flow. NASATM1-2568 (ICOMP-90-12).NASA, Lewis Research Center.

Li, Q., Chen, Z., Flechtner, U., Warnecke, H.J., (1998), Heat transfer and pressure drop characteristics in rectangular channels with elliptic pin fins, Int. J. Heat and Fluid Flow, vol. 19 (3), pp. 245–250.

Li, Q. S., Melbourne, W.H., (1995), Effects of turbulence on surface pressures of a flat plate and rectangular cylinders in separated and reattaching flows, Papers for the 9th Int. Conf. on Wind Engineering, vol. 1,Wiley Eastern Limited, New Delhi.

Liu, G., Kopp, G.A., (2011), High-resolution vortex particle simulations of flows around rectangular cylinders. Comput. Fluids, vol. 40, pp. 2–11.

Liu, X., Wei, A., Luo, K., Fan, J., (2015), Numerical study of the effects of particles on the near wake around a circular cylinder, Int. J. of Computational Fluid Dynamics, vol. 29(2), pp. 150-160.

Menter, F.E., Kubacki, T.S.E., (2013), Transition modeling based on local variables in: Fifth International Symposium on Engineering Turbulence Modeling and Measurements, Mallorca, Spain.

Mittal, R., Balachander, S., (1995), Effect of three-dimensionality on the lift and drag of nominally two-dimensional cylinders, Phy. of Fluids, vol. 7, pp. 1841- 1865.

Mochida, A., Murakami, S., Tominaga, Y., Kobayashi, H., (1996), Large eddy simulation of turbulent vortex shedding flow past 2-D square cylinder using Dynamic SGS model (Part 1), J. of Architecture Planning and Environmental Engineering (Transactions of Architectural Institute of Japan) No. 479, pp. 41-47.
.
Motlagh, A. H. A., Hashemabadi, S. H., (2008), CFD based evaluation of heat transfer coefficient from cylindrical particles, Int. Comm. in Heat and Mass Transfer, vol. 12(35), pp. 674–680.

MurakamI S. Mochida A., (1995), On turbulent vortex shedding flow past 2-D square cylinder predicted by CFD, J. of wind Eng. and Industrial Aerodyn. vol. 54/55, pp. 191-211.

Najjar, F.M., Balachandar, S., (1998), Low frequency unsteadiness in the wake of a normal flat plate, J. of Fluid Mech., vol. 370, pp. 101–147.

Nakagawa, S., Nitta, K., Senda, M., (1999), An experimental study on unsteady turbulent near wake of a rectangular cylinder in, channel flow, Experiments in Fluids, vol.27, pp. 284-294.

Nakagawa, S., Senda, M., Hiraide, A., Kikkawa, S., (1999), Heat transfer characteristics in a channel flow with a rectangular cylinder. JSME Int J B, vol.42(2), pp. 188–96.

Nakaguchi, H., Hasimoto, K., and Muto, S., (1968), J. Japan Soc. Aero. Space Sci, vol. 16(1).

Nakamura, H., Igarashi, T., (2004), Variation of Nusselt number with flow regimes behind a circular cylinder for Reynolds numbers from 70 to 30,000, Int. J. Heat and Mass Transfer, vol.47(23), pp. 5169 –5173.

Nakaguchi, H., Hashimoto, K., Muto, M., (1968), An experimental study on aerodynamics drag of rectangular cylinders, J. Japan Society of Aeronautical and Space Sci., vol.16, pp. 1-5.

Nakamura, Y., Ozono, S., (1987), The effects of turbulence on a separating and reattaching flow, J. Fluid Mech., vol. 178, pp. 477-490.

Nakamura, Y., Mizota, T., (1975), J. Eng. Mech, Div., Proc. ASCE,101:EM2,125.

Norberg, C., (1993), Flow around rectangular cylinders: Pressure forces and wake frequencies, J. of Wind Eng. and Industrial Aerodyn., vol. 40, pp. 187-196.

Nozawa, K., Tamura, T., (1998), An appropriate approach to the application of large-eddy simulation to complex turbulent flow past a square cylinder, J. of Struc. Mech. and Earthquake Eng., vol. I-43, 591, pp. 151-161.

Okajima, A., (1982), Strouhal number of rectangular cylinders, J. of Fluid Mech., vol.123, pp. 379-398.

Okajima A., (1990), Numerical simulation of flow around rectangular cylinders, J. of Wind Eng. and Industrial Aerodyn., vol. 33, pp. 171-180.

Okajima, A., Nagahisa, T., and Rokugoh, A., (1990), A numerical analysis of flow around rectangular cylinders, The Japan Society of Mechanical Engineers, Series II, vol.33 No.4, pp. 702-721.

Okajima, A., Sakuda, Yi. A., and Nakano, T., (1997), Numerical study of blockage effects on aerodynamics characteristics of oscillating rectangular cylinder, J. Wind Engg. Ind. Aerodyn, vol. 67-68, pp. 91-102.

Olawore, A.S., Odesola, I.F., (2013), 2D Flow around a Rectangular Cylinder a Computational Study, An Int. J. of Science and Technology, vol. 2 (1), pp. 1-26.

Paliwal, B, Sharma, A, Chhabra, R.P, Eswaran, V., (2003), Power law fluid flow past a square cylinder: momentum and heat transfer characteristics. Chemical Eng. Science, vol.58, pp. 5315–5329.

Ponta, L. F., Aref, H., (2004), Strouhal-Reynolds number relationship for vortex streets, Phys. Review Letters, vol. 93, No. 8, pp. 1-4.

Posdziech, O., Grundmann, R., (2007), A systematic approach to the numerical calculation of fundamental quantities of the two-dimensional flow over a circular cylinder, J. Fluids Struct., vol. 23, pp. 479 – 499.

Prasad, A., and Williamson, C.H.K., (1997), The instability of the shear layer separating from a bluff body, J. Fluid Mech., vol. 333, pp. 375–492.

Pal, T.K., Chattopadhyay, H., and Mandal, D.K., (2018), Flow and heat transfer due to impinging annular jet, Int. J. Fluid Mechanics Research. (in press).

Park, J., Kwon, K. and Choi, H., (1998), Numerical solutions of flow past a circular cylinder at Reynolds number up to 160.KSME , Int. J. 12, pp. 1200-1205.

Rajani, B. N., Kandasamy, A., Majumdar, S., (2008), Numerical simulation of laminar flow past a circular cylinder, Applied Mathematical Modelling, vol. 33, pp. 1228 - 1247.

Robichuax, J., Balachandar, S., Vanka, S.P., (1999), Three-dimensional floquet instability of the wake of square cylinder, Phys. of Fluids, vol. 1, pp. 560-578.

Rodriguez, I., Lehmkuhl, O., Borrell, R., Oliva, A., (2012), Flow dynamics in the wake of a sphere at sub-critical Reynolds numbers. Computers & Fluids, vol. 80, pp. 223-243.

Rodriguez, I., Lehmkuhl, O., Borrell, R., Paniagua, L., Perez-Segarra, C. D., (2013), High Performance Computing of the flow past a circular cylinder at critical and supercritical Reynolds numbers, Parallel Comp. Fluid Dynamics Conference, Procedia Engineering, vol. 61, pp. 166 – 172.

Rogers, SE., Roth, K., Cao, HV., Slotnick, JP., Whitlock, M., Nash, SM., (2001), Computation of viscous flow for a Boeing 777 aircraft in landing configuration. J Aircraft, vol. 38(6), pp 1060–8.

Rokugou, A., Okajima, A., and Kamiyama, K., (2002), Numerical Analysis of Flow around Rectangular Cylinders with Various Side Ratios. Japan.

Roshko, A., (1954), On the development of turbulent wakes from vortex streets. NACA Rep.,1191.

Roshko, A., (1961), Experiments on the flow past a circular cylinder at very high Reynolds number, J. Fluid Mech, vol. 10, pp. 345–356.

Saha, A. K., Biswas, G., Muralidhar, K., (1999), Numerical study of turbulent unsteady wake behind a partially enclosed square cylinder using RANS Computer Methods, Applied Mechanics and Eng., vol.178(3), pp. 323-341.

Saha, A. K., Biswas, G., Muralidhar, K., (2001), Two-dimensional study of the turbulent wake behind a square cylinder subject to uniform shear, J. Fluids Eng., vol. 123, pp. 595–603.

Saeedi, M., LePoudre, P.P., Wang, B.C., (2014), Direct numerical simulation of turbulent wake behind a surface-mounted square cylinder, Journal of Fluids and Structures, vol. 51, pp. 20–39.

Samani, M., Bergstrom, D.J., (2015), Effect of a wall on the wake dynamics of an infinite square cylinder, Int. J. Heat and Fluid Flow, vol. 55, pp. 158–166.

Sanitjai, S and Goldstein, R.J., (2004), Forced convection heat transfer from a circular cylinder in cross flow to air and liquids, Int. J. Heat and Mass Transfer, vol. 12(47), pp. 4795–4805.

Sen, S., Mittal, S., Biswas, G., (2011), Flow past a square cylinder at low Reynolds numbers, Int. J. Numer. Meth. Fluids, vol. 67, pp. 1160–1174.

Scholeten, J.W. and Murray, D.B., (1998), Unsteady heat transfer and velocity of a cylinder in cross flow- I. Low free stream turbulence, Int. J. Heat Mass Transfer, vol. 10(41), pp. 1139-1148.

Sharma, A. and Eswaran, V., (2004), Heat and fluid flow across a square cylinder in the two-dimensional laminar flow regime, Numerical heat transfer , vol. 45, pp. 247-269.

Shang, J.S., (2004), Three decades of accomplishments in computational fluid dynamics. Progr Aero Sci, vol. 40(3), pp. 173–97.

Shimada, K., Ishihara, T., (2002), Application of a modified k-εmodel to the prediction of aerodynamic characteristics of rectangular cross-section cylinders, J. of Fluids and Struct., vol. 16(4), pp 465-485.

Shu, C., Qu, K., Niu, X.D. and Chew, Y.T., (2005), Numerical simulation of flow past a rotational circular cylinder by Taylor-series-expansion and least squares-based lattice Boltzmann method, Int. J. of Modern Physics C, vol. 16, pp. 1753-1770.

Singh, S.P., Mittal, S., (2005), Flow past a cylinder: shear layer instability and drag crisis numerical., Int. J. numer. meth. fluids, vol. 47, pp. 75–98.

Singh, D., Premachandran, K.B.S., (2015), Effect of nozzle shape on jet impingement heat transfer from a circular cylinder, Int. J. of Thermal Sciences, vol. 96, pp. 45–69.

Smyth, R., Zurit, P., (1994), Heat transfer at the outer surface of a rotating cylinder in the presence of axial flows, Transactions on Eng. Sciences, vol. 5, WIT Press, UK.

Suzuki, K., Suzuki, H., (1994), Unsteady Heat Transfer in a Channel Obstructed by an Immersed Body, Annu. Rev. Heat Transfer, vol.5, pp. 177–206.

Sparrow, E.M., Abraham, J.P. and Jimmy, C.K., (2004), Tong. Archival correlations for average heat transfer coefficients for non-circular and circular cylinders and for spheres in cross-flow, Int. J. Heat and Mass Transfer, vol. 47, pp. 5285–5296.

Srikant, S., Dhiman, A.K. and Bijjam, S., (2010), Confined flow and heat transfer across a triangular cylinder in a channel, Int. J. of Thermal Science, vol. 49, pp. 2191-2200.

Taned, T., (1965), Experimental investigation of vortex streets, J. Phys. Soc. Jpn. vol. 20, pp. 1714–1721.

Tamura, T., Ito, Y., (1996), Aerodynamic characteristics and flow structures around a rectangular cylinder with a section of various depth/breadth ratios. J. of Structure. and Construction Eng., (Rans actions of Architectural Institute of Japan) vol. 486, pp. 153-162.

Taylor, Ian J. (1999), Study of bluff body flow fields and aero elastic stability using a discrete vortex method, Phd thesis.

Thompson, M.C., Leweke, T., Williamson, C.H.K., (2001), The physical mechanism of transition in bluff body wakes, J. of Fluids and Struct.,vol.15, pp. 607-616.

Torii, S., Yang, W.J. and Umeda, S., (2000), Evolution of vortices behind single Diamond-shaped Cylinders in a free stream flow. Proceedings of the ASME/IMECE conference, Orlando.

Valencia, A., (1995), Heat transfer enhancement in a channel with a built-in rectangular cylinder, Heat Mass Transfer, vol.30, pp. 423–427.

Van Leer, B., (1979), Towards the ultimate conservative deference scheme. V. A second-order sequel to Godunoy's method, J. Computational Physics , vol. 32, pp. 101-136.

Venugopal, A, Agrawal, A, Prabhu, S.V., (2015), Spanwise correlations in the wake of a circular cylinder and a trapezoid placed inside a circular pipe, J. of Fluids and Struct. vol. 54, pp. 536–547.

Wang, F., Zhang, J., Wang, S., (2012), Investigation on flow and heat transfer characteristics in rectangular channel with drop-shaped pin fins, Propulsion and Power Research, vol. 1(1): pp. 64–70.

Wang, H., Zhou, Y., Chan, C., Zhou, T., (2009), Momentum and heat transport in a finite-length cylinder wake. Experiments in Fluids, vol. 46, pp. 1173–1185.

Werner, H., Wengle, H., (1989), Large-eddy simulation of turbulent flow over a square rib in a channel. Adv. Turbul., vol. 2, pp. 418–423.

Wang, X. K., Tan, S. K., (2008), Near-wake flow characteristics of a circular cylinder close to a wall, J. Fluids Struct., vol. 24, pp. 605–627.

Williamson, C.H.K., (1996), Vortex Dynamics in the Cylinder Wake, Annual Review of Fluid Mechanics, vol. 28(1), pp. 477–539.

Webb, R.L. and Kim, N.H., (2005), Principles of Enhanced Heat Transfer, Taylor& Francis, New York .

Whitaker, A., (1976), Elementary Heat Transfer Analysis, Pergamon Press, Inc, New York.

Williamson, CHK., (1988a), Defining a universal and continuous Strouhal-Reynolds number relationship for the laminar vortex shedding of a circular cylinder. Phys. Fluids vol. 31: pp. 2742.

Williamson, CHK., (1988b), The existence of two stages in the transition to three dimensionality of a cylinder wake. Phys. Fluids, vol. 31: pp. 3165.

Yoon, D.H., Yang, K.S. and Choi, C.B., (2009), Heat transfer enhancement in channel flow using an inclined square cylinder, J. Heat Transfer – Trans. ASME, vol. 131, no. 7.

Yoon, D.Y., Yang, K.S., Choi, C.B., (2009), Heat Transfer Enhancement in Channel Flow Using an Inclined Square Cylinder, J. of Heat Transfer, vol. 131 / 074503-4.

You, J.Y. and Kwon, O.J., (2012), Numerical assessment of turbulent models at a critical regime on unstructured meshes, J. Mechanical Science and Technology, vol. 26 (5), pp. 1363~1369.

Zheng, D.D., Zheng, T., (2011), Comparison study on flow fields in vortex flow sensors with circular cylinder and trapezoidal cylinder bluff bodies, Proceedings of the International Conference on Machine Learning and Cybernetics, Guilin, 10-13 July.

Zukauskas, A., (1978), Heat transfer from tubes in cross flow in: J.P. Harnett, T.F. Irvine Jr. (Eds.), Advances in Heat Transfer, vol. (8), Academic Press, Inc, New York.